A Study of Interface Crack Branching in Dissimilar Anisotropic Bimaterial Composites Including Thermal Effects

A Thesis

Presented to

The Academic Faculty

by

Renfu Li

In Partial Fulfillment

of the Requirement for the Degree

Doctor of Philosophy in Aerospace Engineering

Georgia Institute of Technology

November 2004

A Study of Interface Crack Branching in Dissimilar Anisotropic Bimaterial Composites Including Thermal Effects

Approved by:

Dr. George A. Kardomateas, Advisor
School of Aerospace Engineering

Dr. Erian A. Armanios
School of Aerospace Engineering

Dr. John Holmes
School of Aerospace Engineering

Evans Harrell
School of Mathematics

Rami Haj-Ali
School of Civil & Environmental Engineering

Date Approved: November 2004

To my Father and Mother,

my Sister and Brothers

Acknowledgements

The accomplishment of this work would not have been possible without the help and support from some very special people during my graduate education here in the school of Aerospace Engineering at the Georgia Institute of Technology.

I would first like to express my deep gratitude to my advisor, mentor and friend, Professor George A. Kardomateas for his invaluable guidance, support and encouragement. He provided me an amicable atmosphere which not only fosters creative thinking, but also working productively.

I also would like to thank my other thesis committee members, Professor Erian A. Armanios, Professor John Holmes from the School of Aerospace Engineering; Professor Evans Harrell from the School of Mathematics and Professor Rami Haj-Ali from the School of Civil and Environmental Engineering, for their constructive suggestions during the course of this thesis.

This research was carried out under the financial support from the Office of Naval Research, Grant N00014-03-1-0189. I am very grateful to the Grant Monitors, Dr. Yapa D.S. Rajapakse and Dr. Patrick C. Potter, for their interests on this project.

I could not have made any achievement in my career without the unfaltering support from my family. Their enduring love and confidence in me have been my source of strength. My mother and father have always been my model of heroes. Their optimism during hard time, their sincerity to friends, to people and their sense of humor have always been a shining torch ahead my way of life. My brothers and elder sister have always been beside me no matter whatever difficulties I encountered. My girl friend, June Chen, gives me unconditional love and passionate support during my completion of this dissertation. I feel so grateful to have such a wonderful family.

I would also like to take this opportunity to express my deep appreciation to many other people who support me during these years of my life in Georgia Institute of Technology.

Finally, great thanks also go to other graduate students in my laboratory for their assistance during my graduate study.

Table of Contents

List of Tables

List of Figures

Summary

The present research investigates the interface crack/delamination branching behavior in dissimilar anisotropic bimaterial media including thermal effects. This was accomplished by using the theory of Stroh's dislocation formalism, extended to thermo-elasticity in matrix notation. The thermoelastic interface delamination problem of dissimilar anisotropic bimedia was re-examined and one compact solution form was derived for general thermo-mechanical loading based on the complex variable method and the analytical continuation principle. A set of Green's functions was proposed for the thermal dislocations(conventional dislocation and heat vortex) in anisotropic bimedia. Using the contour integral method, a closed form solution to the interaction between the dislocations and the interface delamination was obtained. Within the scope of linear elastic fracture mechanics, the thermoelastic problem of interface delamination branching was then solved by modeling the branched portion as a continuous distribution of dislocations. The interface delamination branching growth behavior was examined for three categories: 1) the effects from the variation of the degree of anisotropy(defined by the material compliance constants ratio s_{11}/s_{22}); 2) the influence from thermal loading, hence thermal properties of the materials; 3) the combined effects of thermal properties and the degree of anisotropy.

After the derivation, the study of this thermo-elastic interface crack or interface delamination branching problem was formulated into finding the solution to a set of coupled singular integral equations. Extensive numerical simulation of various cases suggests some possible criteria for predicting the interface delamination branching propagation: I) for general dissimilar anisotropic bimaterial media, there usually exists a significant interaction energy between the thermal loading and mechanical loading for a structure with defects. This may explain why a catastrophic failure could easily happen when an imperfect bimaterial structure is exposed to thermal loading; II) the conventional crack growth criteria based on (1) maximum K_I, (2) zero K_{II}, (3) maximum $\mathcal{G}$, which give identical predictions in the isotropic case for pure mechanical loading, cease to be consistent for anisotropic media, particular for general anisotropy (i.e. the bimaterial constant $\epsilon \neq 0$); III) the G-based criterion may give more reasonable predictions than a K-based criterion for interface delamination branching angles in dissimilar anisotropic bimedia; IV) for some anisotropic bimaterial media, negative K_I (overlapping of the delamination faces around the crack tip) is possible under certain loading conditions due to the thermal effects; V) there exists an optimal orientation angle difference between the two constituents of a bimaterial media. This optimal difference minimizes the value of the maximum energy release rate. Therefore, the results from this research could provide useful guidelines for practical structures

or material optimal design.

The procedure and some essential formulas can be extended in many applications. The first such extension is to use a contact model, eliminating the interpenetration, which may be inappropriate in physical sense, of the two faces around the tips of an interface delamination for general dissimilar anisotropic bimaterials. Some new discovery is found on the conditions in which this contact model would work well. Some clues for how to extend the current research results to investigate the three dimensional thermo-elastic interface delamination branching problem are also suggested in this work.

In this research, the C++ source codes have been implemented to manage the complicated complex operations in the numerical simulation for solving the singular integral equations in a complex matrix form. As a reference for future readers' usage, some relevant specification for this implementation is also presented as appendices.

Chapter I

Introduction

1.1 Background

Interface crack/delamination/debonding along the interface of dissimilar elastic media is a common phenomenon due to possible defects on the bonding surface or impact loading on the structure. Since the pioneering work of Williams (1959)[1] by using the eigenfunction expansion method to obtain the characteristic oscillating stress singularity of the form $r^{-\frac{1}{2}\pm i\epsilon}$, this phenomenon for isotropic bimedia has been extensively investigated. Many results have been obtained for isotropic bimaterials by many authors such as Erdogan (1963)[2], England (1965)[3], Rice and Sih (1965)[4], Suo and Hutchinsion (1990)[5], etc. These works were mostly based on the Muskhelishvili (1953)[6] formulism for isotropic elastic solids. As to the interface crack of anisotropic elastic bimedia, the investigation started with Clements (1971)[7] using Stroh's sextic formalism [8] then by Willis (1971)[9] using the Fourier transform method. Later on, Ting (1986)[10] studied the asymptotic property of the interface crack of dissimilar anisotropic media by assuming a form of stress function; Qu *etal* (1991)[11] addressed this problem by applying a continuous interface dislocation distribution technique with real matrix notation.

From the early sixties of the last century, the problems of **thermo-elastic interface cracks** attracted may researchers' attention. Shih [12] in 1962, Barber and Comninou [13-14], Matin-Moran *et al* [15] studied this problem for **dissimilar isotropic bimaterials**. As to the **dissimilar anisotropic bimedia**, the thermoelastic interface crack problem was first addressed by Clements *et al*[16] in 1983 for a structure consisting of two infinite half space materials. In 1992, Hwu [17] reconsidered the similar interface crack thermoelastic problem in some detail by employing the identities developed by Ting [18]. Choi and Thangjitham [19] studied the interlaminar crack in laminated anisotropic composites with Fourier integral transforms. In 2001, Herrmann and Loboda [20] extended the Comninou [21] contact model which studied the interface crack in dissimilar anisotropic bimedia.

Crack/delamination may easily branch due to severe stress concentration around the crack tip, especially due to thermal stress concentrations when the body is exposed to heat flow with/without mechanical loading. The crack branching/kinking within a cracked material or along the interface of dissimilar materials can often then be observed as shown on Fig.1.1 to Fig.1.3.

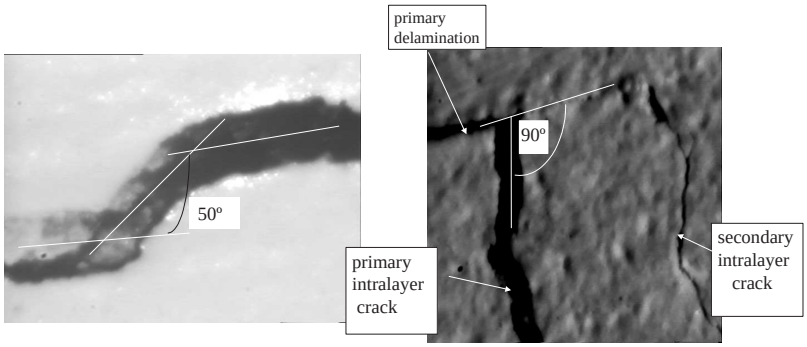

Fig.1.1 Delamination branching in laminated composites

The study of the branching/kinking behavior of a crack is of significant practical importance due to the increasing and wide application of laminated and sandwich composites and thin film structure. After an extensive literature search, it was found that most study on the delamination branching behavior focused on the monolithic **isotropic monolithic** material [22-24] and **isotropic bimaterials** [25]. The crack branching behavior for either **monolithic anisotropic** materials or for **dissimilar anisotropic bimaterial** media has received less attention.

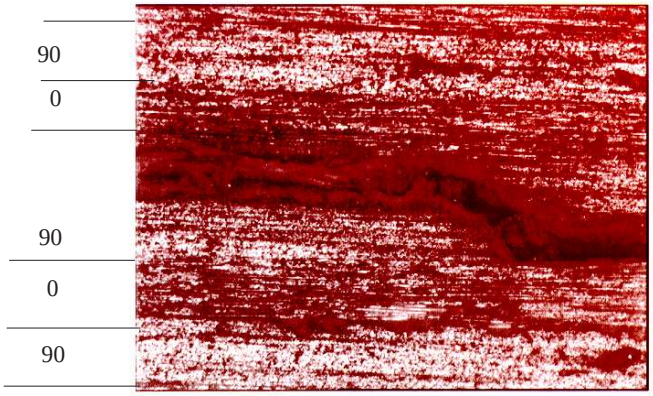

**First branching in same Glass/Epoxy specimen [(0/90)14,0]
under Mixed Mode Bending load**

Fig.1.2 Delamination branching in a Glass/Epoxy specimen

One can find some work on the crack kinking of monolithic anisotropic media, such as Obata *etal*, 1989[26] by Lekhnistkii formulation and Gao *et al*, 1992 [27] by perturbation approach. Gao's paper [27] addresses only a monolithic anisotropic medium and Miller *et al*, 1989 [28] attempted to study a dissimilar anisotropic interface crack branching phenomenon by Lekhnistkii formulas, but their analysis and results are incomplete [27]. Thus some of their conclusion on this phenomenon may be inadequate, based on studying a number of limited cases.

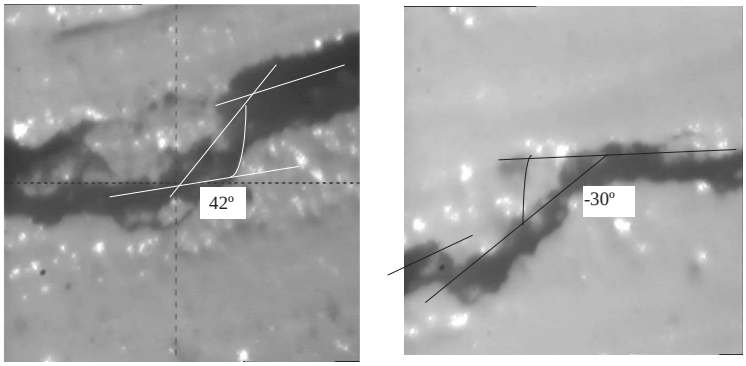

[(0/90) 15], h/T=15/30 [(0/90) 15], h/T=15/30

Crack branching in Glass/Epoxy delaminated specimens (static Mixed-Mode Bending tests)

Fig.1.3 Crack/delamination branching in Mixed-Mode Bending tests

In the meanwhile, in contrast to the **thermo-elastic self-similar** crack propagation or self-similar interface crack problems, very few analyses are available for the **thermo-elastic crack branching** or kinking problems due to the complicated coupling or interaction between thermal effects and mechanical loading. Only two papers tried to deal with this problem, one by Norio *et al* [29, 1986] using rational mapping to the curved crack in isotropic infinite plates and the other one by Chao *et al* [30,1993] using the extended Muskhelishvili's [31] techniques to the curved interface crack of dissimilar isotropic media. But one can easily see that these two papers dealt only with isotropic media and may be hard to be extended to anisotropic media because of the difficulty of finding rational mapping functions for anisotropic dissimilar media

to those in [29] and also because the work in [30] lacks the identities (7) used in this thesis.

Therefore, the delamination branching phenomenon both for monolithic anisotropic and dissimilar anisotropic bimaterial media needs to be further investigated with or without including the thermal effects.

1.2 Research Objectives

The overall purpose of this research is to investigate the interface delamination branching behavior in dissimilar anisotropic bimaterial media. The particular objectives are:

- Develop a general solution to the interface delamination of dissimilar bimaterial media for arbitrary loading (i.e. three cases: pure mechanical applied loading, pure thermal-loading, and a combination of mechanical and thermal loading).

- Formulate the equations for the interface delamination branching of dissimilar bimaterial media and find the solutions to this system of equations

- Examine the influence of thermal properties and degree of anisotropy of the bimaterial media on the delamination branching behavior, thus providing some useful guidelines for practical composite structural design.

1.3 Thesis Outline

The current research is organized as follows:

Chapter 2 presents the derivation of a general solution to the thermo-elastic interface delamination problem under arbitrary loading. This derivation is based on the principle of analytical continuation [31] of complex analysis and an approach similar to the one in Li and Kardomateas in [32]. Although there are some solution forms given in the literature for the thermoelastic interface crack problems, the solution obtained in this chapter can be easily used to obtain the interaction between the thermal dislocations and the interface crack as shown in chapter 4.

Chapter 3 gives the Green's function for thermal dislocation (this term means the combination of heat vortex and conventional/mechanical dislocation). In [32], we studied the thermoelastic crack branching for monolithic anisotropic medium based on extended Stroh's dislocation theory [33] in matrix form. But those thermal-dislocation functions in [32] can not be directly extended to the anisotropic bimedia because of the mismatch of thermal properties along the interface of the dissimilar bimaterials, i.e. these functions cannot satisfy the continuity boundary conditions along the interface. Hence, a different set of thermal dislocation functions is needed and proposed in this paper. In these functions, a mixed term combining heat vortex and conven-

tional dislocation effects is introduced to ensure the continuity condition along the interface of the dissimilar bimaterial media.

Chapter 4 formulates a solution to the interaction between the thermal dislocation and the interface delamination. The introduction of a dislocation into a bimaterial media usually causes the redistribution of the stress and strain fields due to the interaction between the dislocation and the interface delamination. By using the contour integration method, a closed-form solution is found for these interaction functions.

Chapter 5 deals with how to formulate and solve the set of singular integral equations for interface delamination branching problems. Modeling the branched portion of the interface delamination as a continuous distribution of thermal dislocation density and using the superposition principle, one can obtain a system of singular integral equations. But for some simple cases, a closed-form solution may be found by using the Hilbert transformation. In this chapter, a numerical scheme is provided for the general case.

Chapter 6 examines the effects of thermal properties and the degree of anisotropy on the onset of the interface delamination branching behavior by extensive case study. Some important observations can be made regarding interface delamination branching.

Chapter 7 by using a procedure and techniques similar to those in Chapter

2, a contact model is developed to eliminate the interface surfaces interpenetration, a physically implausible phenomenon. It is shown that this model can work well for most practical engineering bimaterials such as laminated composites. The conditions in which the model would be valid for general anisotropic bimedia is also addressed.

Chapter 8 suggests some important conclusions on predicting interface delamination branching. Some clues are presented for potential future applications of the method developed in this research.

Chapter II

A Solution to the Interface Delamination in Dissimilar Anisotropic Bimaterial Media

This chapter will show how to employ the complex variables method and the analytic continuation principle to formulate a general solution to an interface delamination problem. The thermal loading is also taken into account. Some essential fracture quantities such as stresses ahead of the interface delamination and crack open displacements (**COD**) are to be discussed. For the specific case of constant applied loading, a closed form solution will be given.

2.1 Some Basic Thermo-elasticity Formulas for Anisotropic Materials

Thermo-elasticity of anisotropic material in Stroh's formulas can be readily found in the literature. It is briefly summarized in this section. In a fixed Cartesian coordinate system (x_1, x_2, x_3), let us consider an anisotropic elastic medium, in which the displacement u_i, stresses σ_{ij} and temperature fields are independent of x_3. The heat flux can be expressed as

$$h_i = -k_{ij}\frac{\partial T}{\partial x_j}, \quad (i, j = 1, 2, 3) \tag{1}$$

where, $k_{ij} = k_{ji}$ are the coefficients of heat conduction.

The stress-strain law in the presence of thermal fields can be expressed in the following form:

$$\sigma_{ij} = c_{ijkl} \frac{\partial u_k}{\partial x_l} - \beta_{ij} T, \quad (i, j, k, l = 1, 2, 3), \tag{2}$$

where c_{ijkl} is the elastic moduli tensor with the properties that

$$c_{ijkl} = c_{jikl} = c_{ijlk} = c_{klij}, \tag{3}$$

and β_{ij} are the stress-temperature coefficients; the repeated indices imply summation. Equilibrium and conservation of energy lead to

$$\begin{aligned} & \sigma_{ij,j} = 0, \\ \text{i.e.} \qquad & c_{ijkl} \frac{\partial^2 u_k}{\partial x_l \partial x_j} - \beta_{ij} \frac{\partial T}{\partial x_j} = 0 \end{aligned} \tag{4}$$

and

$$\begin{aligned} & \frac{\partial h_i}{\partial x_i} = 0, \\ \text{i.e.} \qquad & k_{ij} \frac{\partial^2 T}{\partial x_i \partial x_j} = 0 \end{aligned} \tag{5}$$

For a plane system, the non-trivial displacement $\mathbf{u} = [u_1, u_2, u_3]^T$, with corresponding stress functions $\varphi = [\varphi_1, \varphi_2, \varphi_3]^T$, and temperature distribution $\mathrm{T}(x_1, x_2)$ (with corresponding heat flux $\mathrm{h}_i, i = 1, 2$) which satisfy equations of

equilibrium (4) and heat conduction (5) be written as

$$\begin{aligned}
&\mathbf{u} = \mathbf{A}\ \phi(z_\alpha) + \overline{\mathbf{A}}\ \overline{\phi(z_\alpha)} + \mathbf{C}\ \chi(z_\tau) + \overline{\mathbf{C}}\ \overline{\chi(z_\tau)},\\
&\varphi = \mathbf{B}\ \phi(z_\alpha) + \overline{\mathbf{B}}\ \overline{\phi(z_\alpha)} + \mathbf{D}\ \chi(z_\tau) + \overline{\mathbf{D}}\ \overline{\chi(z_\tau)},\\
&\mathrm{T}(x_1, x_2) = \chi^{'}(z_\tau) + \overline{\chi^{'}(z_\tau)},\\
&\mathrm{h}_i = -(k_{i1} + \tau k_{i2})\chi^{''}(z_\tau) - (k_{i1} + \overline{\tau} k_{i2})\overline{\chi^{''}(z_\tau)}
\end{aligned} \tag{6}$$

where, $\mathbf{A} = [\mathbf{a}_1, \mathbf{a}_2, \mathbf{a}_3]$ and $\mathbf{B} = [\mathbf{b}_1, \mathbf{b}_2, \mathbf{b}_3]$ are 3×3 matrices which satisfy the identity

$$\begin{vmatrix} B^T & A^T \\ \bar{B}^T & \bar{A}^T \end{vmatrix} \times \begin{vmatrix} A & \bar{A} \\ B & \bar{B} \end{vmatrix} = \begin{vmatrix} I & 0 \\ 0 & I \end{vmatrix} \tag{7}$$

$\mathbf{C}$ and $\mathbf{D}$ are 3×1 vectors; $\phi(z_\alpha)$ is a function vector and $\chi(z_\tau)$ is a scalar function; $z_\alpha = x_1 + p_\alpha x_2$ $(\alpha = 1, 2, 3)$ and $z_\tau = x_1 + \tau x_2$; the overbar $\overline{(\ )}$ denotes the conjugate of a complex variable, the prime $'$ denotes differentiation with respect to z_α or z_τ; the constant τ is the root with positive imaginary part of the equation

$$k_{22}\tau^2 + 2\ k_{12}\tau + k_{11} = 0 \tag{8}$$

the p_α, $\mathbf{a}$, $\mathbf{b}$, $\mathbf{c}$ and $\mathbf{d}$ are constants which satisfy the following equations

$$\mathrm{N} \begin{vmatrix} \mathbf{a} \\ \mathbf{b} \end{vmatrix} = p \begin{vmatrix} \mathbf{a} \\ \mathbf{b} \end{vmatrix},\ \mathrm{N} = \begin{vmatrix} \mathrm{N}_1 & \mathrm{N}_2 \\ \mathrm{N}_3 & \mathrm{N}_1^T \end{vmatrix} \tag{9}$$

$$\mathrm{N} \begin{vmatrix} \mathbf{c} \\ \mathbf{d} \end{vmatrix} = \tau \begin{vmatrix} \mathbf{c} \\ \mathbf{d} \end{vmatrix} - \begin{vmatrix} 0 & \mathrm{N}_2 \\ \mathrm{I} & \mathrm{N}_1^T \end{vmatrix} \begin{vmatrix} \beta_{\mathbf{1}} \\ \beta_{\mathbf{2}} \end{vmatrix}, \qquad (\beta_1)_i = \beta_{i1}, \quad (\beta_2)_i = \beta_{i2} \tag{10}$$

in which, $\mathrm{N}_1 = -\mathrm{T}^{-1}\ R^{\mathrm{T}}$, $\mathrm{N}_2 = \mathrm{T}^{-1}$, $\mathrm{N}_3 = R\ \mathrm{T}^{-1}\ R^{\mathrm{T}} - Q$; the superscript 'T' stands for the transpose of a matrix and

$$Q_{ik} = c_{i1k1}, \quad R_{ik} = c_{i1k2}, \quad \mathrm{T}_{ik} = c_{i2k2}, \quad i,k = 1,2,3 \tag{11}$$

The function vector $\phi(z_\alpha)$ takes the form

$$\begin{aligned} \phi(z_\alpha) &= \ll \mathbf{f}(z_\alpha) \gg \ \mathbf{q}; \\ \ll \mathbf{f}(z_\alpha) \gg &= \mathrm{diag}[\mathbf{f}(z_1),\ \mathbf{f}(z_2),\ \mathbf{f}(z_3)] \end{aligned} \tag{12}$$

where, $\mathbf{f}(z_\alpha)$ and $\mathbf{q}$ are, respectively, unknown functions and constants ; the $\ll\ \gg$ stands for a diagonal matrix.The determination of the unknowns $\mathbf{f}(z_\alpha)$ and $\mathbf{q}$ usually depends on the specifics of problem.

The stresses can be written in term of stress functions as

$$\sigma_{i1} = -\frac{\partial \varphi_i}{\partial x_2} = -\varphi_{i,2}, \quad i = 1,2,3 \tag{13}$$

$$\sigma_{i2} = \frac{\partial \varphi_i}{\partial x_1} = \varphi_{i,1} = \varphi_i^{'}, \quad i = 1,2,3 \tag{14}$$

The relationship

$$\frac{\partial \varphi_i}{\partial x_1} = \frac{d\varphi_i}{dz} = \varphi_i^{'} \tag{15}$$

is used in (14).

If we let $k = k_{22}(\tau - \overline{\tau})/2\mathrm{i}$, then

$$k = \sqrt{k_{11}k_{22} - k_{12}^2} \tag{16}$$

and

$$h_1 = \mathrm{i}k\tau\chi^{''}(z_\tau) - \mathrm{i}k\overline{\tau\chi^{''}(z_\tau)} \tag{17}$$

$$h_2 = -\mathrm{i}k\chi^{''}(z_\tau) + \mathrm{i}k\overline{\chi^{''}(z_\tau)} \tag{18}$$

Here, three useful matrices are defined as

$$H = 2\ i\ AA^T, \quad L = -2\ i\ BB^T, \quad S = i\ (2AB^T - I) \tag{19}$$

where $I = \mathrm{diag}[1, 1, 1]$ is a unit matrix. It can be shown that H and L are symmetric and positive definite and that SH, LS, H^{-1}S, S, SL^{-1} are anti-symmetric [46], and the following relations can be easily verified

$$\begin{aligned} M &= -\mathrm{i}BA^{-1} = H^{-1}(\mathrm{I} + \mathrm{i}S) = (I - \mathrm{i}S^T)H^{-1}, \\ M^{-1} &= \mathrm{i}AB^{-1} = L^{-1}(\mathrm{I} + \mathrm{i}S^T) = (I - \mathrm{i}S)L^{-1} \end{aligned} \tag{20}$$

2.2 A Solution to the Interface Delamination of Anisotropic Bimedia under Thermo-mechanical Loading

Let the medium 'I' occupy the upper half space (denoted by L) and let medium 'II' be in the lower half space (denoted by R) (Fig.2.1). Then from equation (6) and (18) one can have the following expressions for this bimaterial media,

$$\begin{aligned}
\mathbf{u}^I &= \mathbf{A}_{\rm I}\ \phi_{\rm I}(z_\alpha) + \overline{\mathbf{A}}_{\rm I}\ \overline{\phi_{\rm I}(z_\alpha)} + \mathbf{C}_{\rm I}\ \chi_{\rm I}(z_\tau) + \overline{\mathbf{C}}_{\rm I}\ \overline{\chi_{\rm I}(z_\tau)},\\
\varphi^I &= \mathbf{B}_{\rm I}\ \phi_{\rm I}(z_\alpha) + \overline{\mathbf{B}}_{\rm I}\ \overline{\phi_{\rm I}(z_\alpha)} + \mathbf{D}_{\rm I}\ \chi_{\rm I}(z_\tau) + \overline{\mathbf{D}}_{\rm I}\ \overline{\chi_{\rm I}(z_\tau)};\\
T^I &= \chi_{\rm I}^{'}(z_\tau) + \overline{\chi_{\rm I}^{'}(z_\tau)}; \quad h_2^I = -{\rm i}k_{\rm I}\ \chi_{\rm I}^{''}(z_\tau) + {\rm i}k_{\rm I}\ \overline{\chi_{\rm I}^{''}(z_\tau)}
\end{aligned} \tag{21}$$

for $z_\alpha \in L$, and

$$\begin{aligned}
\mathbf{u}^{II} &= \mathbf{A}_{\rm II}\ \phi_{\rm II}(z_\alpha) + \overline{\mathbf{A}}_{\rm II}\ \overline{\phi_{\rm II}(z_\alpha)} + \mathbf{C}_{\rm II}\chi_{\rm II}(z_\tau) + \overline{\mathbf{C}}_{\rm II}\ \overline{\chi_{\rm II}(z_\tau)},\\
\varphi^{II} &= \mathbf{B}_{\rm II}\ \phi_{\rm II}(z_\alpha) + \overline{\mathbf{B}}_{\rm II}\ \overline{\phi_{\rm II}(z_\alpha)} + \mathbf{D}_{\rm II}\ \chi_{\rm II}(z_\tau) + \overline{\mathbf{D}}_{\rm II}\ \overline{\chi_{\rm II}(z_\tau)};\\
T^{II} &= \chi_{\rm II}^{'}(z_\tau) + \overline{\chi_{\rm II}^{'}(z_\tau)}; \quad h_2^{II} = -{\rm i}k_{\rm II}\ \chi_{\rm II}^{''}(z_\tau) + {\rm i}k_{\rm II}\ \overline{\chi_{\rm II}^{''}(z_\tau)}
\end{aligned} \tag{22}$$

for $z_\alpha \in R$.

For the convenience of writing, the symbols 'I' and 'II', denoting the quantities to medium ' L' and ' R', respectively, may be put as supscripts or subscripts. The interface delamination is assumed to be located in the region $a < x_1 < b$, $\infty < x_3 < \infty$ of the plane $x_2 = 0$. A heat flux h_0 and $\sigma_{i2}^{\infty} = p_i$ is applied at infinity (Fig.2.1).

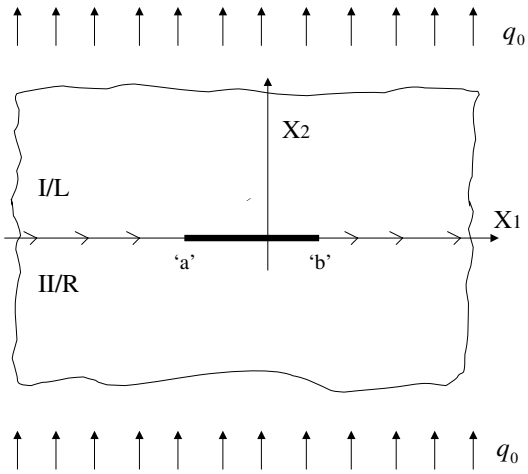

Fig.2.1 A thermo-elastic interface delamination
in a dissimilar anisotropic bimedium

In the scope of linear fracture mechanics, by the superposition principle and making use of equation (14), the boundary conditions for this problem can be written as

$$
\begin{aligned}
h^{I}_{2+}(x_1) &= -h_0(x_1), \\
h^{II}_{2-}(x_1) &= -h_0(x_1), \\
\varphi'^{I}_{+}(x_1) &= \varphi'^{II}_{-}(x_1) = -p(x_1)
\end{aligned}
\tag{23}
$$

for the interface crack region $(a < x_1 < b,\ x_2 = 0)$;

and

$$u_+^I(x_1) = u_-^{II}(x_1),$$

$$\varphi_+^{'I}(x_1) = \varphi_-^{'II}(x_1),$$

$$T_+^I(x_1) = T_-^{II}(x_1),$$

$$h_{2+}^I(x_1) = h_{2-}^{II}(x_1) \tag{24}$$

for the interface outside the crack ($x_1 < a$ and $b < x_1,\ x_2 = 0$);

at infinity

$$h_2^I = h_2^{II} = 0, \quad \sigma_{ij}^I = \sigma_{ij}^{II} = 0 \tag{25}$$

It should be mentioned that the convention $\phi(x_1, x_2) = \phi_\pm(x_1)$ as $x_2 \to 0^\pm$ for any function $\phi(x_1, x_2)$ was used and will be employed in the coming sections.

The temperature continuity condition $(24)_3$ along the bonded interface gives us the following equation

$$\chi_{\text{I}+}^{'}(x_1) + \overline{\chi}_{\text{I}-}^{'}(x_1) = \chi_{\text{II}-}^{'}(x_1) + \overline{\chi}_{\text{II}+}^{'}(x_1) \tag{26}$$

After some rearrangement, it becomes

$$\chi_{\text{I}+}^{'}(x_1) - \overline{\chi}_{\text{II}+}^{'}(x_1) = \chi_{\text{II}-}^{'}(x_1) - \overline{\chi}_{\text{I}-}^{'}(x_1) \tag{27}$$

One can define a function as

$$\theta(z) = \begin{cases} \chi_{\rm I}^{'}(z) - \overline{\chi_{\rm II}^{'}(\bar{z})}, & \text{z} \in \text{L} \\ \\ \chi_{\rm II}^{'}(z) - \overline{\chi_{\rm I}^{'}(\bar{z})}, & \text{z} \in \text{R} \end{cases} \tag{28}$$

which is analytical in the whole plane except at the cut along the $a < x_1 < b$, then equation (27) automatically satisfied.

The heat flux continuity condition $(24)_4$ along the bonded interface leads to:

$$k_{\rm I}[\chi_{\rm I+}^{''}(x_1) - \overline{\chi}_{\rm I-}^{''}(x_1)] = k_{\rm II}[\chi_{\rm II-}^{''}(x_1) - \overline{\chi}_{\rm II+}^{''}(x_1)], \tag{29}$$

or

$$k_{\rm I}\chi_{\rm I+}^{''}(x_1) + k_{\rm II}\overline{\chi}_{\rm II+}^{''}(x_1) = k_{\rm II}\chi_{\rm II-}^{''}(x_1) + k_{\rm I}\overline{\chi}_{\rm I-}^{''}(x_1) \tag{30}$$

Then a function can be defined as

$$\Theta(z) = \begin{cases} k_{\rm I}\chi_{\rm I}^{''}(z) + k_{\rm II}\overline{\chi_{\rm II}^{''}(\bar{z})}, & \text{z} \in \text{L} \\ \\ k_{\rm II}\chi_{\rm II}^{''}(z) + k_{\rm I}\overline{\chi_{\rm I}^{''}(\bar{z})}, & \text{z} \in \text{R} \end{cases} \tag{31}$$

which is analytical in the whole plane except at the cut along the $a < x_1 < b$, then equation (30) is automatically satisfied.

Solving equations (28) and (31), one can obtain

$$k_{\rm I}\chi_{\rm I}^{''}(z) = [k_{\rm I}\Theta(z) + k_{\rm I}\ k_{\rm II}\theta^{'}(z)]/[k_{\rm I} + k_{\rm II}], \tag{32}$$

and

$$k_{\text{II}}\overline{\chi_{\text{II}}^{''}(\bar{z})} = \Theta(z) - [k_{\text{I}}\Theta(z) + k_{\text{I}}\, k_{\text{II}}\theta^{'}(z)]/[k_{\text{I}} + k_{\text{II}}] \tag{33}$$

for the medium occupying the upper space, i.e. $z \in L$;

$$k_{\text{II}}\chi_{\text{II}}^{''}(z) = [k_{\text{II}}\Theta(z) + k_{\text{I}}\, k_{\text{II}}\theta^{'}(z)]/[k_{\text{I}} + k_{\text{II}}], \tag{34}$$

and

$$k_{\text{I}}\overline{\chi_{\text{I}}^{''}(\bar{z})} = \Theta(z) - [k_{\text{II}}\Theta(z) + k_{\text{I}}\, k_{\text{II}}\theta^{'}(z)]/[k_{\text{I}} + k_{\text{II}}] \tag{35}$$

for the medium occupying the lower space, i.e. $z \in R$.

Substituting equation (33) and (35) in condition $(23)_{1,2}$, the following equations can be obtained

$$\frac{1}{k_{\text{I}} + k_{\text{II}}}[k_{\text{I}}\Theta_{+}(x_1) + k_{\text{I}}k_{\text{II}}\theta_{+}^{'}(x_1)] - \Theta_{-}(x_1) + \frac{1}{k_{\text{II}} + k_{\text{II}}}[k_{\text{I}}\Theta_{-}(x_1) + k_{\text{I}}k_{\text{II}}\theta_{-}^{'}(x_1)] = -\text{i}h_0(x_1) \tag{36}$$

and

$$\frac{1}{k_{\text{I}} + k_{\text{II}}}[k_{\text{II}}\Theta_{-}(x_1) + k_{\text{I}}k_{\text{II}}\theta_{-}^{'}(x_1)] - \Theta_{+}(x_1) + \frac{1}{k_{\text{I}} + k_{\text{II}}}[k_{\text{II}}\Theta_{+}(x_1) + k_{\text{I}}k_{\text{II}}\theta_{+}^{'}(x_1)] = -\text{i}h_0(x_1) \tag{37}$$

Subtraction of equation (36) from equation (37) yields

$$\Theta_+(x_1) - \Theta_-(x_1) = 0, \quad a < x_1 < b \tag{38}$$

The equation (38) implies that the function $\Theta(z)$ is also continuous along the region $a < x_1 < b$. Since the function $\Theta(z)$ was defined analytical in the whole plane except the cut $a < x_1 < b$, this function is continuous along the whole interface.

By the statement of the analytical continuation principle [34], the function $\Theta(z)$ shall be analytical on the whole plane. But Liouville's theorem [34] tells that this $\Theta(z)$ must be a constant function in the whole domain. However, the condition in equation $(25)_1$ says this function should be vanish at infinity. Therefore, this constant function must be identically zero in the whole plane, i.e.

$$\Theta(z) = 0, \quad \text{for all z} \tag{39}$$

Hence, the following equations can be obtained from (31)

$$\overline{\chi_{\text{II}}''(\bar{z})} = -\frac{k_{\text{I}}}{k_{\text{II}}}\chi_{\text{I}}''(z) \tag{40}$$

for the upper medium, i.e. $z \in L$; and

$$\overline{\chi_{\text{I}}''(\bar{z})} = -\frac{k_{\text{II}}}{k_{\text{I}}}\chi_{\text{II}}''(z) \tag{41}$$

for the lower medium, i.e. $z \in R$.

Since the temperature field induced by the heat flux at the interface crack tends to zero at infinity, the integration of equations (40) and (41), respectively, gives

$$\overline{\chi'_{\text{II}}(\bar{z})} = -\frac{k_{\text{I}}}{k_{\text{II}}}\chi'_{\text{I}}(z) \tag{42}$$

for the upper medium, i.e. $z \in L$; and

$$\overline{\chi'_{\text{I}}(\bar{z})} = -\frac{k_{\text{II}}}{k_{\text{I}}}\chi'_{\text{II}}(z) \tag{43}$$

for the lower medium, i.e. $z \in R$.

Further integration of equations (42) and (43) leads to:

$$\overline{\chi_{\text{II}}(\bar{z})} = -\frac{k_{\text{I}}}{k_{\text{II}}}\chi_{\text{I}}(z) \tag{44}$$

for $z \in L$; and

$$\overline{\chi_{\text{I}}(\bar{z})} = -\frac{k_{\text{II}}}{k_{\text{I}}}\chi_{\text{II}}(z) \tag{45}$$

for $z \in R$, where the constants contributing to rigid body motion were dropped.

Making use of equations (42) and (43), one can turn equation (28) into the

following form,

$$\theta(z) = \begin{cases} [1 + \frac{k_{\rm I}}{k_{\rm II}}]\chi_{\rm I}^{'}(z), & {\rm z} \in {\rm L} \\ [1 + \frac{k_{\rm II}}{k_{\rm I}}]\chi_{\rm II}^{'}(z), & {\rm z} \in {\rm R} \end{cases} \tag{46}$$

Then either equation (36) or (37) becomes

$$\theta_{+}^{'}(x_1) + \theta_{-}^{'}(x_1) = -\frac{k_{\rm I} + k_{\rm II}}{k_{\rm I} k_{\rm II}} {\rm i} h_0(x_1), \quad a < x_1 < b \tag{47}$$

So far, only the thermal boundary conditions were used. Next, we shall make use of the stress and displacement boundary conditions along the interface.

First, the displacement continuity $(24)_1$ along the bonded interface gives

$$\begin{aligned} &A_{\rm I}\ \phi_{\rm I+}(x_1) + \overline{A}_{\rm I}\ \overline{\phi}_{\rm I-}(x_1) + C_{\rm I}\ \chi_{\rm I+}(x_1) + \overline{C}_{\rm I}\ \overline{\chi}_{\rm I-}(x_1) \\ &\qquad = A_{\rm II}\ \phi_{\rm II-}(x_1) + \overline{A}_{\rm II}\ \overline{\phi}_{\rm I+}(x_1) + C_{\rm II}\ \chi_{\rm II-}(x_1) + \overline{C}_{\rm II}\ \overline{\chi}_{\rm II+}(x_1) \end{aligned} \tag{48}$$

regrouping the '+' and '–' terms, one can have

$$\begin{aligned} &A_{\rm I}\ \phi_{\rm I+}(x_1) - \overline{A}_{\rm II}\ \overline{\phi}_{\rm II+}(x_1) + C_{\rm I}\ \chi_{\rm I+}(x_1) - \overline{C}_{\rm II}\ \overline{\chi}_{\rm II+}(x_1) \\ &\qquad = A_{\rm II}\ \phi_{\rm II-}(x_1) - \overline{A}_{\rm I}\ \overline{\phi}_{\rm I-}(x_1) + C_{\rm II}\ \chi_{\rm II-}(x_1) - \overline{C}_{\rm I}\ \overline{\chi}_{\rm I-}(x_1) \end{aligned} \tag{49}$$

Using similar argument to definition of (31), one may define a function, which is analytical in the whole plane except at the cut along the $a < x_1 < b$,

as :

$$\Phi(z) = \begin{cases} A_{\rm I}\ \phi_{\rm I}(z) - \overline{A}_{\rm II}\ \overline{\phi_{\rm II}(\bar{z})} + C_{\rm I}\ \chi_{\rm I}(z) - \overline{C}_{\rm II}\ \overline{\chi_{\rm II}(\bar{z})}, & \text{z} \in \text{L} \\ A_{\rm II}\ \phi_{\rm II}(z) - \overline{A}_{\rm I}\ \overline{\phi_{\rm I}(\bar{z})} + C_{\rm II}\ \chi_{\rm II}(z) - \overline{C}_{\rm I}\ \overline{\chi_{\rm I}(\bar{z})}, & \text{z} \in \text{R} \end{cases} \tag{50}$$

then equation (48) is automatically satisfied. By using equation (43), the above equation (50) can be recast as follows:

$$\Phi(z) = \begin{cases} A_{\rm I}\ \phi_{\rm I}(z) - \overline{A}_{\rm II}\ \overline{\phi_{\rm II}(\bar{z})} + [k_{\rm II}C_{\rm I} + k_{\rm I}\overline{C}_{\rm II}]\ \chi_{\rm I}(z)/k_{\rm II}, & \text{z} \in \text{L} \\ A_{\rm II}\ \phi_{\rm II}(z) - \overline{A}_{\rm I}\ \overline{\phi_{\rm I}(\bar{z})} + [k_{\rm I}C_{\rm II} + k_{\rm II}\overline{C}_{\rm I}]\ \chi_{\rm II}(z)/k_{\rm I}, & \text{z} \in \text{R} \end{cases} \tag{51}$$

Differentiation of equation (51) and making use of (46) yields

$$\Phi'(z) = \begin{cases} A_{\rm I}\ \phi_{\rm I}^{'}(z) - \overline{A}_{\rm II}\ \overline{\phi_{\rm II}^{'}(\bar{z})} + e_1\ \theta(z), & \text{z} \in \text{L} \\ A_{\rm II}\ \phi_{\rm II}^{'}(z) - \overline{A}_{\rm I}\ \overline{\phi_{\rm I}^{'}(\bar{z})} + \bar{e}_1\ \theta(z), & \text{z} \in \text{R} \end{cases} \tag{52}$$

where, $e_1 = [k_{\rm II}C_{\rm I} + k_{\rm I}\overline{C}_{\rm II}]/[k_{\rm I} + k_{\rm II}]$ is a constant vector.

Secondly, let us consider the stress continuity condition along the bonded interface of this dissimilar bimaterial media. This condition of equation $(24)_2$ leads to:

$$\begin{aligned} &B_{\rm I}\ \phi_{\rm I+}^{'}(x_1) + \overline{B}_{\rm I}\ \overline{\phi}_{\rm I-}^{'}(x_1) + D_{\rm I}\ \chi_{\rm I+}^{'}(x_1) + \overline{D}_{\rm I}\ \overline{\chi}_{\rm I-}^{'}(x_1) \\ &\qquad = B_{\rm II}\ \phi_{\rm II-}^{'}(x_1) + \overline{B}_{\rm II}\ \overline{\phi}_{\rm II+}^{'}(x_1) + D_{\rm II}\ \chi_{\rm II-}^{'}(x_1) + \overline{D}_{\rm II}\ \overline{\chi}_{\rm II+}^{'}(x_1) \end{aligned} \tag{53}$$

rearrangement of both sides of equation (53) reads,

$$B_{\rm I}\ \phi_{\rm I+}^{'}(x_1) - \overline{B}_{\rm II}\ \overline{\phi}_{\rm II+}^{'}(x_1) + D_{\rm I}\ \chi_{\rm I+}^{'}(x_1) - \overline{D}_{\rm II}\ \overline{\chi}_{\rm II+}^{'}(x_1)$$
$$= B_{\rm II}\ \phi_{\rm II-}^{'}(x_1) - \overline{B}_{\rm I}\ \overline{\phi}_{\rm I-}^{'}(x_1) + D_{\rm II}\ \chi_{\rm II-}^{'}(x_1) - \overline{D}_{\rm I}\ \overline{\chi}_{\rm I-}^{'}(x_1) \tag{54}$$

A function which automatically satisfies the condition (54) could be defined as follows:

$$\omega(z) = \begin{cases} B_{\rm I}\ \phi_{\rm I}^{'}(z) - \overline{B}_{\rm II}\ \overline{\phi_{\rm II}^{'}(\bar{z})} + e_2\ \theta(z), & \text{z} \in \text{L} \\ B_{\rm II}\ \phi_{\rm II}^{'}(z) - \overline{B}_{\rm I}\ \overline{\phi_{\rm I}^{'}(\bar{z})} + \overline{e}_2\ \theta(z), & \text{z} \in \text{R} \end{cases} \tag{55}$$

which is analytic on the whole plane except at the cut $a < x_1 < b$ along the interface.

In equation (55),

$$e_2 = [k_{\rm II} D_{\rm I} + k_{\rm I} \overline{D}_{\rm II}]/[k_{\rm I} + k_{\rm II}] \tag{56}$$

is a constant vector and the relationship between $\chi'(z)$ and $\theta(z)$ was used.

From equation (51) and (55), one can obtain

$$B_{\rm I}\ \phi_{\rm I}^{'}(z) = i\ N[\Phi^{'}(z) - e_1\theta(z)] + N\ \overline{M}_{\rm II}^{-1}[\omega(z) - e_2\ \theta(z)] \tag{57}$$

and

$$\overline{B}_{\rm II}\ \overline{\phi_{\rm II}^{'}(\bar{z})} = B_{\rm I}\ \phi_{\rm I}^{'}(z) - \omega(z) + e_2\theta(z) \tag{58}$$

for the upper medium occupying the space $z \in L$;

$$B_{\text{II}}\ \phi^{'}_{\text{II}}(z) = i\ \overline{N}[\Phi^{'}(z) - \overline{e}_1\theta(z)] + \overline{N}\ \overline{M}_{\text{I}}^{-1}[\omega(z) - \overline{e}_2\ \theta(z)] \tag{59}$$

and

$$\overline{B}_{\text{I}}\ \overline{\phi^{'}_{\text{I}}(\bar{z})} = B_{\text{II}}\ \phi^{'}_{\text{II}}(z) - \omega(z) + \overline{e}_2\theta(z) \tag{60}$$

for the lower medium occupying the space $z \in R$.

Substituting of equation (58) and (60) into the condition $(23)_{3,4}$, respectively, gives

$$\begin{aligned} B_{\text{I}}\ \phi^{'}_{\text{I}+}(x_1) + B_{\text{II}}\ \phi^{'}_{\text{II}-}(x_1) - \omega_-(x_1) + \overline{e}_2\theta_-(x_1) \\ + \frac{k_{\text{II}}}{k_{\text{I}} + k_{\text{II}}}[D_{\text{I}}\theta_+(x_1) - \overline{D}_{\text{I}}\theta_-(x_1)] = -p(x_1) \end{aligned} \tag{61}$$

and

$$\begin{aligned} B_{\text{II}}\ \phi^{'}_{\text{II}-}(x_1) + B_{\text{I}}\ \phi^{'}_{\text{I}+}(x_1) - \omega_+(x_1) + e_2\theta_+(x_1) \\ + \frac{k_{\text{I}}}{k_{\text{I}} + k_{\text{II}}}[D_{\text{II}}\theta_-(x_1) - \overline{D}_{\text{II}}\theta_+(x_1)] = -p(x_1) \end{aligned} \tag{62}$$

where, equations (43) and (46) are used.

Subtraction of equation (61) from (62) yields the following equation

$$\omega_+(x_1) - \omega_-(x_1) = 0 \tag{63}$$

which tells that the $\omega(z)$ is continuous on the whole interface. By a similar argument to the on in obtaining equation (39), one may has

$$\omega(z) = 0, \quad \text{for all z} \tag{64}$$

Either equation (61) or (62) leads to:

$$\Phi_+^{'}(x_1) + N^{-1}\overline{N}\Phi_-^{'}(x_1) = \mathrm{i}N^{-1}[p(x_1) + \varrho_1\,\theta_+(x_1) + \varrho_2\,\theta_-(x_1)], \quad a < x_1 < b \tag{65}$$

where

$$\begin{aligned} \varrho_1 &= \frac{k_{\mathrm{II}}}{k_{\mathrm{I}} + k_{\mathrm{II}}} D_I - N[\mathrm{i}\, e_1 + \overline{M}_{\mathrm{II}}^{-1}\, e_2], \\ \varrho_2 &= \frac{k_{\mathrm{I}}}{k_{\mathrm{I}} + k_{\mathrm{II}}} D_{II} - \overline{N}[\mathrm{i}\,\overline{e}_1 + \overline{M}_{\mathrm{I}}^{-1}\overline{e}_2]; \\ N^{-1} &= M_{\mathrm{I}}^{-1} + \overline{M}_{\mathrm{II}}^{-1} \end{aligned} \tag{66}$$

The general solutions to equations (47) and (65) can be obtained by employing the procedure in [32]. These solutions read, respectively as (Appendix A)

$$\theta^{'}(z) = -\frac{k_{\mathrm{I}} + k_{\mathrm{II}}}{2\pi\; k_{\mathrm{I}}\; k_{\mathrm{II}}}\mathrm{x}(z)[\int_a^b \frac{\mathrm{x}_+^{-1}(x_1)h_0(x_1)}{x_1 - z}dx_1 + P(z)] \tag{67}$$

$$\Phi^{'}(z)=\frac{1}{2\pi}\mathrm{X}(z)[\int_{a}^{b}\frac{\mathrm{X}_{+}^{-1}(x_1)}{x_1-z}N^{-1}[p(x_1)+\varrho_1\,\theta_{+}(x_1)+\varrho_2\,\theta_{-}(x_1)]dx_1+Q(z)] \tag{68}$$

where, $P(z)$ and $Q(z)$ are constants to be determined by the boundary conditions,

$$\begin{aligned}&\mathrm{x}(z)=\frac{1}{\sqrt{(z-a)(z-b)}},\quad \mathrm{X}(z)=\mathbf{v}\;\mathrm{x}(z)\;\Delta(z;\epsilon),\\&\Delta(z;\epsilon)=\mathrm{dia}[(\frac{z-b}{z-a})^{i\epsilon},(\frac{z-b}{z-a})^{-i\epsilon},1]\end{aligned} \tag{69}$$

and

$$\mathbf{v}=[v_1,v_2,v_3], \tag{70}$$

in which, v_j(j = 1, 2, 3) are the eigenvectors of the equation

$$(N+e^{2\pi i\delta}\;\overline{N})\;\mathbf{v}=\mathbf{0}. \tag{71}$$

The matrix N can be expressed in terms of a symmetric matrix D and an anti-symmetric matrix W [19]

$$N^{-1}=D-\mathrm{i}W,\quad D=L_1^{-1}+L_2^{-1},\quad W=S_1L_1^{-1}-S_2L_2^{-1}. \tag{72}$$

The explicit expressions to eigenvalues of equation (71) are:

$$\begin{aligned}&\delta_1=\frac{1}{2}+i\epsilon,\;\delta_2=\frac{1}{2}-i\epsilon,\;\delta_3=\frac{1}{2},\\&\epsilon=\frac{1}{2\pi}\log[\frac{1+\beta}{1-\beta}],\;\beta=[-\frac{1}{2}\mathrm{tr}(D^{-1}W)^2]^{\frac{1}{2}}.\end{aligned} \tag{73}$$

It can be seen that equations () and (68) are singular integral equations. Usaully, the contour integral approach is applied to this type of integrations. The method employed in the current paper could be viewed as the generalization of the technique in [6, §110, §70] which is for a single equation.

Once the applied loading $h_0(x_1)$ and $p(x_1)$ is given, the solution to the functions $\theta(z)$ and $\Phi(z)$, hence fields functions $\chi_j(z)$ and $\phi_j(z)$ (j = 'I' and 'II'), can be found. Therefore, a general solution to the thermoelastic interface crack problem of dissimilar bimedia is obtained.

The traction $\sigma_{i2} = \varphi^{'}$ ahead of the interface crack reads

$$[\sigma_{12}, \sigma_{22}, \sigma_{32}]^T = \varphi^{'} = N^* \Phi^{'}(x_1) - e^* \theta(x_1), \quad x_1 < a \ \text{ or } \ b < x_1 \tag{74}$$

where,

$$N^* = i(N + \overline{N}), \quad e_3 = \frac{k_{\text{II}} D_{\text{I}} + \ k_{\text{I}} D_{\text{II}}}{k_{\text{I}} + k_{\text{I}}}$$
$$e^* = i\ (Ne_1 + \overline{N}\ \overline{e}_1) - (NM_{\text{I}}^{-1} e_2 - \overline{NM}_{\text{I}}^{-1} \overline{e}_2) + e_2 + e_3. \tag{75}$$

and the crack open displacements (**COD**) can be derived after some manipulation

$$\Delta \mathbf{u} = \mathbf{u}_+^I(x_1) - \mathbf{u}_-^{II}(x_1) = \Phi_+(x_1) - \Phi_-(x_1), \quad a < x_1 < b \tag{76}$$

2.3 Solution for the Constant Applied Loading

For constant applied loading, a contour integral can give a closed form to the general solution. Let us assume the general applied loading p is constant in the following equation,

$$\Phi^{'}(z) = \frac{\mathbf{X}(z)}{2\pi} \int_{\overline{ab}} \frac{[\mathbf{X}_{+}(x_1)]^{-1}\ N^{-1}}{x_1 - z}\, dx_1\ p \tag{77}$$

Where, $\mathbf{X}(z)$ is defined in (69).

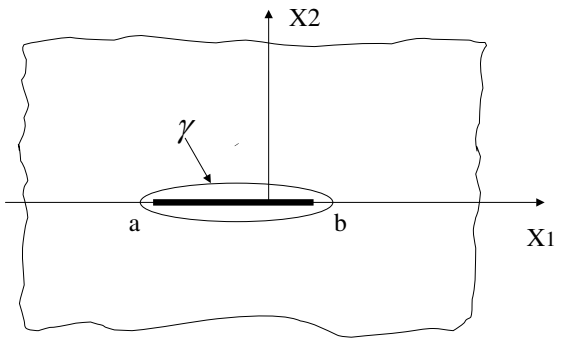

Fig.2.2 Contour integral path

Let γ be a contour which includes the arc $\overline{ab}$, and let this contour shrink

into the arc $\overline{ab}$(Fig.2.2), then

$$\int_{\gamma} \frac{[X(\xi)]^{-1}N^{-1}}{\xi - z}d\xi = \int_{\overline{ab}} \frac{[X_+(t)]^{-1}N^{-1}}{t - z}dt + \int_{\overline{ba}} \frac{[X_-(t)]^{-1}N^{-1}}{t - z}dt$$
$$= \int_{\overline{ab}} \frac{[X_+(t)]^{-1}N^{-1}}{t - z}dt - \int_{\overline{ab}} \frac{[X_-(t)]^{-1}N^{-1}}{t - z}dt \tag{78}$$

From equation (65), one can have

$$X_-(t) = -\bar{N}^{-1}NX_+(t), \qquad a < \ t \ < b \tag{79}$$

Substituting equation (79) into (78) leads to:

$$\int_{\gamma} \frac{[X(\xi)]^{-1}N^{-1}}{\xi - z}d\xi = \int_{\overline{ab}} \frac{[X_+(t)]^{-1}N^{-1}[I + \bar{N}N^{-1}]}{t - z}dt \tag{80}$$

Then,

$$\int_{\overline{ab}} \frac{[X_+(t)]^{-1}N^{-1}}{t - z}dt = \int_{\gamma} \frac{[X(\xi)]^{-1}N^{-1}[I + \bar{N}N^{-1}]^{-1}}{\xi - z}d\xi$$
$$= \int_{\gamma} \frac{[X(\xi)]^{-1}[N + \bar{N}]^{-1}}{\xi - z}d\xi \tag{81}$$

Hence, the line singular integral becomes a contour integral.

Specifically in our problems, the constant loading are $h_0(x_1) = h_0$ and $p(x_1) = p_0$. Then contour integration of equation () leads to:

$$\theta^{'}(z) = -\mathrm{i}\frac{(k_{\mathrm{I}} + k_{\mathrm{II}})h_0}{2\ k_{\mathrm{I}}\ k_{\mathrm{II}}}[1 - \frac{z - (a + b)/2}{\sqrt{(z - a)(z - b)}}] \tag{82}$$

Integration of equation (82) gives

$$\theta(z) = -\mathrm{i}\frac{(k_{\mathrm{I}} + k_{\mathrm{II}})h_0}{2\ k_{\mathrm{I}}\ k_{\mathrm{II}}}[z - \sqrt{(z-a)(z-b)}] \tag{83}$$

where the integral constant is dropped.

The stress function can be found from (68) and it reads (Appendix A)

$$\Phi^{'}(z) = \mathrm{v}\ [\phi_1(z)\ \mathrm{v}^{-1}(N + \overline{N})^{-1}(\mathrm{i}p_0) + \phi_2(z)\mathrm{v}^{-1}(N + \overline{N})^{-1}(\mathrm{i}p_1^*)$$
$$+ \phi_3(z)\mathrm{v}^{-1}(N + \overline{N})^{-1}(\mathrm{i}p_2^*)] \tag{84}$$

where,

$$\phi_1(z) = \mathrm{I} - \mathrm{x}(z)\Delta(z;\epsilon)[\Xi(z) + \Pi_1] \tag{85}$$

$$\phi_2(z) = \Xi(z) - \mathrm{x}(z)\Delta(z;\epsilon)[\Xi(z^2) + \Pi_1\Xi(z) - \Pi_2] + \mathbf{x}(z)\Pi_5 \tag{86}$$

$$\phi_3(z) = \mathrm{x}^{-1}(z) - \mathrm{x}(z)\Delta(z;\epsilon)[\Xi(z^2) - \Pi_3\Xi(z) + \Pi_4 + \mathbf{x}(z)\Pi_6 \tag{87}$$

and Π_k ($k = 1$ to 6) are defined in Appendix A.

If the constant which only contributes to rigid body motion is omitted, integration of the above function gives (Appendix A),

$$\Phi(z) = \mathrm{v}\ [\Xi(z) - \mathrm{x}^{-1}(z)\Delta(z;\epsilon)]\ \mathrm{v}^{-1}(N + \overline{N})^{-1}(\mathrm{i}p_0) + \mathrm{v}[\Xi(z^2) -$$
$$\mathrm{x}^{-1}\Delta(z;\epsilon)\Xi(z) - Y_1(z;\epsilon) - Y_2(z;\epsilon)\Pi_2]\ \mathrm{v}^{-1}(N + \overline{N})^{-1}(\mathrm{i}p_1^*) + \mathrm{v}[Y_3(z)$$
$$- \mathrm{x}^{-1}\Delta(z;\epsilon)(\Xi(z) - \widetilde{\Pi}_1) - Y_1(z;\epsilon) - Y_2(z;\epsilon)\widetilde{\Pi}_2]\ \mathrm{v}^{-1}(N + \overline{N})^{-1}(\mathrm{i}p_2^*) \tag{88}$$

where,

$$\widetilde{\Pi}_1 = \mathrm{diag}[\frac{a+b}{2} + (b-a)i\epsilon,\ \frac{a+b}{2} - (b-a)i\epsilon,\ \frac{a+b}{2}] \tag{89}$$

$$\begin{aligned}\widetilde{\Pi}_2 = \mathrm{diag}[&\frac{b^2-a^2}{2}i\epsilon - (1+4\epsilon^2)\frac{(b-a)^2}{2}, \\ &-\frac{b^2-a^2}{2}i\epsilon - (1+4\epsilon^2)\frac{(b-a)^2}{2}, -\frac{(b-a)^2}{2}]\end{aligned} \tag{90}$$

$\Xi(z)$, $Y_1(z;\epsilon)$, $Y_2(z;\epsilon)$ and $Y_3(z)$ are matrix functions defined in Appendix A.

Once the temperature potential functions and stress functions are found, the heat flux and stress fields for this bimedia with the presence of the interface may readily be obtained. Here given are the heat flux for the upper medium of this bimaterial

$$h_1^c(x_1,x_2) = -\mathrm{Re}[(1 - \frac{z-\frac{a+b}{2}}{\sqrt{(z-a)(z-b)}})\tau]h_0 \tag{91}$$

$$h_2^c(x_1,x_2) = \mathrm{Re}[1 - \frac{z-\frac{a+b}{2}}{\sqrt{(z-a)(z-b)}}]h_0 \tag{92}$$

and the stress fields for the upper medium read as

$$[\sigma_{11},\sigma_{21},\sigma_{31}]_{1c}^T = -2\mathrm{Re}[\mathrm{i}N\mathrm{v} \ll p_\alpha \gg \mathrm{v}^{-1}\Phi^{'}(z) - \mathrm{i}\overline{D_c}\ \tau\ \theta(z)] \tag{93}$$

$$[\sigma_{11},\sigma_{21},\sigma_{31}]_{2c}^T = 2\mathrm{Re}[\mathrm{i}N\Phi^{'}(z) - \mathrm{i}\overline{D_c}\theta(z)] \tag{94}$$

where,

$$\overline{D_c} = \mathrm{i}Ne_1 + N\overline{M}_{II}^{-1}e_2 - D_I\frac{k_{II}}{k_I + k_{II}} \tag{95}$$

The **COD** for this case can then be expressed as

$$\begin{aligned}\Delta\mathbf{u}(x_1) = 4\sqrt{(x_1-a)(b-x_1)}\mathrm{cosch}(\epsilon\pi)\{\mathbf{u}_1(x_1,\epsilon)[p_0 + x_1(p_1^* + p_2^*) - \widetilde{\Pi}_1 p_2^*] \\ + \frac{a+b-2x_1}{8}(N+\overline{N})^{-1}p_2^*\}\end{aligned} \tag{96}$$

where,

$$\mathbf{u}_1(x_1,\epsilon) = \mathbf{v}\mathrm{diag}[(\frac{b-x_1}{x_1-a})^{i\epsilon}, (\frac{b-x_1}{x_1-a})^{-i\epsilon}, \mathrm{cosch}^{-1}(\epsilon\pi)]\mathbf{v}^{-1}(N+\overline{N})^{-1} \tag{97}$$

The traction ahead of the crack tip may then read

$$\begin{aligned}\mathbf{t}(x_1) = [\sigma_{12},\sigma_{22},\sigma_{32}]^T = N^*\Phi^{'}(x_1) - e^*\theta(x_1) = \frac{N^*}{\sqrt{(x_1-\mathrm{a})(x_1-\mathrm{b})}}\mathrm{v} \\ \times\{[\sqrt{(x_1-\mathrm{a})(x_1-\mathrm{b})}\mathrm{I} - \Delta(x_1;\epsilon)(\Xi(x_1)+\Pi_1)]\mathrm{v}^{-1}(N+\overline{N})^{-1}(\mathrm{i}p_0) \\ + [x_1\sqrt{(x_1-\mathrm{a})(x_1-\mathrm{b})}\mathrm{I} - \Delta(x_1;\epsilon)(\Xi(x_1^2)+x_1\Pi_1-\Pi_2)+\Pi_5]\times \\ \mathrm{v}^{-1}(N+\overline{N})^{-1}(\mathrm{i}p_1^*) + [(x_1-\mathrm{a})(x_1-\mathrm{b})\mathrm{I} - \Delta(x_1;\epsilon)(\Xi(x_1^2)-x_1\Pi_3+\Pi_4) \\ + \Pi_6]\mathrm{v}^{-1}(N+\overline{N})^{-1}(\mathrm{i}p_2^*)\} - e^*[x_1 - \sqrt{(x_1-a)(x_1-b)}]h_0^*\end{aligned} \tag{98}$$

the notation $\mathrm{I} = \mathrm{diag}[1,\ 1,\ 1]$.

The conventional Stress Intensity Factors (**SIF**s) ahead of the crack tip

such as for $x_1 = b$ may be expressed as

$$[\mathbf{K}_{\text{II}}, \mathbf{K}_{\text{I}}, \mathbf{K}_{\text{III}}]^T = \lim_{x_1 \to \text{b}} \sqrt{2\pi(x_1 - \text{b})}[\sigma_{12}, \sigma_{22}, \sigma_{32}]^T$$
$$= \sqrt{2\pi(\text{b} - \text{a})} N^* \text{v} \lim_{x_1 \to \text{b}} \Delta(x_1; \epsilon)[\text{k}_1 \text{v}^{-1}(N + \overline{N})^{-1}(\text{i}p_0)$$
$$+ \text{k}_2 \text{v}^{-1}(N + \overline{N})^{-1}(\text{i}p_1^*) + \text{k}_3 \text{v}^{-1}(N + \overline{N})^{-1}(\text{i}p_2^*)] \tag{99}$$

where,

$$\text{k}_1 = -\text{diag}[\frac{1}{2} + \text{i}\epsilon, \frac{1}{2} - \text{i}\epsilon, \frac{1}{2}] \tag{100}$$

$$\text{k}_2 = (\text{b} - \text{a})\text{diag}[\epsilon^2 - \frac{\text{b} + \text{a}}{4(\text{b} - \text{a})} - \text{bi}\epsilon, \epsilon^2 - \frac{\text{b} + \text{a}}{4(\text{b} - \text{a})} + \text{bi}\epsilon, -\frac{\text{b} + \text{a}}{4(\text{b} - \text{a})} + \frac{1}{8}] \tag{101}$$

$$\text{k}_3 = (\text{b} - \text{a})\text{diag}[0.375 + \epsilon^2 + 2\text{i}\epsilon, 0.375 + \epsilon^2 - 2\text{i}\epsilon, -0.25] \tag{102}$$

Now the energy release rate G_0 can also be calculated for this interface crack propagation. Assuming the crack tip grows from $'\text{b}'$ to $'\text{b} + \delta b'$, then from equations (76), (88) and (98), G_0 reads as:

$$G_0 = \lim_{\delta b \to 0} \frac{1}{2\ \delta b} \int_0^{\Delta b} \delta \mathbf{u}^T(x_1 - \delta b)\ \mathbf{t}(x_1) dx_1 \tag{103}$$

For the simple case where two media which are identical, an explicit expression for the energy release rate can be obtained as

$$G_0 = \frac{\pi(b - a)}{2}[p_0^T L^{-1} p_0 + (b - a) p_0^T L^{-1} \widetilde{p}_1^* + p_0^T L^{-1} e_1^* h_0^* + b p_1^{*T} L^{-1} p_0$$
$$+ b p_1^{*T} L^{-1} \hat{p}_1^*/4] \tag{104}$$

where

$$p_1^{*T} = p_1^*[1,\ 1,\ 1]; \qquad \widetilde{p}_1 = p_1^*[1,\ 1,\ \frac{3}{2}]^T, \qquad \hat{p}_1^* = p_1^*[b+a,\ b+a,\ \frac{b+3a}{2}]^T \tag{105}$$

If there is no mechanically applied loading, i.e $p_0 = [0,\ 0,\ 0]^T$, then equation (104) can be expressed as

$$G_0 = \frac{\pi b(b-a)}{8} p_1^{*T} L^{-1} \hat{p}_1^* \tag{106}$$

In this section, a solution as well as the method leading to the solution for the crack of a thermo-mechanically loaded anisotropic medium was presented in detail. And one can see that the general solution given here lays the foundation for the study of the branched delamination phenomena.

Chapter III

Green's Functions for Dislocations in Bimaterials

Due to the introduction of a dislocation into either one of the elastic bimaterial media under thermal loading, a temperature discontinuity (also called heat vortex[13]) may be induced across the cut plane by which a conventional (or mechanical) dislocation is formulated (Fig.3.1).

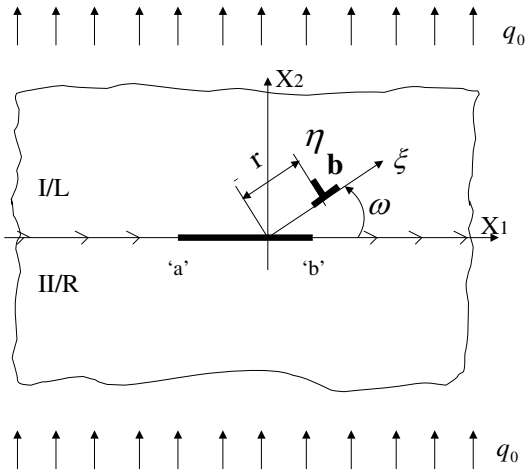

Fig.3.1 A thermo-elastic dislocation in a dissimilar anisotropic bimedium

This concept of heat vortex first appeared in the literature several decades ago and has been studied by many authors. But most of the functions of displacement and stress fields due to the heat vortex can hardly be directly extended to the dissimilar anisotropic media. To offset this difficulty, mixed terms are introduced in the expressions for displacement and stress functions.

For the dissimilar anisotropic bimaterial media, the functions of the heat vortex may be assumed as

$$T_{\mathrm{I}}^{d} = 2\ \mathrm{Re}[q_{0\tau}\log(z_\tau - z_{\tau 0}) + q_{1\tau}\log(z_\tau - \overline{z}_{\tau 0})] \tag{107}$$

for the medium in the upper space, i.e. z $\in L$;

$$T_{\mathrm{II}}^{d} = 2\ \mathrm{Re}[q_{2\tau}\log(z_\tau - z_{\tau 0})] \tag{108}$$

for the medium in the lower space, i.e. z $\in R$.

The corresponding heat flux h_2 can then be expressed as

$$h_{2\mathrm{I}}^{d} = 2\ k_{\mathrm{I}}\mathrm{Im}[\frac{q_{0\tau}}{z_\tau - z_{\tau 0}} + \frac{q_{1\tau}}{z_\tau - \overline{z}_{\tau 0}}],\ \ \mathrm{z} \in L \tag{109}$$

$$h_{2\mathrm{II}}^{d} = 2\ k_{\mathrm{II}}\mathrm{Im}[\frac{q_{2\tau}}{z_\tau - z_{\tau 0}}],\ \ \mathrm{z} \in R \tag{110}$$

where,

$$q_{0\tau} = \frac{T}{4\pi \mathrm{i}} \tag{111}$$

$q_{1\tau}$ and $q_{2\tau}$ are constants to be determined by the conditions along the interface.

The displacement and stress functions may then take the form:

$$\mathbf{u}_{\mathrm{I}}^{d} = 2\mathrm{Re}[A_{\mathrm{I}} \ll \log(z_\alpha - z_{\mathrm{d}0}) \gg q_{\mathrm{d}0}] + \sum_{k=1}^{3} A_{\mathrm{I}} \ll \log(z_\alpha - \overline{z}_{\mathrm{d}0\mathrm{k}}) \gg q_{1k}]$$
$$+ 2\mathrm{Re}[A_{\mathrm{I}} \ll (\log(z_\alpha - z_{\tau 0}) - 1)(z_\alpha - z_{\tau 0}) \gg q_{1\mathrm{d}\tau}]$$
$$+ 2\ \mathrm{Re}[C_{\mathrm{I}}(q_{0\tau}(\log(z_\tau - z_{\tau 0}) - 1)(z_\tau - z_{\tau 0})$$
$$+ q_{1\tau}(\log(z_\tau - \overline{z}_{\tau 0}) - 1)(z_\tau - \overline{z}_{\tau 0}))] \tag{112}$$

$$\phi_{\mathrm{I}}^{d} = 2\mathrm{Re}[B_{\mathrm{I}} \ll \log(z_\alpha - z_{\mathrm{d}0}) \gg q_{\mathrm{d}0}] + 2\mathrm{Re}[\sum_{k=1}^{3} B_{\mathrm{I}} \ll \log(z_\alpha - \overline{z}_{\mathrm{d}0\mathrm{k}}) \gg q_{1k}]$$
$$+ 2\mathrm{Re}[B_{\mathrm{I}} \ll (\log(z_\alpha - z_{\tau 0}) - 1)(z_\alpha - z_{\tau 0}) \gg q_{1\mathrm{d}\tau}]$$
$$+ 2\ \mathrm{Re}[D_{\mathrm{I}}(q_{0\tau}(\log(z_\tau - z_{\tau 0}) - 1)(z_\tau - z_{\tau 0})$$
$$+ q_{1\tau}(\log(z_\tau - \overline{z}_{\tau 0}) - 1)(z_\tau - \overline{z}_{\tau 0})] \tag{113}$$

for the upper half-space($x_2 > 0$), and

$$\mathbf{u}_{\mathrm{II}}^{d} = 2\mathrm{Re}[\sum_{k=1}^{3} A_{\mathrm{II}} \ll \log(z_\alpha - z_{\mathrm{d}0k}) \gg q_{2k}]$$
$$+ 2\mathrm{Re}[A_{\mathrm{II}} \ll (\log(z_\alpha - \bar{z}_{\tau 0}) - 1)(z_\alpha - \bar{z}_{\tau 0}) \gg q_{2\mathrm{d}\tau}]$$
$$+ 2\ \mathrm{Re}[C_{\mathrm{II}}(\log(z_\tau - z_{\tau 0}) - 1)(z_\tau - z_{\tau 0})q_{2\tau}] \tag{114}$$

$$\phi_{\mathrm{II}}^{d} = 2\mathrm{Re}[\sum_{k=1}^{3} B_{\mathrm{II}} \ll \log(z_\alpha - z_{\mathrm{d}0k}) \gg q_{2k}]$$
$$+ 2\mathrm{Re}[B_{\mathrm{II}} \ll (\log(z_\alpha - \bar{z}_{\tau 0}) - 1)(z_\alpha - \bar{z}_{\tau 0}) \gg q_{2\mathrm{d}\tau}]$$
$$+ 2\ \mathrm{Re}[D_{\mathrm{II}}(\log(z_\tau - z_{\tau 0}) - 1)(z_\tau - z_{\tau 0})q_{2\tau}] \tag{115}$$

for the lower half-space ($x_2 < 0$). Where [33]

$$q_{\mathrm{d}0} = \frac{1}{2\pi \mathrm{i}} B_{\mathrm{I}}^{T} \mathbf{b} \tag{116}$$

We may need to point out that in the term $\ll$ ($\log(z_\alpha - z_{\tau 0}) - 1)(z_\alpha - z_{\tau 0}) \gg$ and $\ll$ ($\log(z_\alpha - \bar{z}_{\tau 0}) - 1)(z_\alpha - \bar{z}_{\tau 0}) \gg$, the variable z_α and $z_{\tau 0}$ interacts. These mixed terms were introduced to reflect the interaction between the heat vortex (represented by $z_{\tau 0}$) and the conventional dislocation (represented by z_α) due to the mismatch of the properties of the upper and lower medium. This consideration plays a very important role to ensure the continuity of the displacements and tractions along the interface of the dissimilar bimaterials.

Substituting equations (108), (110), (113), and (115) into the boundary conditions along the interface,

$$
\begin{aligned}
&T^d_{\mathrm{I}}(x_1, x_2 = 0^+) = T^d_{\mathrm{II}}(x_1, x_2 = 0^-), \\
&h^d_{2\mathrm{I}}(x_1, x_2 = 0^+) = h^d_{2\mathrm{II}}(x_1, x_2 = 0^-), \\
&\mathbf{u}^d_{\mathrm{I}}(x_1, x_2 = 0^+) = \mathbf{u}^d_{\mathrm{II}}(x_1, x_2 = 0^-), \\
&\phi'^d_{\mathrm{I}}(x_1, x_2 = 0^+) = \phi'^d_{\mathrm{II}}(x_1, x_2 = 0^-)
\end{aligned}
\tag{117}
$$

one can obtain (Appendix C)

$$
\begin{aligned}
q_{1\tau} &= \frac{k_{\rm I} - k_{\rm II}}{k_{\rm I} + k_{\rm II}}\, \overline{q}_{0\tau}, \\
q_{2\tau} &= \frac{2k_{\rm I}}{k_{\rm I} + k_{\rm II}} q_{0\tau} \\
B_{\rm I} q_{1k} &= N(-N^{-1} + 2L_{\rm I}^{-1})\overline{B}_{\rm I} I_k \overline{q}_{\rm d0}, \\
B_{\rm II} q_{2k} &= 2\ \overline{N} L_{\rm I}^{-1} B_{\rm I} I_k q_{\rm d0}, \\
B_{\rm I} q_{1{\rm d}\tau} &= N[\overline{M}_{\rm II}^{-1} D + {\rm i}C] q_{0\tau}, \\
B_{\rm II} q_{2{\rm d}\tau} &= -\overline{N}[\overline{M}_{\rm I}^{-1}\overline{D} + {\rm i}\overline{C}] q_{0\tau}
\end{aligned} \tag{118}
$$

The heat flux and stress fields can then be readily calculated. Here recorded are the quantities for the medium in the upper space,

$$
\begin{aligned}
h_{1{\rm I}}^{td} &= -2\ k_{\rm I} {\rm Im}[\frac{q_{0\tau}}{z_\tau - z_{\tau 0}}\tau + \frac{q_{1\tau}}{z_\tau - \overline{z}_{\tau 0}}\tau], \\
h_{2{\rm I}}^{td} &= 2\ k_{\rm I} {\rm Im}[\frac{q_{0\tau}}{z_\tau - z_{\tau 0}} + \frac{q_{1\tau}}{z_\tau - \overline{z}_{\tau 0}}]
\end{aligned} \tag{119}
$$

and

$$
\begin{aligned}
[\sigma_{11}, \sigma_{21}, \sigma_{31}]_{\rm I1}^{{\rm td}T} = -2{\rm Re} \sum_{k=1}^{3} [B_{\rm I} \ll \frac{p_\alpha}{z_\alpha - z_{d0k}} \gg I_k q_0 + B_{\rm I} \ll \frac{p_\alpha}{z_\alpha - \overline{z}_{d0k}} \gg q_{1k}] \\
+ 2{\rm Re}[B_{\rm I} \ll p_\alpha {\rm log}(z_\alpha - z_{\tau 0}) \gg q_{1d\tau} \\
+ D_{\rm I}(\tau {\rm log}(z_\tau - z_{\tau 0}) q_{0\tau} + \tau {\rm log}(z_\tau - \overline{z}_{\tau 0}) q_{1\tau})]
\end{aligned} \tag{120}
$$

$$[\sigma_{12},\sigma_{22},\sigma_{32}]_{\mathrm{I2}}^{\mathrm{td}T}=2\mathrm{Re}\sum_{k=1}^{3}[B_{\mathrm{I}}\ll\frac{1}{z_{\alpha}-z_{d0k}}\gg I_{k}q_{0}+B_{\mathrm{I}}\ll\frac{1}{z_{\alpha}-\overline{z}_{d0k}}\gg q_{1k}]$$
$$+2\mathrm{Re}[B_{\mathrm{I}}\ll\log(z_{\alpha}-z_{\tau0})\gg q_{1d\tau}$$
$$+D_{\mathrm{I}}(\log(z_{\tau}-z_{\tau0})q_{0\tau}+\log(z_{\tau}-\overline{z}_{\tau0})q_{1\tau})] \tag{121}$$

The heat flux and traction along the interface are, respectively,

$$h_{2}^{d}(x_{1})=\frac{4k_{\mathrm{I}}k_{\mathrm{II}}}{k_{\mathrm{I}}+k_{\mathrm{II}}}\mathrm{Im}[\frac{q_{0\tau}}{x_{1}-z_{\tau0}}] \tag{122}$$

and

$$\mathbf{t}_{\mathrm{d}\tau}=[\sigma_{12},\sigma_{22},\sigma_{32}]_{\mathrm{d}\tau}^{\mathrm{T}}$$
$$=2\mathrm{Re}\{\sum_{k=1}^{3}[\frac{2}{x_{1}-z_{\mathrm{d0k}}}\ \overline{N}L_{\mathrm{I}}^{-1}\ B_{\mathrm{I}}\mathrm{I}_{k}q_{\mathrm{d0}}]-[\log(x_{1}-\overline{z}_{\tau0})\overline{N}(\overline{M}_{\mathrm{I}}^{-1}\overline{D}+\mathrm{i}\overline{C})$$
$$-\log(x_{1}-z_{\tau0})\frac{2k_{\mathrm{I}}}{k_{\mathrm{I}}+k_{\mathrm{II}}}D_{\mathrm{II}}]q_{0\tau}\} \tag{123}$$

$$\mathbf{t}_{\mathrm{d}\tau}=2\mathrm{Re}\{\sum_{k=1}^{3}[\frac{2}{x_{1}-z_{\mathrm{d0k}}}\ \overline{N}L_{\mathrm{I}}^{-1}\ B_{\mathrm{I}}\mathrm{I}_{k}q_{\mathrm{d0}}]$$
$$+\log(x_{1}-z_{\tau0})[N(M_{\mathrm{I}}^{-1}D-\mathrm{i}C)+\frac{2k_{\mathrm{I}}}{k_{\mathrm{I}}+k_{\mathrm{II}}}D_{\mathrm{II}}]q_{0\tau}\} \tag{124}$$

where the relationships $\mathrm{Re}[1/(x_{1}-z_{d0k})]=\mathrm{Re}[1/(x_{1}-\overline{z}_{d0k})]$ and $\mathrm{Re}[\log(x_{1}-z_{\tau0}]=\mathrm{Re}[\log(x_{1}-\overline{z}_{\tau0}]$ were used.

Chapter IV

Thermo-elastic Interaction between the Interface Delamination and the Dislocations

Replacing the $h_0(x_1)$ of equation () with $-h_2^d(x_1)$ of equation (122), one can obtain a closed form solution to the interaction temperature potential function, and it reads

$$\theta'_{\text{int}}(z) = \frac{T}{4\pi}[\, y(z, z_{\tau 0}) + y(z, \bar{z}_{\tau 0})] \tag{125}$$

where,

$$y(z, z_{\tau 0}) = \frac{1}{z - z_{\tau 0}}[1 - \mathbf{x}(z)\, \mathbf{x}^{-1}(z_{\tau 0})] - \mathbf{x}(z) \tag{126}$$

Integrating equation (125) and dropping some constants yields

$$\theta_{\text{int}}(z) = \frac{T}{4\pi}[\, \widetilde{y}(z, z_{\tau 0}) + \widetilde{y}(z, \bar{z}_{\tau 0})] \tag{127}$$

with

$$\widetilde{y}(z, z_{\tau 0}) = \log[\frac{\mathbf{x}^{-1}(z) + \mathbf{x}^{-1}(z_{\tau 0}) + (z_{\tau 0} - \frac{a+b}{2})(z - z_{\tau 0})\mathbf{x}(z_{\tau 0})}{z - \frac{a+b}{2} + \sqrt{(z-a)(z-b)}}] \tag{128}$$

It can be seen that the interaction thermal potential function is not singular at the point $z = z_{\tau^0}$. Comparing with the contribution from the term $\frac{1}{z - z_{\tau 0}}$ for

simulating the onset of the interface delamination branching, the influence of the function $\theta_{\rm int}(z)$ on the interaction stress functions, which can be obtained by replacing $p(x_1)$ of equation (68) with - $\mathbf{t}_{{\rm d}\tau}$ of equation (124), can be ignored .

Therefore, the interaction stress functions can be expressed as

$$\Phi^{'}_{\rm int}(z) = \sum_{k=1}^{3}[\mathbf{v}\mathbf{Y}_k(z, z_{\rm d0k}; \epsilon)\ \mathbf{v}^{-1}(N + \overline{N})^{-1}\mathcal{A}_k - \mathbf{v}\mathbf{Y}_k(z, \bar{z}_{\rm d0k}; \epsilon) \mathbf{v}^{-1}(N + \overline{N})^{-1}\overline{\mathcal{A}}_k\ ]\mathbf{b} \tag{129}$$

where

$$\mathbf{Y}_k(z, z_{\rm d0k}; \epsilon) = \ll \frac{1}{z - z_{\rm d0k}} \gg [{\rm I} - \sqrt{\frac{(z_{\rm d0k} - a)(z_{\rm d0k} - b)}{(z - a)(z - b)}}\Delta(z; \epsilon)\Delta^{-1}(z_{\rm d0k}; \epsilon)] - \frac{\Delta(z; \epsilon)}{\sqrt{(z - a)(z - b)}},$$
$$\mathcal{A}_k = \overline{N}L_{\rm I}^{-1}B_{\rm I}I_kB_{\rm I}^T/\pi, \tag{130}$$

and the following notation is employed

$$\frac{\Delta(z; \epsilon)}{\sqrt{(z - a)(z - b)}} = {\rm diag}[(z_1 - b)^{-\frac{1}{2}+i\epsilon}(z_1 - a)^{-\frac{1}{2}-i\epsilon}, (z_2 - b)^{-\frac{1}{2}-i\epsilon}(z_2 - a)^{-\frac{1}{2}+i\epsilon},\ (z_3 - b)^{-\frac{1}{2}}(z_3 - a)^{-\frac{1}{2}}] \tag{131}$$

By employing *L'Hôpital*'s rule, one can easily show that the $y(z, z_{\tau 0})$ and $\mathbf{Y}_k(z, z_{\rm d0k}; \epsilon)$ are not singular when $z \to z_\tau$ and $z \to z_{\rm d0k}$, respectively.

The heat flux and stress fields induced by the interaction for the upper

medium can then be written, respectively as

$$h_1^{\text{int}} = -2\frac{k_{\text{I}}k_{\text{II}}}{k_{\text{I}}+k_{\text{II}}}\text{Re}[\tau\theta_{\text{int}}^{'}(z)]$$
$$h_2^{\text{int}} = 2\frac{k_{\text{I}}k_{\text{II}}}{k_{\text{I}}+k_{\text{II}}}\text{Re}[\theta_{\text{int}}^{'}(z)] \tag{132}$$

and

$$[\sigma_{11},\sigma_{21},\sigma_{31}]_{\text{I}}^{\text{int}T} = -2\text{Re}[\text{i}N\text{v} \ll p_\alpha \gg \text{v}^{-1}\Phi_{\text{int}}^{'}(z) - \text{i}\overline{D_{\text{int}}}\tau\theta_{\text{int}}(z)],$$
$$[\sigma_{12},\sigma_{22},\sigma_{32}]_{\text{I}}^{\text{int}T} = 2\text{Re}[\text{i}N\Phi_{\text{int}}^{'}(z) - \text{i}\overline{D_{\text{int}}}\theta_{\text{int}}(z)] \tag{133}$$

where, the constant vector $\overline{D_{\text{int}}} = \overline{D_c}$.

Chapter V

Interface Delamination Branching of Dissimilar Anisotropic Bimaterial Media

Let the main delamination be located at the $a < x_1 < b, x_2 = 0$ of a coordinate system (x_1, x_2, x_3). This delamination is assumed to branch into $x_2 > 0$ (or $x_2 < 0$) at an angle $\theta = \omega$ shown in Fig. 5.1.

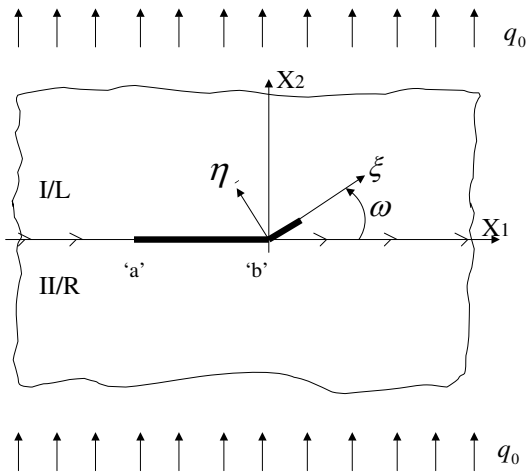

Fig.5.1 A branched thermo-elastic interface delamination in a dissimilar anisotropic bimaterial medium

In Fig. 5.1, a new coordinate system (ξ, η, x_3) was introduced for the sake of convenient derivation. Similarly to the conditions for the main crack, the

boundary conditions for this branched portion may be written in this new coordinate system as

$$
\begin{aligned}
&h_2(\xi, 0^+) = -h(\xi), \\
&h_2(\xi, 0^-) = -h(\xi), \\
&[\sigma_{\xi\eta}(\xi, 0^+), \sigma_{\eta\eta}(\xi, 0^+), \sigma_{3\eta}(\xi, 0^+)]^T = -p(\xi), \\
&[\sigma_{\xi\eta}(\xi, 0^-), \sigma_{\eta\eta}(\xi, 0^-), \sigma_{3\eta}(\xi, 0^-)]^T = -p(\xi)
\end{aligned} \tag{134}
$$

If the applied thermomechanical loading at infinity is constant, then one has the following conditions along the cut $\eta = 0$

$$
h(\xi) = h_0 \cos(\omega),
$$

$$
p(\xi) = \begin{vmatrix} \cos(2\omega), & \frac{1}{2}\sin(2\omega) & 0 \\ -\sin(2\omega), & \cos^2(\omega) & 0 \\ 0, & 0 & \cos(\omega) \end{vmatrix} p_0 \tag{135}
$$

where the vector $p_0 = [\sigma_{12}, \sigma_{22}, \sigma_{32}]^T$ is the constant applied traction at infinity.

Now let us consider the total heat flux and traction at any point on the plane $\eta = 0$, i.e. $\theta = \omega$ in the cylindrical coordinate system $(\mathrm{r}, \theta, x_3)$, the

superposition leads to:

$$h_2^{\mathrm{tot}}(\xi,0) = h_\theta^{\mathrm{c}}(\mathrm{r},\omega) + h_\theta^{\mathrm{int}}(\mathrm{r},\omega) + h_\theta^{\mathrm{td}}(\mathrm{r},\omega)$$

$$\mathbf{t}^{\mathrm{tot}}(\xi,0) = \mathbf{t}_\theta^{\mathrm{c}}(\mathrm{r},\omega) + \mathbf{t}_\theta^{\mathrm{int}}(\mathrm{r},\omega) + \mathbf{t}_\theta^{\mathrm{td}}(\mathrm{r},\omega) \tag{136}$$

where the superscript 'c' and 'td' denote the corresponding fields induced by the main delamination and the thermal-mechanical dislocations, respectively; 'int' denotes the fields induced by the interaction between the delamination and the dislocation; 'tot' is the summation from all contributions.

It would be more convenient for calculation if the terms on the right side of the equations (136) expressed in the coordinate system (x_1, x_2, x_3) could be transformed into the corresponding quantities in the coordinate system $(\mathrm{r}, \theta, x_3)$ or the system (ξ, η, x_3). Following is the transformation relationship

$$h = h_2\cos(\omega) - h_1\sin(\omega)$$

$$\mathbf{t} = \Omega_2(\omega)[\sigma_{12}, \sigma_{22}, \sigma_{32}]^T - \Omega_1(\omega)[\sigma_{11}, \sigma_{21}, \sigma_{31}]^T \tag{137}$$

where

$$\Omega_2(\theta) = \begin{vmatrix} \cos^2(\theta) & \frac{1}{2}\sin(2\theta) & 0 \\ -\frac{1}{2}\sin(2\theta) & \cos^2(\theta) & 0 \\ 0 & 0 & \cos(\theta) \end{vmatrix} \tag{138}$$

$$\Omega_1(\theta) = \begin{vmatrix} \frac{1}{2}\sin(2\theta) & \sin^2(\theta) & 0 \\ -\sin^2(\theta) & \frac{1}{2}\sin(2\theta) & 0 \\ 0 & 0 & \sin(\theta) \end{vmatrix} \tag{139}$$

The σ_{i1} and σ_{i2} in equation (137) are stresses which are measured in the system (x_1, x_2, x_3) and defined by equations (13) and (14); h_1 and h_2 are heat fluxes measured in the system (x_1, x_2, x_3) and defined by equations (17) and (18).

Using the above transformation, each term of the right hand side of equation (136) can be easily expressed in terms of the temperature potential functions and stress functions obtained in the previous sections.

Denoting

$$\mu = \cos(\omega) + \tau \sin(\omega) \tag{140}$$

and

$$\zeta = \cos(\omega) + p_\alpha \sin(\omega), \tag{141}$$

then

$$z_\tau = \mathrm{r}\mu, \quad z_{\tau 0} = \mathrm{r}_0\mu, \quad z_\alpha = \mathrm{r}\zeta, \quad z_{\alpha 0} = \mathrm{r}_0\zeta. \tag{142}$$

One can relate the heat flux and tractions in the cylindrical coordinate system $(\mathrm{r}, \theta, x_3)$ to the those in the Cartesian coordinate system (x_1, x_2, x_3).

The heat fluxes read as

$$h_\theta^{\rm c}({\rm r},\omega) = h_2^{\rm c}({\rm r}\mu)\cos(\omega) - h_1^{\rm c}({\rm r}\mu)\sin(\omega),$$

$$h_\theta^{\rm int}({\rm r},\omega) = h_2^{\rm int}({\rm r}\mu)\cos(\omega) - h_1^{\rm int}({\rm r}\mu)\sin(\omega),$$

$$h_\theta^{\rm td}({\rm r},\omega) = h_2^{\rm td}({\rm r}\mu)\cos(\omega) - h_1^{\rm td}({\rm r}\mu)\sin(\omega) \tag{143}$$

and the tractions are

$$\mathbf{t}_\theta^{\rm c}({\rm r},\omega) = \Omega_2(\omega)[\sigma_{12},\sigma_{22},\sigma_{32}]_c^T - \Omega_1(\omega)[\sigma_{11},\sigma_{21},\sigma_{31}]_c^T,$$

$$\mathbf{t}_\theta^{\rm int}({\rm r},\omega) = \Omega_2(\omega)[\sigma_{12},\sigma_{22},\sigma_{32}]_{\rm int}^T - \Omega_1(\omega)[\sigma_{11},\sigma_{21},\sigma_{31}]_{\rm int}^T$$

$$\mathbf{t}_\theta^{\rm td}({\rm r},\omega) = \Omega_2(\omega)[\sigma_{12},\sigma_{22},\sigma_{32}]_{\rm td}^T - \Omega_1(\omega)[\sigma_{11},\sigma_{21},\sigma_{31}]_{\rm td}^T \tag{144}$$

Without loss of generality, it can be assumed that the interface delamination branches into the upper medium. The branched portion of the delamination may be viewed as a continuous distribution of the heat vortex and conventional dislocations. If the densities of these dislocations are defined as

$$T_0({\rm r}_0) = -dT_0({\rm r}_0)/d{\rm r}_0,$$

$$\mathbf{b}({\rm r}_0) = -d\mathbf{b}({\rm r}_0)/d{\rm r}_0 \tag{145}$$

then the boundary condition(134) and equation (136) lead to a system of singular integral equations as

$$\frac{k_{\rm I}}{2\pi}\int_b^c \frac{T_0}{{\rm r}-{\rm r}_0}\,d{\rm r}_0 + \frac{k_{\rm I}}{2\pi}\int_b^c {\rm K}_t({\rm r},{\rm r}_0)T_0\,d{\rm r}_0 = h_0\cos(\omega) + h_\theta^c({\rm r},\omega), \tag{146}$$

where,

$$\mathrm{K}_t(\mathrm{r},\mathrm{r}_0) = -\frac{k_{\mathrm{I}}-k_{\mathrm{II}}}{k+k_{\mathrm{II}}}\mathrm{Re}[\frac{\mu}{\mathrm{r}\mu-\mathrm{r}_0\overline{\mu}}] + \frac{k_{\mathrm{II}}}{k_{\mathrm{I}}+k_{\mathrm{II}}}\mathrm{Re}[\frac{1}{\mathrm{r}-\mathrm{r}_0}(1- \sqrt{\frac{(\mathrm{r}_0\mu-a)(\mathrm{r}_0\mu-b)}{(\mathrm{r}\mu-a)(\mathrm{r}\mu-b)}}) + \frac{\mu}{\mathrm{r}\mu-\mathrm{r}_0\overline{\mu}}(1-\sqrt{\frac{(\mathrm{r}_0\overline{\mu}-a)(\mathrm{r}_0\overline{\mu}-b)}{(\mathrm{r}\mu-a)(\mathrm{r}\mu-b)}}) - \frac{2\mu}{\sqrt{(\mathrm{r}\mu-a)(\mathrm{r}\mu-b)}}] \tag{147}$$

$$h^c_\theta(\mathrm{r},\omega) = h_0\mathrm{Re}[\mu(1-\frac{\mathrm{r}\mu-(a+b)/2}{\sqrt{(\mathrm{r}\mu-a)(\mathrm{r}\mu-b)}})] \tag{148}$$

and

$$\frac{1}{\pi}\int_b^c \frac{\mathcal{A}_b(\omega)}{\mathrm{r}-\mathrm{r}_0}\mathbf{b}\; d\mathrm{r}_0 + \frac{1}{\pi}\int_b^c \mathrm{K}_b(\mathrm{r},\mathrm{r}_0)\mathbf{b}\; d\mathrm{r}_0 + \frac{1}{2\pi}\int_b^c \mathrm{K}_{bt}(\mathrm{r},\mathrm{r}_0)T_0\; d\mathrm{r}_0 = \Omega_2 p_0 + \mathbf{t}^c_\theta(\mathrm{r},\omega) \tag{149}$$

in which,

$$\mathcal{A}_b(\omega) = \mathrm{Im}[\Omega_2 B_{\mathrm{I}} \ll \frac{1}{\zeta} \gg B_{\mathrm{I}}^{-1} + \Omega_1 B_{\mathrm{I}} \ll \frac{p_\alpha}{\zeta} \gg B_{\mathrm{I}}^{-1}] \tag{150}$$

$$
\begin{aligned}
\mathrm{K}_b(\mathrm{r},\mathrm{r}_0) = \sum_{k=1}^{3} \mathrm{Im}[\Omega_2\ B_{\mathrm{I}} \ll \frac{1}{\mathrm{r}\zeta - \mathrm{r}_0\overline{\zeta}_0} \gg B_{\mathrm{I}}^{-1}(\mathrm{I} - 2NL_{\mathrm{I}}^{-1})\overline{B}_{\mathrm{I}}\mathrm{I}_k\overline{B}_{\mathrm{I}}^{T} \\
+ \Omega_1\ B_{\mathrm{I}} \ll \frac{p_\alpha}{\mathrm{r}\zeta - \mathrm{r}_0\overline{\zeta}_0} \gg B_{\mathrm{I}}^{-1}(\mathrm{I} - 2NL_{\mathrm{I}}^{-1})\overline{B}_{\mathrm{I}}\mathrm{I}_k\overline{B}_{\mathrm{I}}^{T} \\
- \frac{2}{\pi}\Omega_2 N(\mathrm{v}\mathbf{Y}_k(\mathrm{r}\zeta,\mathrm{r}_0\zeta_k;\epsilon)\mathrm{v}^{-1}(N+\overline{N})^{-1}\mathcal{A}_k \\
- \mathrm{v}\mathbf{Y}_k(\mathrm{r}\zeta,\mathrm{r}_0\overline{\zeta}_k;\epsilon)\mathrm{v}^{-1}(N+\overline{N})^{-1}\overline{\mathcal{A}}_k) \\
- \frac{2}{\pi}\Omega_1 N(\mathrm{v} \ll p_\alpha \gg \mathbf{Y}_k(\mathrm{r}\zeta,\mathrm{r}_0\zeta_k;\epsilon)\mathrm{v}^{-1}(N+\overline{N})^{-1}\mathcal{A}_k \\
- \mathrm{v} \ll p_\alpha \gg \mathbf{Y}_k(\mathrm{r}\zeta,\mathrm{r}_0\overline{\zeta}_k;\epsilon)\mathrm{v}^{-1}(N+\overline{N})^{-1}\overline{\mathcal{A}}_k), \qquad (151)
\end{aligned}
$$

$$
\begin{aligned}
\mathrm{K}_{bt}(\mathrm{r},\mathrm{r}_0) = \Omega_2\mathrm{Im}[B_{\mathrm{I}} \ll \log(\mathrm{r}\zeta - \mathrm{r}_0\mu \gg B_{\mathrm{I}}^{-1}N(\overline{M}_{\mathrm{II}}D + \mathrm{i}C) \\
+ D_{\mathrm{I}}(\log(\mathrm{r}\mu - \mathrm{r}_0\mu) - \frac{k_{\mathrm{I}} - k_{\mathrm{II}}}{k_{\mathrm{I}} + k_{\mathrm{II}}}\log(\mathrm{r}\mu - \mathrm{r}_0\overline{\mu})) \\
+ \overline{D}_{\mathrm{int}}(\widetilde{y}(\mathrm{r}\mu,\mathrm{r}_0\mu) + \widetilde{y}(\mathrm{r}\mu,\mathrm{r}_0\overline{\mu}))] \\
+ \Omega_1\mathrm{Im}[B_{\mathrm{I}} \ll p_\alpha\log(\mathrm{r}\zeta - \mathrm{r}_0\mu \gg B_{\mathrm{I}}^{-1}N(\overline{M}_{\mathrm{II}}D + \mathrm{i}C) \\
+ D_{\mathrm{I}}(\log(\mathrm{r}\mu - \mathrm{r}_0\mu) - \frac{k_{\mathrm{I}} - k_{\mathrm{II}}}{k_{\mathrm{I}} + k_{\mathrm{II}}}\log(\mathrm{r}\mu - \mathrm{r}_0\overline{\mu}))\tau \\
+ \overline{D}_{\mathrm{int}}(\widetilde{y}(\mathrm{r}\mu,\mathrm{r}_0\mu) + \widetilde{y}(\mathrm{r}\mu,\mathrm{r}_0\overline{\mu}))\tau] \qquad (152)
\end{aligned}
$$

In the above equations,

$$
\begin{aligned}
\widetilde{\mathrm{I}}_1 &= \mathrm{diag}[0,1,1], \\
\widetilde{\mathrm{I}}_2 &= \mathrm{diag}[1,0,1], \\
\widetilde{\mathrm{I}}_3 &= \mathrm{diag}[1,1,0] \qquad (153)
\end{aligned}
$$

were introduced.

Next, let

$$\mathrm{r} = \frac{(1+x)l}{2}, \quad \mathrm{r}_0 = \frac{(1+t)l}{2}, \quad l = c - b \tag{154}$$

where, $|x| < 1$ and $|t| < 1$. Then equation (146) and (149) can be rewritten as

$$\frac{k_{\mathrm{I}}}{2\pi}\int_{-1}^{1}\frac{T_0}{x-t}\,dt + \frac{k_{\mathrm{I}}}{2\pi}\int_{-1}^{1}\widetilde{\mathrm{K}}_t(x,t)T_0\,dt = h_0\cos(\omega) + h_\theta^c(x,\omega) \tag{155}$$

$$\begin{aligned}\frac{1}{\pi}\int_{-1}^{1}\frac{\mathcal{A}_b(\omega)}{x-t}\mathbf{b}\,dt + \frac{1}{\pi}\int_{-1}^{1}\widetilde{\mathrm{K}}_b(x,t)\mathbf{b}\,dt + \frac{1}{2\pi}\int_{-1}^{1}\widetilde{\mathrm{K}}_{bt}(x,t)T_0\,dt \\ = \Omega_2 p_0 + \mathbf{t}_\theta^c(x,\omega)\end{aligned} \tag{156}$$

Where, $\widetilde{\mathrm{K}}_t(x,t), \widetilde{\mathrm{K}}_b(x,t)$ and $\widetilde{\mathrm{K}}_{bt}(x,t)$ are obtained by substituting (154) in $\mathrm{K}_t(\mathrm{r},\mathrm{r}_0)$, $\mathrm{K}_b(\mathrm{r},\mathrm{r}_0)$ and $\mathrm{K}_{bt}(\mathrm{r},\mathrm{r}_0)$, respectively.

It can be easily seen that this system of singular equations (155) and (156) involves two unknowns, namely T_0 and $\mathbf{b}$, which are coupled through the term $\widetilde{\mathrm{K}}_{bt}$ in (156). This coupling comes from the interaction between the heat vortex and the conventional mechanical dislocation.

One can let [36,37]

$$\begin{aligned}T_0 &= w_1(t)\mathcal{T}(t), \quad w_1(t) = (1+t)^{-s_1}(1-t)^{\frac{1}{2}} \\ \mathbf{b}(t) &= w_2(t)b(t), \quad w_2(t) = (1+t)^{-s_2}/(1-t)^{\frac{1}{2}}\end{aligned} \tag{157}$$

Since the heat vortex density at both ends of branched potion of the crack usually is assumed to be bounded and the singularity at the intersection point of the main delamination and the branched portion is to be of order less then $\frac{1}{2}$, then one can have $s_1 = -1/2$ and $s_2 = 1/2$ [32]. Therefore, $(156)_1$ can be solved by using the Gauss-Chebvshev integration. Once the solution for T_0 is obtained, substitution into $(156)_2$ and using the Gauss-Jacobi integration formulas leads to the whole system of equations.

By a similar token as in [32], the numerical schemes for solving equations (155) and (156) can be, respectively, written as:

$$\sum_{i=1}^{\mathrm{n}} \frac{1-t_i^2}{n+1}\mathcal{T}(t_i)[\frac{1}{t_i-x_k} - \widetilde{\mathrm{K}}_t(t_i,x_k)] = \frac{2}{k_I}[h_0\cos(\omega) + h_\theta^c(x_k,\omega)],$$
$$t_i = \cos(\frac{i\pi}{n+1},) \quad (i=1....n); \qquad x_k = \cos(\frac{\pi}{2}\frac{2k-1}{n+1}), \quad (k=1....n+1) \tag{158}$$

and

$$\sum_{i=1}^{n} \frac{1}{n}[\frac{\mathcal{A}_b(\omega)}{t_i-x_k} - \widetilde{\mathrm{K}}_b(t_i,x_k)]b(t_i) = -\Omega_2 p_0 - \mathbf{t}_\theta^c(x_k,\omega) + \frac{1}{2\pi}\int_{-1}^{1} \widetilde{\mathrm{K}}_{bt}(x_k,t)T_0\ dt,$$
$$\sum_{i}^{n} \frac{\pi}{n} b(t_i) = \Delta u,$$
$$t_i = \cos(\pi\frac{2i-1}{2n}), \quad (i=1....n); \qquad x_k = \cos(\frac{\pi k}{n}), \quad (k=1....n-1) \tag{159}$$

where the second equation, i.e. $(159)_2$, comes from the condition $\int_{-1}^{1}\mathbf{b}(t)\ dt = \Delta u$, which satisfies the continuity condition of displacement at the intersection point between the main delamination and the branched portion. For

an approximation, one may take $\int_{-1}^{1} \mathbf{b}(t)\ dt \approx 0$. But for a more accurate computation , one would use equation (76) to evaluate the Δu by letting $\mathrm{a} = -(\mathrm{L} + l\cos(\omega))/2$, $\mathrm{b} = (\mathrm{L} + l\cos(\omega))/2$, and $x_1 = \mathrm{L}/2$, where 'l' denotes the length of the branched portion of the crack and 'L' the length of the main crack.

The integration of the third term on the right hand side of $(159)_1$ was performed by using Simpson's rule. Since the nodes used in (158) and (159) are different, the polynomial interpolations were also used in order to get the values of $\widetilde{\mathrm{K}}_{bt}(x,t)$ and $T_0(t)$ from the nodes in (158) for those values needed for the nodes in $(159)_1$.

The conventional stress intensity factors (**SIF**)s at the branched crack tip may be defined as

$$\mathbf{K} = [\mathbf{K}_{\mathrm{II}}, \mathbf{K}_{\mathrm{I}}, \mathbf{K}_{\mathrm{III}}]^T = \lim_{\mathrm{r}\to\mathrm{l}^+} \sqrt{2\pi(\mathrm{r}-\mathrm{l})}\mathbf{t}^{\mathrm{tot}}(\mathrm{r},\omega) \tag{160}$$

Using the technique given by Muskhelishvili (1953), the **SIF**s can be evaluated as

$$\begin{aligned}\mathbf{K} &= \lim_{\mathrm{r}\to\mathrm{l}^+} \sqrt{2\pi(\mathrm{r}-\mathrm{l})}[\frac{1}{\pi}\int_{-1}^{1} \frac{\mathcal{A}_b(\omega)}{x-t} w_2(t)b(t)dt + \frac{1}{2\pi}\int_{-1}^{1} \widetilde{\mathrm{K}}_{bt}(x,t)w_1(t)\mathcal{T}(t)dt] \\ &= \sqrt{\frac{\pi l}{2}}\mathcal{A}(\omega)\Omega_0(\omega)b(1)\end{aligned} \tag{161}$$

where an elementary relationship $\lim_{x\to 1^+} \sqrt{(x-1)}\log(x-1) \to 0$ is employed

and

$$\Omega_0(\omega) = \begin{vmatrix} \cos(\omega) & \sin(\omega) & 0 \\ -\sin(\omega) & \cos(\omega) & 0 \\ 0 & 0 & 1 \end{vmatrix} \tag{162}$$

Once the onset of the branching of an interface delamination happens, this delamination usually propagates in one of the medium of the bimaterials. Therefore, the energy release rate can be approximated as stated in [38] by

$$\begin{aligned} \mathcal{G}(\omega) &= \frac{1}{2}\mathbf{K}^T \widetilde{L}^{-1}\ \mathbf{K}, \\ \widetilde{L} &= \Omega_0^T(\omega)\ L\ \Omega_0(\omega) \end{aligned} \tag{163}$$

where, 'L' is the bi-material property matrix.

From expressions (161) and (163), it is not difficult to figure out that the stress intensity factors and the energy release rate of a branched interface delamination usually are functions of the branching angle ω. It could also be seen that the stress intensity factors and the energy release rate may often be non-linear functions of the branching angle ω. Therefore, there probably exist angles which could maximize the stress intensity factors and the energy release rate for a given bimaterial structure. These angles may or may not be identical as will be shown in the next chapter.

Chapter VI

Numerical Simulation

In this chapter, the results of the numerical simulation from the preceding theory of interface delamination branching will be presented. As discussed in the introduction, the issue of anisotropic crack branching behavior has not been adequately addressed in literature, especially with thermal loading. Here we first consider the cases of delamination branching behavior without thermal loading. Sections 6.1 and 6.2 are devoted to this case. To do this, only the (156) needs to be solved and set to zero all those terms which are related to the vortex dislocation in (156). Secondly, we will study the cases in which thermal loading is applied. This study will be discussed in detail in sections 6.3 and 6.4.

6.1 Delamination Branching in Monolithic Anisotropic Solids

As the first application of the formulas developed in the current work, we re-investigate the crack branching in monoclinic anisotropic media. This problem has been studied in the literature, but incompletely as mentioned in Chapter I. Here in our study of this problem as a special application of our powerful method, i.e. to solve this problem one only needs to assume a

fictitious interface between the upper and lower half plane of the media with identical materials (monolithic anisotropic), one has (72)

$$L_1 = L_2 = L,$$

$$S_1 = S_2 = S \tag{164}$$

which implies

$$D = 2\ L_1 = 2\ L_2 = 2\ L, \quad W = \mathbf{0},$$

$$\beta = 0 \qquad \epsilon = 0 \tag{165}$$

The constant matrix in (70) would then be taken as an identity matrix and the singular equation (156) can be solved.

This monolithic case was first studied in [26] and later on in [27]. The results in [27] look more detailed than those in [26]. For the sake of easy of comparison, we choose the orthotropic material as the authors of [26] and [27], i.e. let the elastic constants be

$$\nu_{12} = -s_{12}/s_{11} = 0.25, \qquad s_{66} = 2\ (s_{11} - s_{12}) \tag{166}$$

and the degree of anisotropy be defined as s_{11}/s_{22} or s_{22}/s_{11}. Here, ν_{12} is the Poisson's ratio and s_{ij} $(i, j = 1, 2, 3)$ are the martial compliance coefficients. An infinitesimal crack branch is considered with the ratio $l/L = 0.001$, where 'l' is the length of the branched portion of the crack and 'L' is the half length

of the main crack. For this case, the main crack is assumed lying along the x_1 axis, which is the weaker material axis ($s_{11}/s_{22} > 1$). As used in literature like [23, 26, 27, etc.], the degree of anisotropy ranging from 1 to 10 is physically acceptable.

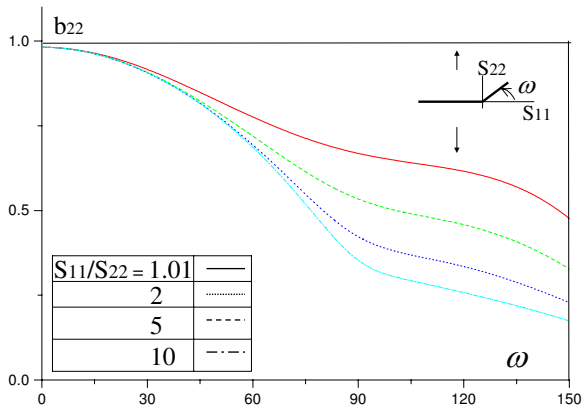

Fig.6.1 Dislocation Density at the branched crack tip
with the main crack lying along the weaker material axis

Plotted in Fig. 6.1 is the normalized dislocation density $\mathbf{b}_{22}$ at the branched crack tip in the x_2 direction of the (x_1, x_2, x_3) coordinate system. Figs. 6.2 -

6.3 show the mode I and mode II stress intensity factors versus various degrees of anisotropy. It can be easily seen that the curves in the Fig. 6.1 are strikingly similar to those in Fig. 2 of [26] and close to those in Fig. 6 of [27]. Though the variation of the K_I and K_{II} with respect to the branching angles in our Fig.6.2 and Fig. 6.3 follows the same pattern as those in [26] and [27], the values differ from those in [26] and [27], especially at large branching angles. In Fig. 6.2, one can see that K_I is negative when the branching angle ω is bigger than 80^o. The negative value of K_I means that the crack surfaces are not separated, but contacted. In this thesis, the contribution from negative K_I to the energy release rate, $\mathcal{G}$, is excluded.

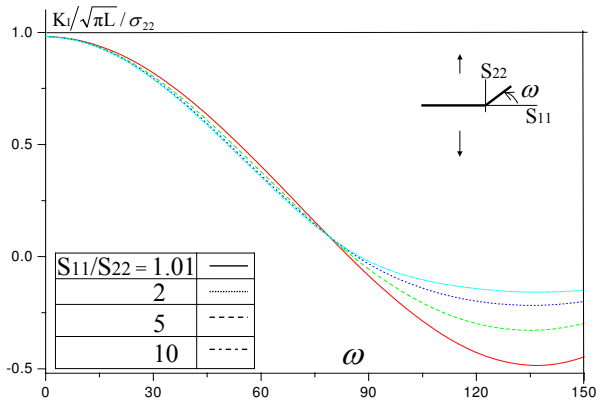

Fig.6.2 Mode I Stress Intensity Factor at the branched crack tip with the main crack lying along the weaker material axis

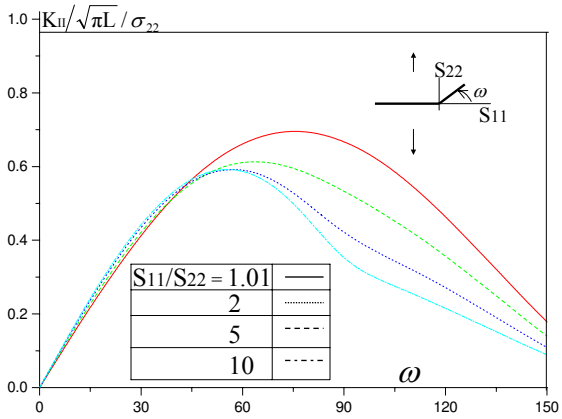

Fig.6.3 Mode II Stress Intensity Factor at the branched crack tip with the main crack lying along the weaker material axis

The energy release rate, $\mathcal{G}$, for the branched crack tip was calculated by using (163). For monolithic anisotropic media, the energy release rate can also be computed by the following formula, which was first derived in [39]

$$\mathcal{G} = -\frac{s_{11}}{2}\mathrm{Im}[K_I^2(p_1+p_2)\bar{p}_1\bar{p}_2 + 2K_IK_{II}\bar{p}_1\bar{p}_2 - K_{II}^2(p_1+p_2)] \qquad (167)$$

where, the $p_i (i = 1, 2)$ are the eigenvalues of equation (10) and all the quantities are referred to the (ξ, η, x_3) coordinate system associated with the branched crack tip. The results by the formulas (163) and (167) are the same for this case, and the normalized results are plotted on Fig. 6.4. Here, some differences also can be seen between these results and those in [26] and [27].

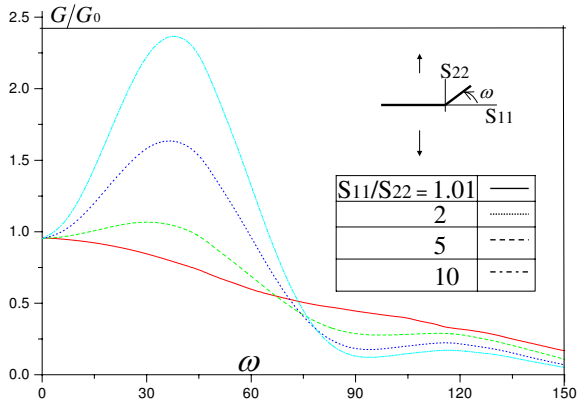

Fig.6.4 Energy release rate for the branched crack tip
with the main crack lying along the weaker material axis

The differences between our results and those in [26] may arise because the authors of [26] seem to have evaluated their results in the (x_1, x_2, x_3) coordinate system which actually should be transformed into the crack branching coordinate system (ξ, η , x_3) system, as was also pointed by the authors of [27] for the compliance coefficients. Quantitatively, the normalized dislocation density in Fig. 6.1 is equal to the stress intensity factor of mode I if measured in the (x_1, x_2, x_3) coordinate system. Therefore, the similarity between the curves of b_{11} and those of K_I in Fig. 2 of [26] directly supports the above explanation on the differences between these two sets of results. In the mean while, a close examination can be seen that the differences between present results and those in [27] come from two facts: 1). First, the equation (76) in [27] used by those authors to calculate energy release rate for branched crack

tip is incorrect (Appendix D), i.e. the sign of the second term of that formula in [27] should be $'-'$, not $'+'$. This error happened because the authors of [27] seem to have mixed up the imaginary part of a complex variable with that of its conjugate. Therefore, it would not be surprising that all their results with regard to the energy release rate in [27] may lead to some incorrect conclusions; 2). Secondly, the perturbation method employed in [27] could fail in nonlinear problems like the one considered, or just could only capture some linear features of the problem. The second fact can be more clear if we make a comparison with regard to the results of the energy release rate. The results of energy release rate for the branched crack tip in Fig. 6.4 of this paper and those in Fig. 4 of [26] both show the high non-linearity on the curves, although some errors were made on the values in [26] due to the lack of coordinate system transformation. However, in the derivation of their formulas in [27], the fundamental assumption $\mathbf{sin}(\omega) \cong \omega$ and $\mathbf{cos}(\omega) \cong 1$ used by those authors may be applied only when the ω is very small. But the ω they considered was ranged from $0^o \sim 150^0$ for which this assumption would not be valid. The results in Figure 8 of [27] show that he deviation of energy release rate for anisotropic media with respect to the isotropic medium is relatively small as the degree of anisotropy increases. This may tell us that their perturbation method might only capture the linear (or some slight non-linear) deviation portion of the total energy release rate for the branched crack tip

of anisotropic, as a perturbation usually does. Therefore, their perturbation method may be inadequate for the cases considered in [27]. Perhaps, in order to achieve high accurate results by their perturbation, more than second higher order approximation should be used.

Nevertheless, for the symmetric case there is a remarkable agreement among the present paper and [26] and [27] in that the well-known independence of the stress intensity factors on the material properties behavior at zero degrees (Sih, Paris, and Irwin, 1965) has been shown by the results in all these three work. Furthermore, our results in Fig. 6.4 also show that the branching angle at which the energy release rate reaches its maximum value increases as the degree of anisotropy increases. This tells us that the orientation of crack branching tends to the direction of the stiffer material axis. This along with the results shown in Fig. 6.7 of the next case may well explain the often observed phenomenon that in fiber-reinforced composites, cracks usually propagate parallel to the fibers, i.e. the stiffer material axis.

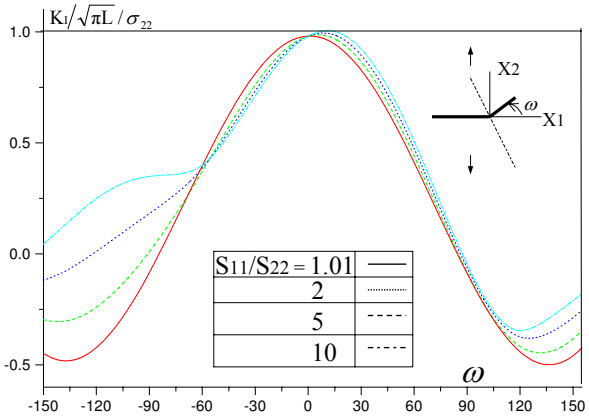

Fig.6.5 Mode I Stress Intensity Factor at the tip of a branched asymmetric crack.

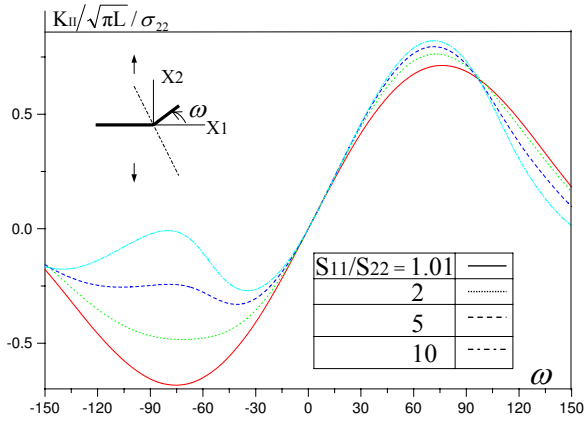

Fig.6.6 Mode II Stress Intensity Factor at the tip of a branched asymmetric crack.

Figs. 6.5-6.7 give the results of the asymmetric case at which the norm of the main crack makes a 30^o angle with respect to the material stiffer axis and the loading is the same as previous case. There are also some differences

among the results in this paper and those in [26] and [27] due to the same reasons explained in the discussion of the previous case. It can be seen that the variation of the K_I and K_{II} versus the variation of branching angle and the degree of anisotropy in Fig. 6.5 and Fig. 6.6 follow a similar pattern as those in [26] and [27].

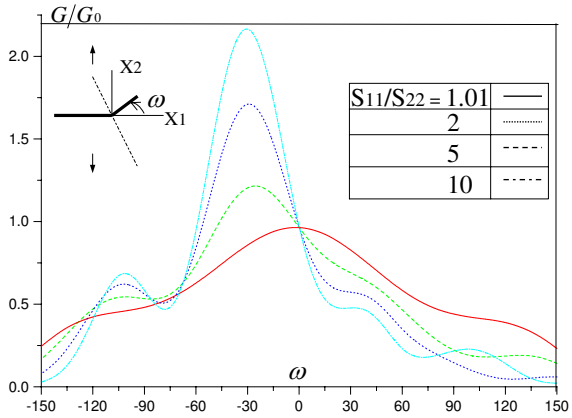

Fig.6.7 Energy release rate at the branched tip for the asymmetric case

Both Fig. 6.7 of the current result and Fig. 7 of [26] show again the high non-linearity of the energy release rate for the branched crack tip while Fig. 11 in [27] captures the linear/slight non-linear portion of the total energy release rate.

In these two cases, one may find that the changes of mode I and mode II stress intensity factors are relatively small at small branching angles as the

degree of anisotropy increases. However the changes in the maximum values of the energy release rate for the branched crack tip are dramatically increased as the degree of anisotropy increases, and these branching angles also increases as the degree of anisotropy increases. We can also see that, for each of these two cases, the angle which maximizes the K_I but makes K_{II} zero is not equal to the angle at which the maximum energy release rate is reached for a given degree of anisotropy. The results of the energy release rate for the asymmetric case more clearly show that the tendency of crack branching is in favor to the stiffer material axis as shown Figure 6.7, in which when the degree of anisotropy $s_{11}/s_{22} = 10.0$, the branching angle at which the maximum energy release rate occurs is - 42.15^o that tends to the direction of -60^0, the stiffer material axis orientation.

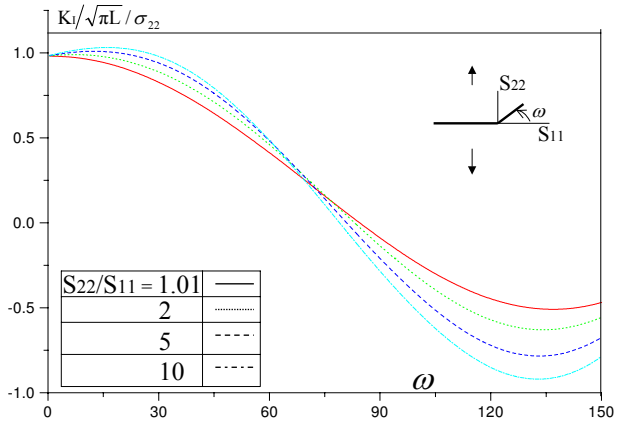

Fig. 6.8 Mode I Stress Intensity Factors at the branched crack tip for the main crack lying along the stiffer material axis

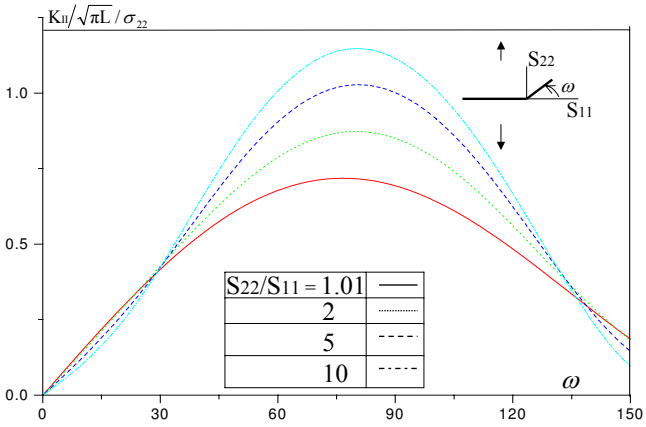

Fig. 6.9 Mode II Stress Intensity Factors at the branched crack tip for the main crack lying along the stiffer material axis

Another application of the present method to the crack/delamination branching problem is to consider the case of a main crack located along the stiffer material axis, i.e. $s_{11}/s_{22} < 1$, which was studied in [27] but not in [26]. The stress intensity factors and energy release rate for this case are plotted in Figs. 6.8-6.10.

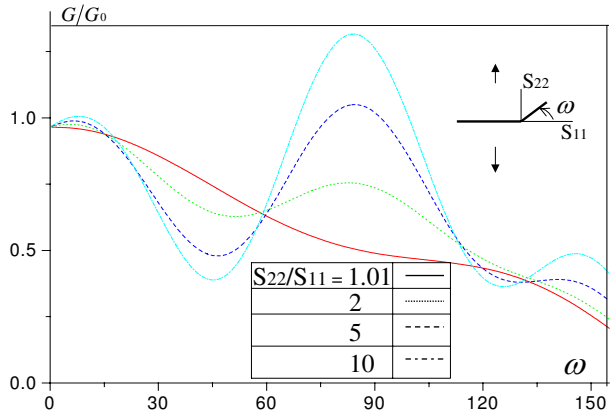

Fig.6.10 Energy release rate at the branched crack tip for the main crack lying along the stiffer material axis

For the reason pointed above, some differences can also be seen between the present results and those in Figs. 12-14 of [27], especially for the energy release rate. It can be seen that, as the degree of anisotropy increases, the mode I stress intensity factor becomes a local maximum with regard to the branching angles. The transition angle happens when the $s_{22}/s_{11} \cong 1.65$. There are some very interesting features on the energy release rate results of Fig. 6.10, i.e. there are two local maximum values $\mathcal{G}_{1c}$ and $\mathcal{G}_{2c}$ appearing on the energy release rate curves if the material is not isotropic. The relationship between $\mathcal{G}_{1c}$ and $\mathcal{G}_{2c}$ reverses as the degree of anisotropy increase: $\mathcal{G}_{1c} \geq \mathcal{G}_{2c}$ when $s_{22}/s_{11} < 4.15$; $\mathcal{G}_{1c} < \mathcal{G}_{2c}$ when $s_{22}/s_{11} \geq 4.15$. Both $\mathcal{G}_{1c}$ and $\mathcal{G}_{2c}$ increase as the degree of anisotropy increases, so do the corresponding branching angles ω_{1c} and ω_{2c} (see Table 3).

The values of the branching angle ω_{1c} are relatively small, $0^o \sim 10^o$, i.e. almost parrel to the direction of the main crack; while these ω_{2c} are very large, $75^o \sim 90^o$, i.e. almost perpendicular to the orientation of the original crack. This observation may give a rough but reasonable explanation for two often observed fracture phenomena:

(1) the first one is the secondary delamination observed in some experiments for delaminated laminated composites. The secondary delamination is usually parrel to the direction along which the original delamination lies. This phenomenon may happen for some composites such that the degree of

anisotropy is under the transition value and $\mathcal{G}_{1c} \geq \mathcal{G}_c$ (where $\mathcal{G}_c$ is the critical value of energy release rate of the material), the branching occurs at the ω_{1c}. Since the branching angle in this case is not too large, therefore, it is easily to force the branched crack back in the direction of the stiffer material axis, which is the orientation of the original delamination.

(2) the second is the matrix cracks in the fiber reinforced composites which are mostly observed perpendicular to the fibers. For this kind of composites, the value of the degree of anisotropy easily exceeds the transition value and a delamination often originates between the reinforcing fibers and the matrix media, i.e. the original delamination lying along the orientation of the stiffer material axis. If $\mathcal{G}_{2c} \geq \mathcal{G}_c$, the branching happens and grow along the angle of ω_{2c}, i.e. almost perpendicular to the fibers.

The results obtained in this research so far are in a agreement with some often observed fracture phenomena. This agreement and the results in the following section can provide some justification of the validity of the method developed in this paper. Next, we shall use this method to further study some complicated practical applications of crack/delamination branching problems.

.

Table 1 Maximum value of G and the corresponding branching angle for the symmetric case

S_{11}/S_{22}	ω_c	G_{Max}/G_0
1.01	0.0	1.00
2.0	30.13	1.074
5.0	35.12	1.65
10.0	37.64	2.36

Table 2 Maximum value of G and the corresponding branching angle for the asymmetric case

S_{11}/S_{22}	ω_c	G_{Max}/G_0
1.01	0.0	1.00
2.0	-22.5	1.21
5.0	-24.25	1.71
10.0	-42.15	2.16

.

Table 3 Maximum values of KI , G and the corresponding branching angles for the case of the main crack lying along the stiffer material axis

S22/S11	ω_c	K_I	ω_{c1}	G_{Max1}/G_0	ω_{c2}	G_{Max2}/G_0
1.01	0.00	1.00	0.00	1.00		
2.0	0.00	1.00	5.75	1.08	77.7	0.83
5.0	7.72	1.02	7.25	1.09	82.0	1.16
10.0	15.5	1.03	10.5	1.12	85.5	1.42

6.2 Interface Crack Branching of Anisotropic Bimaterial Media

The authors of [28] attempted a study of interface crack branching in dissimilar anisotropic bimaterials by using the Lekhnistkii formulization. But the cases studied were actually for a very special material, not for general bimaterial media, since the bimaterial characteristic parameter ϵ is equal to 0.0 in the cases considered in [28]. Therefore, the conclusion drawn from the results of the cases analyzed may not be accurate, as will be pointed out later on in this section. Here, the case for which $\epsilon = 0.0$ is defined as the quasi-bimaterial case and the corresponding materials are called quasi-bimaterials. In this section, the raw or original material constants are chosen as

$$\begin{aligned} &E_{11} = 9.79GPa, \quad E_{22} = E_{33} = 0.407GPa, \\ &G_{21} = 0.979GPa, \quad \nu_{21} = \nu_{23} = \nu_{31} = 0.01 \end{aligned} \tag{168}$$

where $E_{ij}(i, j = 1, 2, 3)$ are the Young's moduli. The materials produced by the method in [28], i.e. by simply rotating the principal material axis of the upper or lower side of the body at different angles with respect to the coordinates x_1 and x_2, can be proved to be quasi-bimaterials (Appendix E). This is a very interesting construction. It looks like a bimaterial media, but there is no oscillatory character on the stress and displacement fields ahead of the interface crack tip [1].

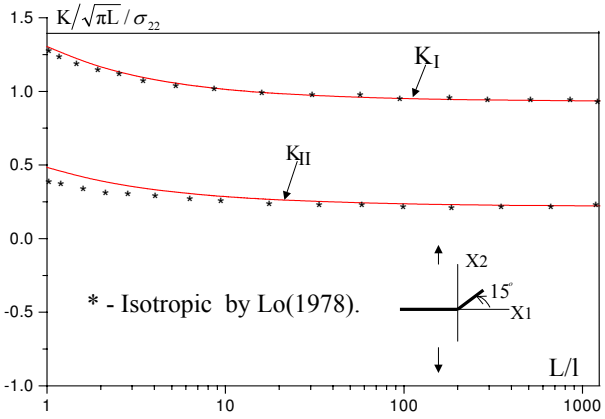

Fig.6.11 Variation of Stress Intensity Factors at the branched crack tip v.s. variation of l/L for $\omega = 15^o$.

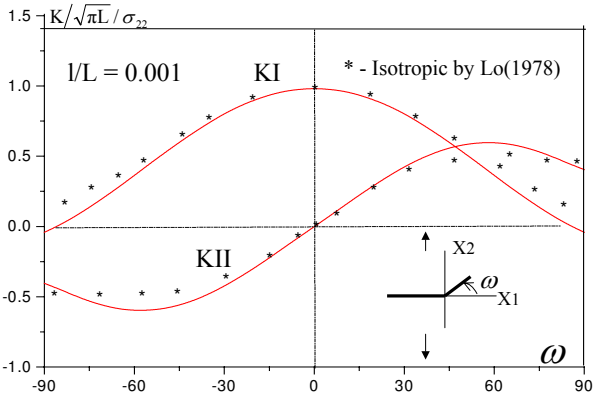

Fig.6.12 Variation of Stress Intensity Factors v.s. variation of branching angles with l/L = 0.001.

Fig. 6.11 shows the results of the variation of the mode I and mode II stress intensity factors at the branched crack tip with respect to the change of the ratio l/L under the assumed branching angle $\omega = 15^o$. Fig. 6.12 is the

variation of the mode I and mode II stress intensity factors at the branched crack tip versus the variation of branching angles. The materials for these two cases satisfy

$$E_{22} = E_{11}/1.01, \quad E_{33} = E_{22} \tag{169}$$

which is very close to an isotropic material.

On these two figures, the results by Lo (1978)[22] for an isotropic material under the same geometric and loading conditions were also plotted. These two sets of results are remarkably close to each other, especially for the infinitesimal branched crack tip. This closeness provides a validation and also further proves that the method in our current research, though derived from the anisotropic theory, can be properly applied to crack branching problems in isotropic media. In Figs. 6.13-6.14 are the mode I and mode II stress intensity factors and energy release rate versus the branching angles for the case $l/L = 0.001$ of a quasi-bimaterial media.

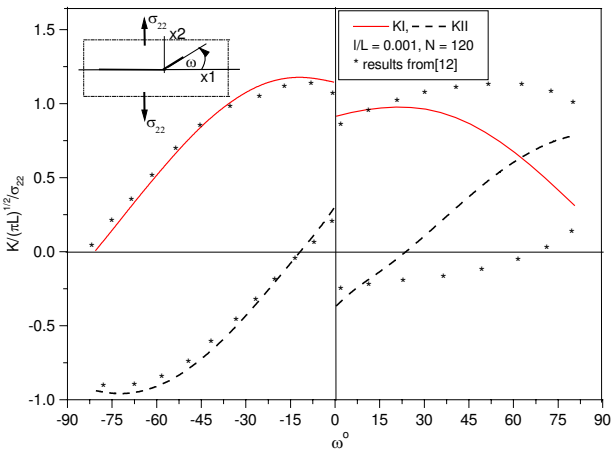

Fig.6.13 Stress Intensity Factors at the branched crack tip in a quasi-bimaterial medium , l/L = 0.001

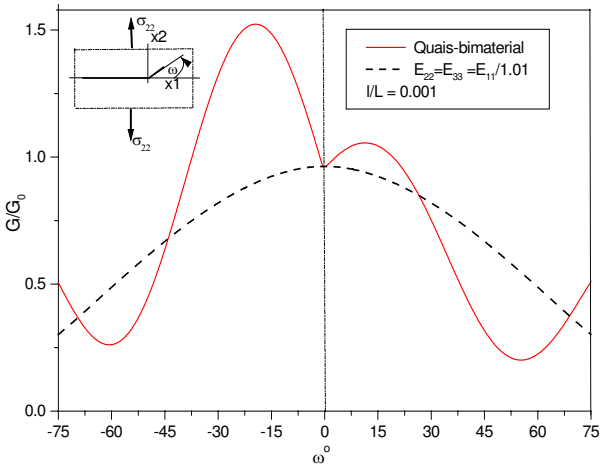

Fig.6.14 Variation of Energy release rate for a branched crack in a quasi-bimaterial medium, l/L = 0.001

In this case, the upper medium or medium 'I' is the raw material as above, the lower medium or medium 'II' is also made from the above raw material but with the principal material axis being rotated -30^o with respect to the

$(x_1\ ,\ x_2,\ x_3)$ coordinate system. The results for the stress intensity factors from our calculations and those on Fig. 8 of [28] both agree that the branching angles at which the maximum values of K_I attains are those angles where K_{II} approaches zero, and there is a discontinuity on the stress intensity factors across the $\omega = 0^o$. But the results in [28] can not clearly predict in which direction the crack branching would happen. From the plotting of Fig.8 in [28] and based on their K_I prediction criterion, it looks that the crack would prefer to branch into the upper medium since the maximum K_I is slightly larger than that for the lower material. This prediction obviously contradicts to the observed phenomenon that crack branching usually tends to occur parrel to the orientation of fibers (which is 0^o for the upper medium or -30^o for the lower medium in the present case) in fiber-reinforced composite media. However, from our results on Fig. 6.14, it can be seen that the maximum energy release rate occurs around the branching angle $\omega = -22.5^o$, and the maximum K_I zero K_{II} happens in the same medium with branching angle $\omega = -10.5^0$.

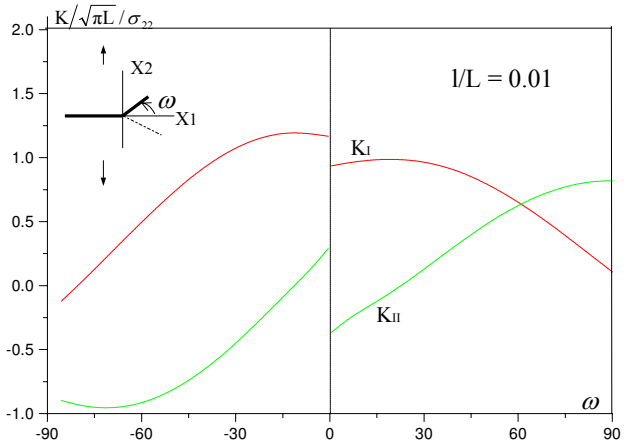

Fig.6.15 Stress Intensity Factors at the branched crack tip in the quasi-bimaterial medium, l/L = 0.01

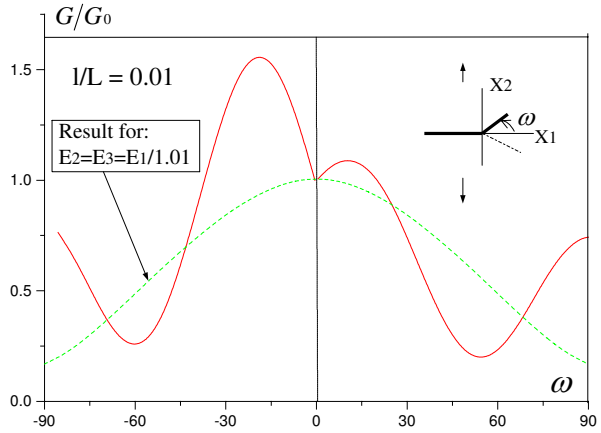

Fig.6.16 Energy release rate for the branched crack in a quasi-bimaterial medium, l/L = 0.01

A similar observation can also be made from Figs. 6.15-6.16 which shows the results of stress intensity factors and energy release rate for the same material properties and loading condition as the above case, but with the ratio $l/L = 0.01$. Here, it should be mentioned that the similarity between Figs. 6.13-6.14 and Figs. 6.15-6.16 comes from the convergence of K_I and K_{II} when $L/l > 50$ as shown on Fig.6.11. Therefore, the more accurate predicated behavior for this kind of quasi-bimaterial media may be: the interface crack would propagate into the lower medium, which is more compliant than the upper medium in the $(x_1\ x_2\ x_3)$ coordinates system, and try to follow the stiffer material axis of the lower/compliant medium.

Now let's study a more general anisotropic bimaterial medium case. The material constants for the upper medium are same as those of the raw material given above, while these constants for the lower medium are

$$E_{11} = 2.312GPa, \quad E_{22} = E_{33} = 0.517GPa,$$
$$G_{21} = 0.0174GPa, \quad \nu_{21} = \nu_{23} = \nu_{31} = 0.1 \tag{170}$$

A angle of -30^o rotation was imposed on the principal material axis of the lower medium with respect to the x_1. From the given elastic constants, it can be seen that the lower medium is much weaker than the upper medium. The value of the bimaterial parameter for this solid is $\epsilon = 0.00917367$.

Presented in Figs. 6.17-6.18 are the mode I and mode II stress intensity factors and energy release rate for the case of an interface crack branching for this general anisotropic bimaterial.

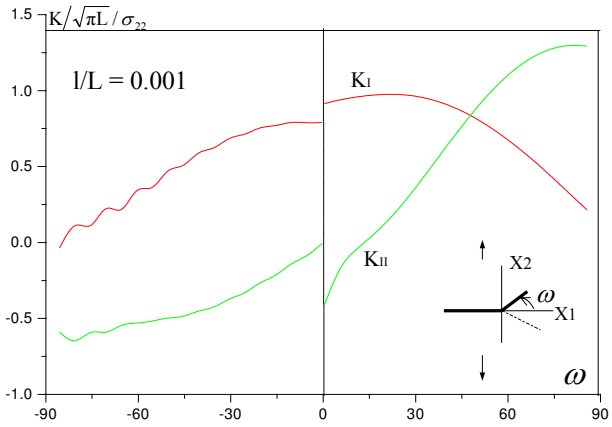

Fig.6.17 Variation of Stress Intensity Factors at the branched crack tip for a general anisotropic bimaterial

The results in Fig.6.17 show that the maximum value of K_I for the upper medium is much higher than that for the lower medium. If K-based criteria would be used to predict branching angles as suggested by the authors of [28], it would be in conflict with the observed fact that cracks usually branch into the weaker (more compliant) medium, as seen in experiments on debond branching in sandwich, i.e. debonding often branches into the core, seldom into the face sheet. But from our results in Fig. 6.18, it can be easily seen that the energy release rate reaches its maximum value at the branching angle

$\omega = -25.5^o$, which is very close to the orientation of the stiffer material axis of the weaker or more compliant medium. This again tells us that if crack branching happens, it will not only branch into the weaker (lower) medium, but also follow the orientation of the stiffer material axis of this medium.

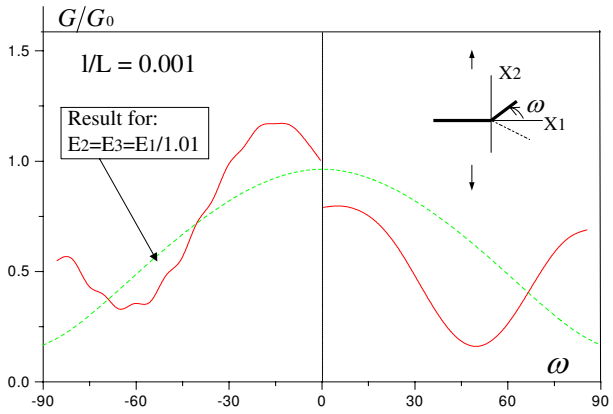

Fig.6.18 Variation of the Energy release rate for the branched crack tip in a general anisotropic bimaterial

These remarkable results significantly illustrate the validity and power of our method in the present research. The observation on the above case and other cases studied in section 5.1 and 5.2 may give sufficient evidence to reach the conclusion that the usual crack growth criteria based on (i) maximum K_I; (ii) zero K_{II}; (iii) maximum $\mathcal{G}$, which give identical predictions in the isotropic case, cease to be consistent for monoclinic anisotropic media and dissimilar anisotropic bimedia. This conclusion was also partially claimed by some authors [26,27,28] based on their partially correct results for the ho-

mogenous anisotropic solids. But our results based on extensive cases studies, which agree well with often observed fracture phenomena, provide adequate validation to this claim.

6.3 Thermo-elastic Crack Branching in Monolithic Anisotropic Solids

From this section, our attention moves toward the study of crack/delamination behavior under thermal loading. Without loss of generality, let us check the temperature change in the upper medium under unit applied heat flux. From equations $(21)_3$, (32) and (83), the variation of temperature in the medium ' I' can be written as

$$T = \frac{h_0}{k_I}\mathrm{Im}[z - \sqrt{(z-a)(z-b)}] = \frac{1}{k_I}\mathrm{Im}[z - \sqrt{(z-a)(z-b)}] \qquad (171)$$

One can see that the $T \to 0$ as z approach infinity, i.e. the temperature variation is bounded. One can further find that when $|z| \simeq 50(b-a)$, $T <= 0.2^0 C$, a small value.

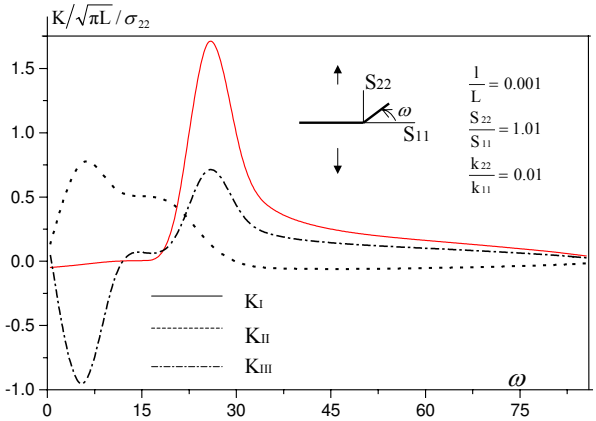

Fig.6.19 Stress Intensity Factors v.s. branching angles for a nearly isotropic material

Therefore, in the following computation, the material property constants can be assumed not varied with the temperature change under unit applied

heat flux. Fig. 6.19 and Fig. 6.20 show, respectively, the stress intensity factors and energy release rate for a nearly isotropic material, i.e. $S_{22} = 1.01\ S_{11}$. In Fig. 6.21 and Fig. 6.22 are the stress intensity factors and energy release rate for mechanically anisotropic material, the degree of anisotropy is $S_{22} = 2.50\ S_{11}$. In these cases the ratios k_{22}/k_{11} of the heat conduction coefficients are assumed to be 0.01.

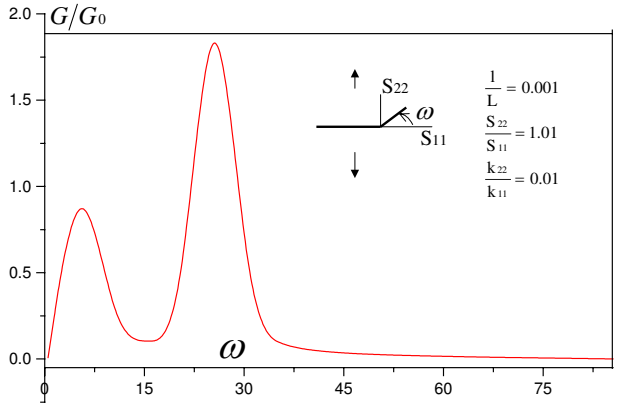

Fig.6.20 Energy Release Rate v.s. branching angles for a nearly isotropic material

From the results in Fig. 6.19 and Fig. 6.20, it can be seen that the branching angle at which the K_I attains its maximum value (K_{II} reaching its minimum value) coincide with the angle which makes the energy release rate attain its maximum value; while those angles in Fig. 6.21 and Fig. 6.22 are different. This observation shows that K-based criteria are still valid for thermoelastic problem of mechanically isotropic materials. But for the thermoelastic problem of a mechanically anisotropic solid, the G-based criteria should be more accurate.

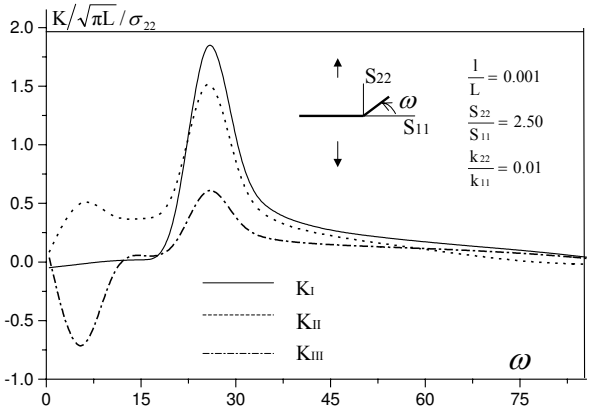

Fig.6.21 Stress Intensity Factors v.s. branching angles for an anisotropic material

The K_{III} does not disappear in Fig. 6.19 and Fig. 6.21 although the material is orthotropic and the only applied load is σ_{22}; also a negative K_I can be observed when the branching angles are very small. These two interesting phenomena are due to the thermal loading effects. The influence of the degree of anisotropy is also illustrated in these cases, say when $S_{22} = 1.01$ S_{11}, the G_{max}/G_0 is 1.875 with corresponding branching angle $\omega_{\max} = 22.5^0$ (see Fig.6.20); while $S_{22} = 2.5$ S_{11}, the $G_{max}/G_0 = 2.925$ with corresponding branching angle $\omega_{\max} = 27.25^0$(see Fig.6.22). Here, G_0 is the value without branching.

Presented in Fig. 6.23 is the combined influence of the thermal conduction properties and the degree of anisotropy on the branching angles. From this picture, one can observe that the branching angles increase as the degree of

anisotropy (S_{22}/S_{11}) increases when $0.01 < k_{22}/k_{11} < 0.275$; while these results are reversed at $0.275 < k_{22}/k_{11} < 0.425$. When $0.425 < k_{22}/k_{11} < 0.5$, the tendency is mixed. The plotting can provide a guideline for selecting the thermal properties of anisotropic materials.

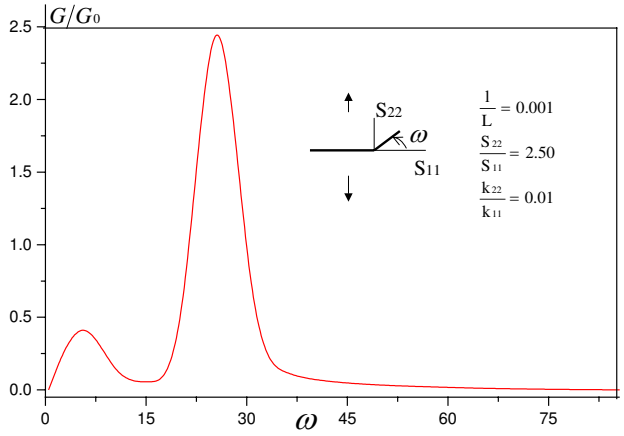

Fig.6.22 Energy Release Rate v.s. branching angles for an anisotropic material

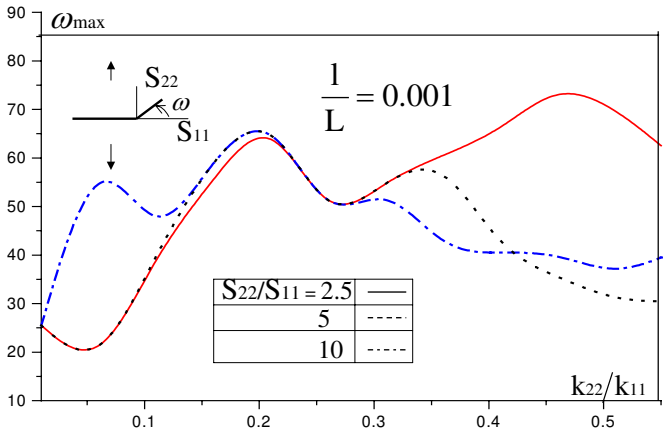

Fig.6.23 Max. branching angles v.s. ratios of coefficient of heat conduction

6.4 Thermo-elastic Interface Delamination Branching Behavior in Dissimilar Anisotropic Bimaterials

In this section, the influence of thermal loading on the delamination branching in composite bimaterials will be demonstrated. Some typical composites were used as ' raw' or ' basic' material in the numerical simulation.

The first raw material called material-I is selected with thermo-elastic properties as following:

$$
\begin{aligned}
&E_{11}^{\mathrm{I}} = 5.69GPa, \quad E_{22}^{\mathrm{I}} = E_{33}^{\mathrm{I}} = 0.407GPa,\\
&G_{21}^{\mathrm{I}} = 0.979GPa, \quad \nu_{21}^{\mathrm{I}} = \nu_{23}^{\mathrm{I}} = \nu_{31}^{\mathrm{I}} = 0.01,\\
&k_{11}^{\mathrm{I}} = 42.1\mathrm{W/m/K}, \quad k_{22}^{\mathrm{I}} = k_{33}^{\mathrm{I}} = 0.47\mathrm{W/m/K},\\
&\alpha_{11}^{\mathrm{I}} = 0.025 \times 10^{-6}\mathrm{m/m/K}, \quad \alpha_{22}^{\mathrm{I}} = \alpha_{33}^{\mathrm{I}} = 32.4 \times 10^{-6}\mathrm{m/m/K} \qquad (172)
\end{aligned}
$$

Where $E_{ij}(i,j=1,2,3)$ are Young's moduli, ν_{ij} are the Poisson ratios, k_{ij} and α_{ij} are, respectively, the coefficients of heat conductivity and coefficients of thermal expansion.

Thermo-elastic properties of the second raw material (material-II) read as:

$$E_{11}^{\mathrm{II}} = 2.312 \times GPa, \quad E_{22}^{\mathrm{II}} = E_{33}^{\mathrm{II}} = 0.517 \times GPa,$$

$$G_{21}^{\mathrm{II}} = 0.0174 \times GPa, \quad \nu_{21}^{\mathrm{II}} = \nu_{23}^{\mathrm{II}} = \nu_{31}^{\mathrm{II}} = 0.1,$$

$$k_{11}^{\mathrm{II}} = 53.7\mathrm{W/m/K}, \quad k_{22}^{\mathrm{II}} = k_{33}^{\mathrm{II}} = 0.73\mathrm{W/m/K},$$

$$\alpha_{11}^{\mathrm{II}} = 0.034 \times 10^{-6}\mathrm{m/m/K}, \quad \alpha_{22}^{\mathrm{II}} = \alpha_{33}^{\mathrm{II}} = 34.2 \times 10^{-6}\mathrm{m/m/K} \qquad (173)$$

The angles θ_I and θ_{II} define the angles between the material principal axis and the x_1 axis for the medium occupying the upper and lower space, respectively. The unit axial tension σ_{22} and the unit heat flux q_0 in the x_2 direction are considered to be the applied loading (Fig.3.1).

Fig. 6.24 and Fig. 6.25 are the convergent illustrations of the numerical scheme employed in chapter V. The bimaterial medium used here in consists of material-I as the upper medium and material-II as the lower medium and its bimaterial parameter ϵ, defined in equation (73), equals 0.0662693.

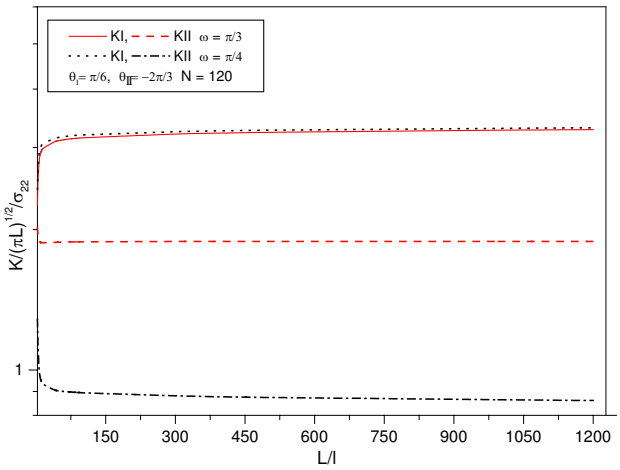

Fig.6.24 Variations of the Stress Intensity Factors v.s the relative length(l/L) of the branched crack

Depicted in Fig. 6.24 are the Mode I (K_I) and Mode II (K_{II}) stress intensity factors around the branched crack tip as functions of L/l . The partition points in (158) and (159) are n = 120. Results of two cases were plotted, one for the assumed branching angle $\omega = \pi/3$ and the other for $\omega = \pi/4$. It can be seen that when $l/L > 0.1$, both values of K_I and K_{II} converge very well. When $l/L > 0.00125$, these values almost do not vary with the change of l/L. Therefore, the behavior of a branched crack with $l/L = 0.001$ can be considered as the behavior at the onset of an interface crack branching. Usually, the onset of a crack branching is of great interest in the study of interface crack problems.

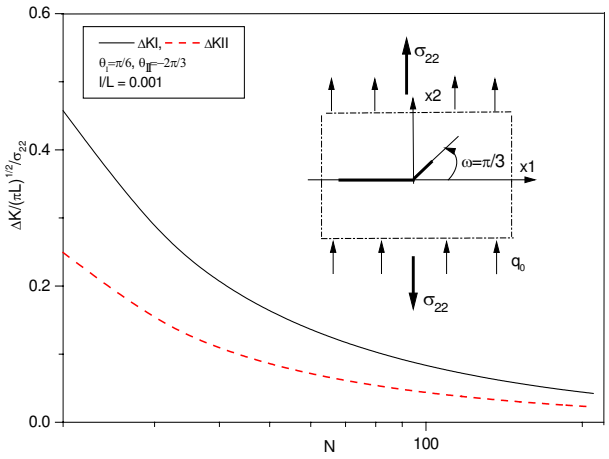

Fig. 6.25 Variation of Stress Intensity Factors versus the number of partition points N

Fig. 6.25 gives the variation of K_I and K_{II} versus the number of partition points n. The value $l/L = 0.001$ was used here. To obtain these results , Δn was set to be 10 and ΔK is defined as the difference of the K evaluated at n = i + 10 and n = i ($i >= 20$), respectively. It can be seen that $\Delta K \to 0$ as $n \to \infty$. This means that K_I and K_{II} converge with the increase of n. The plot shows that one could get a good approximation by using n = 60 in the computation if one's computer memory is not big enough, and the choice of partition points n = 120 in this paper shall be very reasonable. Of course, if the computer memory permits, one can set n to be a big number. Thus, the infinitesimal crack branch was assumed to be $l/L = 0.001$ and the n was taken to be 120 in the thesis.

Thermo-elastic interface delamination branching for a general bimaterial

As described in the above convergence study, the raw material properties (thermal and mechanical ones) of the upper and lower medium for this general bi-material structure are completely different. This type of bimaterial medium can often be found to have applications in many areas such as electronic packaging, bio-materials, aircraft structure, etc. The components of a structure in these applications often have different thermal and mechanical properties and operate under severe temperature gradients. Therefore, the study of thermo-elastic interface delamination branching behavior is not only of theoretical importance but also of practical significance.

Fig. 6.26 and Fig. 6.27 are the results of mode I and mode II stress intensity factors and energy release rates versus the variation of branching angle under different applied loading conditions. The orientation for the components of this bimaterial medium is $\theta_I = \pi/6$ and $\theta_{II} = -2\pi/3$. Three sets of results are plotted for three loading conditions: solid line for combined loading of unit σ_{22} and q_0; dash-dot line for only unit σ_{22} applied; dash line for only unit q_0 applied. Several interesting observations can be made from the results in these two figures. In Fig. 6.26, the branching angle at which the K_I attains its maximum under combined loading is different from the corresponding angle under pure mechanical loading or thermal loading. When $\omega = 51.44^o$, $K_{Imax} = 3.3394$ for combined loading, while $\omega = 43.45^o$, $K_{Imax} = 1.5507$ for pure mechanical loading and $\omega = 57.4665^o$, $K_{Imax} = 1.8198$ for pure thermal loading. If the bimaterial media were originally under pure mechanical loading, then the K_{Imax} would increase by 115.3% due to the additional thermal loading;

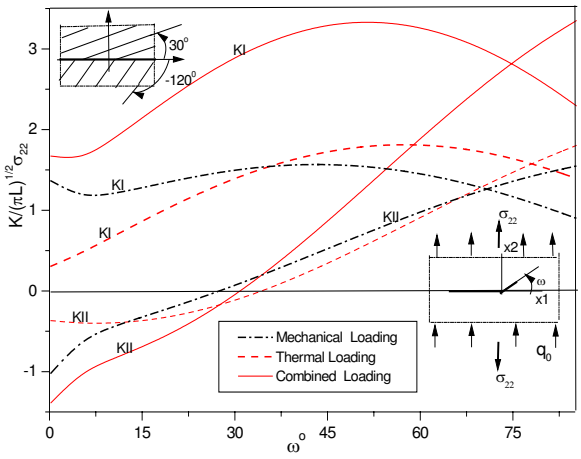

Fig. 6.26 Stress Intensity Factors for an anisotropic bimaterial ($\theta_I = 30^o$, $\theta_{II} = -120^0$)

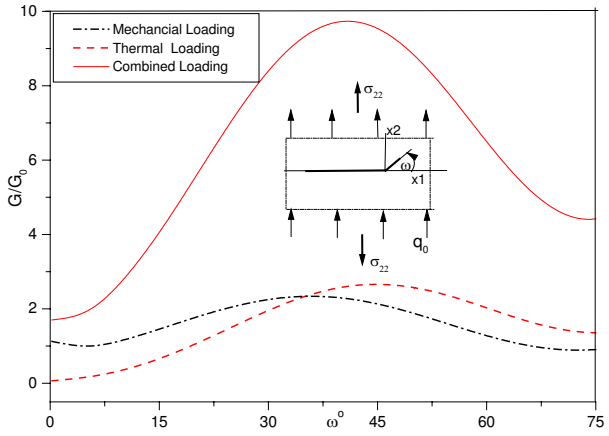

Fig. 6.27 Energy Release Rate for an anisotropic bimaterial ($\theta_I = 30^o$, $\theta_{II} = -120^0$)

or on the other hand, if the bi-material medium were originally under pure thermal loading, then the K_{Imax} would increase by 83.5% after an additional

mechanical loading applied. The result for the energy release rate G, plotted in Fig. 6.27 shares a similar tendency as these for K_I in Fig.6.26. The angles at which the Gs reach their maximum values are also different: when $\omega = 40.94^o$, $G_{max} = 9.7478$ for combined loading, $\omega = 34.78^o$, $G_{max} = 2.3294$ for pure mechanical loading and $\omega = 45.23^o$, $G_{max} = 2.7123$ for pure thermal loading. If the assumed original loading is purely mechanical, as in many engineering applications, then G_{max} would increase by 318.5% (7.4284) due to the additional thermal loading. One can see that though the energy release rate is a scalar quantity, its value under combined loading is not the summation of the values from the purely applied mechanical loading and purely thermal loading. It is much bigger than the summation. The difference of these two values reflects the fact that a huge interaction energy would be produced once a heat flux is added onto a mechanically loaded structure which includes defects. This observation will have significance in practical structural design. According to the K-based criterion, a structure, usually operating in a constant temperature environment, could still survive from a sudden fire since the increased value of K may still fall into the design tolerance. However, there would be a strong interaction energy induced by the heat flux according to the energy release rate criterion, hence cracks in this structure may actually grow very quickly. Therefore, for the safety of the structure, the designer should pay more attention to the G-based criterion.

There are also some other interesting observations. In Fig. 6.26, one can see that when K_I reaches its maximum, the K_{II} does not equal to zero for each loading condition. This observation differs from that in monolithic isotropic medium or dissimilar quasi-bimaterial medium (which will be studied in detail the in next section) under pure mechanical loading in which K_I is maximum while $K_{II} = 0$ simultaneously as to be discussed in the next example. Two aspects may contribute to this difference: (1). the bimaterial parameter $\epsilon \neq 0$ and/or; (2). the thermal loading effects. The above observations suggest that the G-based criteria may be more suitable than the usual K-based criteria to predict thermoelastic interface crack branching propagation for dissimilar anisotropic bimaterial media.

Thermo-elastic interface delamination branching for quasi-bimedia

Since quasi-bimaterial structures are the most commonly used composites in engineering applications, hence, we devote a section specifically to study the interface delamination branching behavior of this type of media.

For general dissimilar anisotropic bimaterial media, the bimaterial parameter ϵ is not zero. However, we often use a set of bimaterial media whose constituents can be dissimilar but its bimaterial parameter $\epsilon = 0$. As defined in section 6.2, this type of bimaterial media is referred to as 'quasi-bimaterial media'. Many engineering composite materials belong to this category. One way to produce such composites is to use one raw material and rotate the material axis with respect to the structure axis by different angles for the upper and lower components. It can be easily proven that $\epsilon = 0$ for this type of dissimilar bi-material medium (Appendix E). Because of its special character $\epsilon = 0$, the quasi-bimaterial medium is found to have some interesting behavior during the interface delamination branching growth.

The 'basic' material elastic constants are similar to those in [29], i.e.

$$E_{11} = 4.89GPa, \quad E_{22} = E_{33} = 0.407GPa,$$
$$G_{21} = 0.731GPa, \quad \nu_{21} = \nu_{23} = \nu_{31} = 0.02 \tag{174}$$

This raw material used as the upper medium rotates at θ_I with respect

to the $(x_1,\ x_2,\ x_3)$ coordinate system; the lower medium was also made from this raw material but with the principal material axis being rotated θ_{II} with respect to the $(x_1,\ x_2,\ x_3)$ coordinate system. The bimaterial parameter ϵ equals zero as shown in Appendix E.

It might not be difficult to know that the overall thermo-elastic properties of a bimaterial medium may vary with the changes of θ_I and θ_{II}, so do the mismatches between the constituents of this bimaterial.

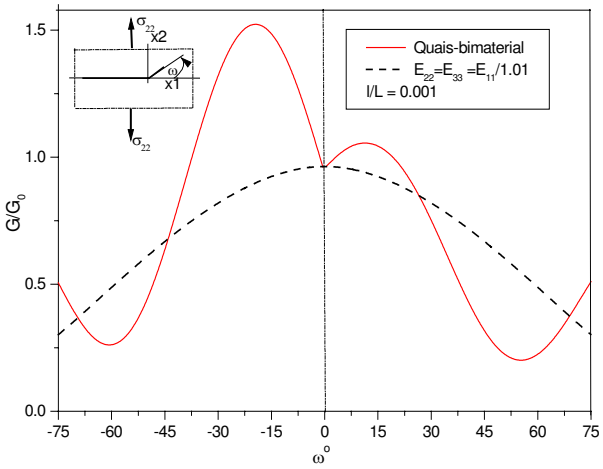

Fig.6.28 Energy release rate for the branched crack v.s. branching angle for a quasi-bimaterial under pure tension loading

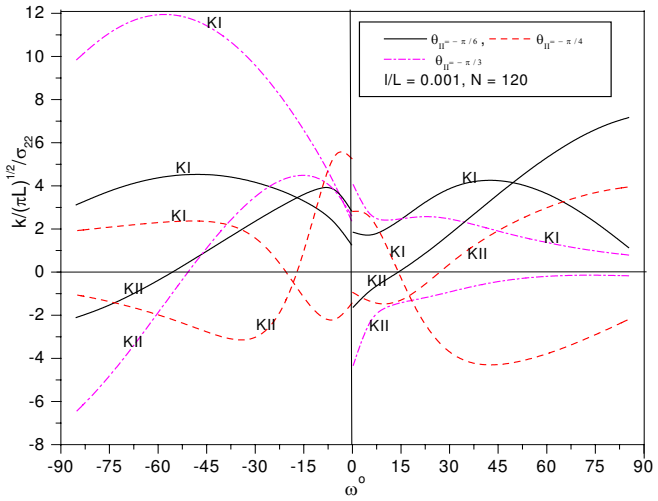

Fig.6.29 SIFs at the branched delamination tip vs. branching angle for a quasi-bimaterial

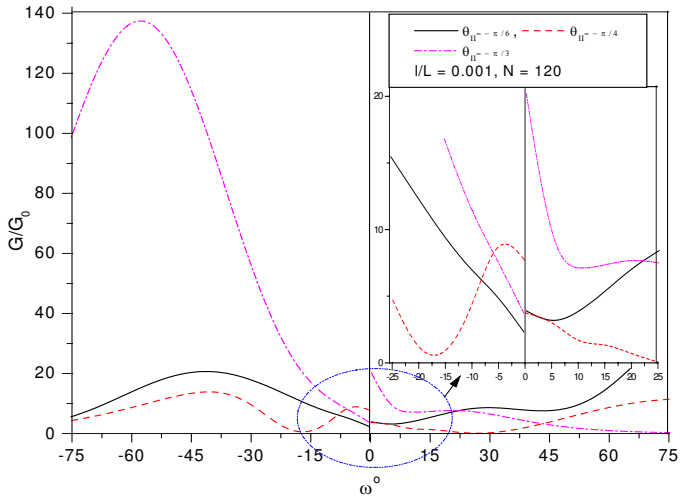

Fig.6.30 Energy release rate for the branched delamination vs. branching angle for a quasi-bimaterial

Fig. 6.29 and Fig. 6.30 are, respectively, the results of Mode I and Mode

II stress intensity factors and energy release rate versus the branching angles for three different bi-material media, which are formulated by letting $\theta_I = 0.0$ while $\theta_{II} = -\pi/6$, $\theta_{II} = -\pi/4$ and $\theta_{II} = -\pi/3$. Besides some observations similar to those in Fig. 6.26-Fig. 6.27, some other observations are also presented in Fig. 6.29 - Fig. 6.30. One may see there is a discontinuity in the stress intensity factors and energy release rate when the branching angle ω approaches $0^{\mp}$, respectively. This discontinuity for K_I and K_{II} was also shown on Fig. 6.13 and in the results of [28]. But for pure mechanical loading there is no such discontinuity for the energy release rate as plotted in Fig. 6.28. This discontinuity on energy release rate on Fig. 6.30 is another effect of the thermal loading.

Negative K_I (contact of the crack faces around the crack tip) [32] appears for the bi-material of $\theta_I = 0.0$, $\theta_{II} = -\pi/4$ when the branching angle $\omega > 13.75^o$ or $-21.25^o < \omega < 0^o$ (the '$-$' sign means the interface delamination possibly branches into the lower medium), an observation being consistent with the one in [22]. Some other interesting results can also be observed in the plotting of the energy release rate. It can be seen from Fig. 6.30 that the interface tends to branch into the lower medium, a result being consist with the observation in Fig. 6.27. But the corresponding maximum energy release rate, which is $G_{max} = 21.03$ for the bimaterial media with $\theta_{II} = -\pi/6$, $G_{max} = 13.12$ for the bimaterial media with $\theta_{II} = -\pi/4$, $G_{max} = 138.15$ for the

bimaterial media with $\theta_{II} = -\pi/6$, does not simply increase as the orientation angle β_{II} increases. The G_{max} reaches its minimum value when $\theta_{II} = -\pi/4$. This observation may indicate that $\theta_{II} = -\pi/4$ could be the optimal orientation angle between the upper and lower medium for this bimaterial media. Therefore, the results may be useful for structure optimal design.

Chapter VII

A Contact Model for Interface Delamination of Dissimilar Bi-materials

It can be seen in Chapter II that the stress and displacement fields around the tip of the interface delamination of dissimilar bimaterial media have the oscillatory property. In 1965, England pointed out in his work [3] that there exists a physical inadequate overlapping and interpenetration between the two surfaces of the dissimilar bimedia in the oscillatory solution of [1]. This implausible physical interpenetration character attracted the attention of many authors such as Hutchinson *et al* (1987) [41], Rice (1988) [42] and Suo *et al* (1988)[43], etc., who have extensively addressed the influence of the bimaterial parameter ϵ on the fracture quantities such as stress intensity factors, crack open displacements and energy release rate, and the conditions under which the ϵ effect could be neglected.

The two faces interpenetration may not be acceptable or at least not that perfect in strictly physical sense though the overlapping fields may only be confined in very small zone around the interface delamination tips. The oscillatory property would naturally disappear so does the interpenetration if the bimaterial matrix W would be null. This result was well proven by Qu

and Bassani in [44,1989] and further discussed in [45, 1993] and by other authors like Ting[46], etc in literature. Probably inspired by the results of [1] and [47], Comninou (1977) [21] looked at this phenomenon in other direction and assumed that the interface crack may not be fully opened, but partially contacted near the ends of the interface crack. Based on this assumption, Comniuou obtained a reasonable non-oscillating solution for general isotropic dissimilar bimedia. This assumption was then referred as the Comninou contact model by some scholars afterwards. In 1980's, the contact model began its extensions to anisotropic dissimilar media. By Lekhnitskii's formulism, Wang and Choi (1983a, b) [48,49] used the contact model to find an non-oscillatory solution to the case in which the roots p_α of the characteristic equation are purely imaginary for the interface crack between the particular high-modulus, graphite-expoy fiber-reinforced laminated composites. Wu and Hwang (1990) [50] obtained the non-oscillatory solution to the problem for materials with $[SL^{-1}]_{13} = L_{12} = L_{23} = 0$ by using method and formulas developed by Willis (1971) [9] and Clements (1971) [7] in dealing with Griffith type interface anisotropic dissimilar bimedia. All the above studies were for some kind of special dissimilar bimaterials. In this chapter, the limitation and conditions in which the Comniuou contact model is valid for the interface crack problems will be investigated for general anisotropic dissimilar bimedia by extending the approaches developed in Chapter II.

7.1 Formulas for an Interface Delamination of General Dissimilar Bimaterials of Comninou Contact Model

The procedure in this section is similar to the one in chapter II, but not exactly the same because of the consideration of the contact zone.

As in Chapter II, let the upper half-plane be occupied by medium 'I', while the lower half-plane occupied by medium 'II' as shown in Fig.7.1.

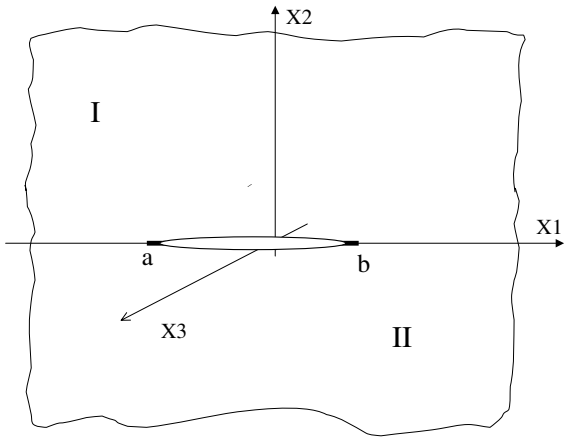

Fig. 7.1 An interface delamination with contact zone for dissimilar anisotropic bimedia

Then the displacement and stress functions for the bimaterials can be expressed as

$$\mathbf{u}^I = A^I\psi(z_\alpha) + \overline{A^I}\,\overline{\psi(z_\alpha)}, \qquad \mathbf{t}^I = B^I\psi'(z_\alpha) + \overline{B^I}\,\overline{\psi'(z_\alpha)}. \tag{175}$$

for z_α in medium $'I'$; and

$$\mathbf{u}^{II} = A^{II}\omega(z_\alpha) + \overline{A^{II}}\,\overline{\omega(z_\alpha)}, \qquad \mathbf{t}^{II} = B^{II}\omega'(z_\alpha) + \overline{B^{II}}\,\overline{\omega'(z_\alpha)}. \tag{176}$$

for z_α in medium $'II'$. The delamination of length 2L lying on the interface of two dissimilar elastic solids as shown in Fig. 7.1 opens at the interval (a, b) under applied loading at infinity. The frictionless contact zones are assumed in the intervals (-L, a) and (b, L) so that the boundary conditions for this interface crack problem can be written as

$$\begin{aligned} &\mathbf{u}_2^I(x_2 = 0^+) = \mathbf{u}_2^{II}(x_2 = 0^-), \quad x_1 < \text{a} \quad \text{and} \quad \text{b} < x_1 \\ &\mathbf{u}_\beta^I(x_2 = 0^+) = \mathbf{u}_\beta^{II}(x_2 = 0^-), \quad \beta = 1, 3 \quad |x_1| \geq \text{L} \end{aligned} \tag{177}$$

$$\begin{aligned} &\sigma_{22}^I(x_2 = 0^+) = \sigma_{22}^{II}(x_2 = 0^-), \qquad x_1 < \text{a} \quad \text{and} \quad \text{b} < x_1 \\ &\sigma_{\beta 2}^I(x_2 = 0^+) = \sigma_{\beta 2}^{II}(x_2 = 0^-), \qquad \beta = 1, 3 \qquad |x_1| \geq \text{L} \end{aligned} \tag{178}$$

and

$$\begin{aligned} &\sigma_{22}^I(x_2 = 0^+) = -\sigma_{22}^\infty, \quad \sigma_{22}^{II}(x_2 = 0^-) = -\sigma_{22}^\infty, \qquad a < x_1 < b \\ &\sigma_{\beta 2}^I(x_2 = 0^+) = -\sigma_{\beta 2}^\infty, \quad \sigma_{\beta 2}^{II}(x_2 = 0^-) = -\sigma_{\beta 2}^\infty, \qquad \beta = 1, 3 \qquad |x_1| < \text{L} \end{aligned} \tag{179}$$

then substitution of the equations of $(175)_1$ and $(176)_1$ into the equation (177)

yields the displacement continuous conditions along the bonded interface as,

$$a^I_{2\alpha}\psi_{\alpha+}(x_1) + \overline{a^I}_{2\alpha}\overline{\psi}_{\alpha-}(x_1) = a^{II}_{2\alpha}\omega_{\alpha-}(x_1) + \overline{a^{II}}_{2\alpha}\overline{\omega}_{\alpha+}(x_1),$$

$$x_1 < \mathrm{a} \quad \text{and} \quad \mathrm{b} < x_1$$

$$a^I_{\beta\alpha}\psi_{\alpha+}(x_1) + \overline{a^I}_{\beta\alpha}\overline{\psi}_{\alpha-}(x_1) = a^{II}_{\beta\alpha}\omega_{\alpha-}(x_1) + \overline{a^{II}}_{\beta\alpha}\overline{\omega}_{\alpha+}(x_1), \beta = 1, 3$$

$$|x_1| \geq \mathrm{L} \tag{180}$$

or

$$a^I_{2\alpha}\psi_{\alpha+}(x_1) - \overline{a^{II}}_{2\alpha}\overline{\omega}_{\alpha+}(x_1) = a^{II}_{2\alpha}\omega_{\alpha-}(x_1) - \overline{a^I}_{2\alpha}\overline{\psi}_{\alpha-}(x_1),$$

$$x_1 < \mathrm{a} \quad \text{and} \quad \mathrm{b} < x_1$$

$$a^I_{\beta\alpha}\psi_{\alpha+}(x_1) - \overline{a^{II}}_{\beta\alpha}\overline{\omega}_{\alpha+}(x_1) = a^{II}_{\beta\alpha}\omega_{\alpha-}(x_1) - \overline{a^I}_{\beta\alpha}\overline{\psi}_{\alpha-}(x_1),$$

$$\beta = 1, 3 \qquad |x_1| \geq \mathrm{L} \tag{181}$$

If we define a function vector

$$\mathbf{\Phi}(z) = \begin{cases} A^I\psi(z) - \overline{A^{II}}\,\overline{\omega(\bar{z})}, & \mathrm{z} \in {}'I' \\ A^{II}\omega(z) - \overline{A^I}\,\overline{\psi(\bar{z})}, & \mathrm{z} \in {}'II' \end{cases} \tag{182}$$

which is analytic in the whole plane with $\mathbf{\Phi}_2(z)$ cutting along $a < x_1 < b$; and $\mathbf{\Phi}_\beta(z)\{\beta = 1, 3\}$ cutting along $|x_1| < L$, then the equation (180) or (181) is identically satisfied.

Similarly from the stress continuity along the bonded interface and closed

portion of the interface crack, we can get

$$b^I_{2\alpha}\psi\prime_{\alpha+}(x_1) - \overline{b^{II}}_{2\alpha}\overline{\omega\prime}_{\alpha+}(x_1) = b^{II}_{2\alpha}\omega\prime_{\alpha-}(x_1) - \overline{b^I}_{2\alpha}\overline{\psi\prime}_{\alpha-}(x_1),$$

$$x_1 < \mathrm{a} \quad \text{and} \quad \mathrm{b} < x_1$$

$$b^I_{\beta\alpha}\psi\prime_{\alpha+}(x_1) - \overline{b^{II}}_{\beta\alpha}\overline{\omega\prime}_{\alpha+}(x_1) = b^{II}_{\beta\alpha}\omega\prime_{\alpha-}(x_1) - \overline{b^I}_{\beta\alpha}\overline{\psi\prime}_{\alpha-}(x_1),$$

$$\beta = 1, 3 \qquad |x_1| \geq \mathrm{L} \tag{183}$$

and, define a function vector

$$\mathbf{\Theta}(z) = \begin{cases} B^I\psi'(z) - \overline{B^{II}}\ \overline{\omega'(\bar{z})}, & \mathrm{z} \in {}'I' \\ B^{II}\omega'(z) - \overline{B^I}\ \overline{\psi'(\bar{z})}, & \mathrm{z} \in {}'II' \end{cases} \tag{184}$$

which is analytical in the whole plane with $\mathbf{\Theta}_2(z)$ cutting along $a < x_1 < b$; and $\mathbf{\Theta}_\beta(z)\{\beta = 1, 3\}$ cutting along $|x_1| < L$, then the equation (183) is identically satisfied.

Differentiating $(182)_1$ with respect to z gives

$$A^I\psi'(z) - \overline{A^{II}}\ \overline{\omega'(\bar{z})} = \Phi'(z), \qquad \mathrm{z} \in {}'I' \tag{185}$$

A re-arrangement of equation (185) can lead to

$$A^I B^{I^{-1}} B^I\psi'(z) - \overline{A^{II}B^{II^{-1}}}\ \overline{B^{II}}\ \overline{\omega'(\bar{z})} = \Phi'(z), \qquad \mathrm{z} \in {}'I' \tag{186}$$

Solving equations $(184)_1$ and (186) for $B_1\psi'(z)$ yields,

$$(A^I B^{I^{-1}} - \overline{A^{II}B^{II}}^{-1})B^I\psi'(z) = \Phi'(z) - \overline{A^{II}B^{II}}^{-1}\Theta(z), \qquad \mathrm{z} \in {}'I' \tag{187}$$

or

$$(i\ A^I B^{I^{-1}} + \overline{i\ A^{II} B^{II^{-1}}}) B^I \psi'(z) = i\ \Phi'(z) + \overline{i\ A^{II} B^{II^{-1}}} \Theta(z), \qquad \mathrm{z} \in {}'I' \tag{188}$$

As it was defined in Chapter II,

$$M^{-1} = iAB^{-1}, \quad \text{and} \quad N^{-1} = M_1^{-1} + \overline{M_2}^{-1} \tag{189}$$

then,

$$B^I \psi'(z) = N[i\Phi'(z) + \bar{M}_2^{-1}\Theta(z)], \qquad \mathrm{z} \in {}'I' \tag{190}$$

Next, substitution of (190) into $(184)_1$ leads

$$\bar{B^{II}}\ \overline{\omega'(\bar{z})} = N[i\Phi'(z) + \bar{M}_2^{-1}\Theta(z)] - \Theta(z), \qquad \mathrm{z} \in {}'I' \tag{191}$$

By similar procedure, we can find following equations for $\mathrm{z} \in {}'II'$,

$$\begin{aligned} &\bar{B}^I \overline{\psi'(\bar{z})} = \bar{N}[i\Phi'(z) - M_2^{-1}\Theta(z)], \\ &B^{II}\omega'(z) = \bar{N}[i\Phi'(z) - M_2^{-1}\Theta(z)] + \Theta(z), \quad \mathrm{z} \in {}'II' \end{aligned} \tag{192}$$

Making use of equations (190), (191), and (192), the boundary condition on the crack face $(179)_2$ can be rewritten as

$$N_\beta[i\Phi'_+(x_1) + \bar{M}_2^{-1}\Theta_+(x_1)] + \bar{N}_\beta[i\Phi'_-(x_1) - M_2^{-1}\Theta_-(x_1)] = -\sigma^\infty_{\beta 2}(x_1) \tag{193}$$

$$\begin{aligned} &\bar{N}_\beta[i\Phi'_-(x_1) - M_2^{-1}\Theta_-(x_1)] + \Theta_-(x_1) \\ &\quad + N_\beta[i\Phi'_+(x_1) + \bar{M}_2^{-1}\Theta_+(x_1)] - \Theta_+(x_1) = -\sigma^\infty_{\beta 2}(x_1) \end{aligned} \tag{194}$$

where $|x_1| < L$ and $\beta = 1, 3$ and N_β is the β^{th} row of matrix N; a significant remark should be made here that, since domain on which $\Phi_2(x_1)$ and $\Theta_2(x_1)$ are analytical includes the domain of $\Phi_\beta(x_1)$ and $\Theta_\beta(x_1)$, the equations (194) and (193) naturally make sense.

By subtraction of (193) from (194), we obtain

$$\Theta_{\beta-}(x_1) - \Theta_{\beta+}(x_1) = 0, \quad |x_1| < L, \quad \beta = 1, 3. \tag{195}$$

Equation (195) shows that $\Theta_\beta(z)\{\beta = 1, 3\}$ is continuous on the whole interface plane($x_2 = 0$). Based on an argument similar to the one in Chapter II on using the analytic continuation principle, (195) also implies that the functions $\Theta_\beta(z)\{\beta = 1, 3\}$ are analytical in the whole media including the whole plane $x_2 = 0$. However, since the stress and rotation of the elastic body must be vanished at infinity when the media only subjected to loading on the crack surface. Therefore these functions must identically be zero in the whole domain, i.e.

$$\Theta_\beta(z) = 0, \quad \text{for all z} \quad \beta = 1, 3. \tag{196}$$

Similarly, from the condition $(179)_1$ the following equations can be obtained

$$N_2[i\Phi'_+(x_1) + \bar{M}_2^{-1}\Theta_+(x_1)] + \bar{N}_2[i\Phi'_-(x_1) - M_2^{-1}\Theta_-(x_1)] = -\sigma_{22}^{\infty}(x_1) \tag{197}$$

$$\bar{N}_2[i\Phi'_-(x_1) - M_2^{-1}\Theta_-(x_1)] + \Theta_-(x_1)$$
$$+ N_2[i\Phi'_+(x_1) + \bar{M}_2^{-1}\Theta_+(x_1)] - \Theta_{2+}(x_1) = -\sigma_{22}^{\infty}(x_1) \tag{198}$$

where, N_2 is the 2^{nd} row of matrix N and $a < x_1 < b$. Here, it may also be necessary to point out though the domain on which $\Phi_\beta(x_1)$ and $\Theta_\beta(x_1)$ are analytical is smaller than that of $\Phi_2(x_1)$ and $\Theta_2(x_1)$, all these functions are continuous on the x_2 axis according to their definitions. Thus, equations (197) and (198) are valid, and then yield

$$\Theta_{2-}(x_1) - \Theta_{2+}(x_1) = 0, \quad a < x_1 < b \; . \tag{199}$$

which imply

$$\Theta_2(z) = 0, \quad \text{for all z.} \tag{200}$$

Therefore, we have

$$\Theta(z) = 0, \quad \text{for all z} \tag{201}$$

Consequently, from equations (197) or (198) and (193) or (194), a typical Hilbert equation can be formulated as

$$\begin{aligned} &N_2\Phi'_+(x_1) + \overline{N_2}\Phi'_-(x_1) = i\ \sigma^\infty_{22}(x_1), \quad \text{a} < x_1 < \text{b} \\ &N_\beta\Phi'_+(x_1) + \overline{N_\beta}\Phi'_-(x_1) = i\ \sigma^\infty_{\beta 2}(x_1), \quad |x_1| < \text{L}, \quad \beta = 1, 3. \end{aligned} \tag{202}$$

As shown in Appendix F that $N = \widetilde{D} + \text{i}\widetilde{W}$ with $\widetilde{D}$ is symmetry and $\widetilde{W}$ is skew-symmetry. Hence, equation (202) can be rewritten as

$$\begin{aligned} &[\widetilde{d}_{12} - i\widetilde{w}_3, \quad \widetilde{d}_{23} + i\widetilde{w}_1] \begin{vmatrix} \Phi'_{1+}(x_1) \\ \Phi'_{3+}(x_1) \end{vmatrix} + [\widetilde{d}_{12} + i\widetilde{w}_3, \quad \widetilde{d}_{23} - i\widetilde{w}_1] \begin{vmatrix} \Phi'_{1-}(x_1) \\ \Phi'_{3-}(x_1) \end{vmatrix} + \\ &\widetilde{d}_{22}[\Phi'_{2+}(x_1) + \Phi'_{2-}(x_1)] = i\ \sigma^\infty_{22}(x_1), \quad \text{a} < x_1 < \text{b} \end{aligned} \tag{203}$$

and

$$\begin{vmatrix} \widetilde{d}_{11} & \widetilde{d}_{13}-i\widetilde{w}_2 \\ \widetilde{d}_{13}+i\widetilde{w}_2 & \widetilde{d}_{33} \end{vmatrix} \begin{vmatrix} \Phi'_{1+}(x_1) \\ \Phi'_{3+}(x_1) \end{vmatrix} + \begin{vmatrix} \widetilde{d}_{11} & \widetilde{d}_{13}+i\widetilde{w}_2 \\ \widetilde{d}_{13}-i\widetilde{w}_2 & \widetilde{d}_{33} \end{vmatrix} \begin{vmatrix} \Phi'_{1-}(x_1) \\ \Phi'_{3-}(x_1) \end{vmatrix} + \begin{vmatrix} \widetilde{d}_{12} \\ \widetilde{d}_{23} \end{vmatrix} [\Phi'_{2+}(x_1)+\Phi'_{2-}(x_1)] + \begin{vmatrix} i\widetilde{w}_3 \\ -i\widetilde{w}_1 \end{vmatrix} [\Phi'_{2+}(x_1)-\Phi'_{2-}(x_1)]$$
$$= \begin{vmatrix} i\,\sigma^{\infty}_{12}(x_1) \\ i\,\sigma^{\infty}_{32}(x_1) \end{vmatrix}, \quad |x_1| < \mathrm{L} \tag{204}$$

Let $\phi(s) = \Phi'_{2+}(s) - \Phi'_{2-}(s)$, and making use of the following Plemelj formulae [36, pp.43]

$$\Phi'_{2+}(x_1) + \Phi'_{2-}(x_1) = \frac{1}{\pi i}\int_{-L}^{L} \frac{\phi(s)}{s-x_1}\, ds, = \frac{1}{\pi i}\int_{a}^{b} \frac{\phi(s)}{s-x_1}\, ds \tag{205}$$

where in (205), the following relationship related crack open displacement is employed

$$\phi(x_1) = \Phi'_{2+}(x_1) - \Phi'_{2-}(x_1) = 0 \qquad \text{for } -L < x_1 < a \ \text{ and } \ b < x_1 < L \tag{206}$$

Therefore, equations (204) then can further be written as

$$\widehat{N} \begin{vmatrix} \Phi'_{1+}(x_1) \\ \Phi'_{3+}(x_1) \end{vmatrix} + \overline{\widehat{N}} \begin{vmatrix} \Phi'_{1-}(x_1) \\ \Phi'_{3-}(x_1) \end{vmatrix} = i \begin{vmatrix} \sigma^{\infty}_{12}(x_1) \\ \sigma^{\infty}_{32}(x_1) \end{vmatrix} + i \begin{vmatrix} -\widetilde{w}_3 \\ \widetilde{w}_1 \end{vmatrix} \phi(x_1) + \frac{i}{\pi} \begin{vmatrix} \widetilde{d}_{12} \\ \widetilde{d}_{23} \end{vmatrix} \int_a^b \frac{\phi(s)}{s-x_1} ds \tag{207}$$

where

$$\widehat{N} = \begin{vmatrix} \widetilde{d}_{11} & \widetilde{d}_{13}-i\widetilde{w}_2 \\ \widetilde{d}_{13}+i\widetilde{w}_2 & \widetilde{d}_{33} \end{vmatrix} \tag{208}$$

is a positive definite Hermitian matrix, since it is the major submatrix of N.

The non-homogenous Hilbert equation (207) can be solved, and it may be of the following form:

$$\begin{vmatrix} \Phi_1'(z) \\ \Phi_3'(z) \end{vmatrix} = \frac{\mathbf{X}(z)}{2\pi} \int_{-L}^{L} \frac{[\mathbf{X}_+(s)]^{-1}}{s-z} \widehat{N}^{-1} \begin{vmatrix} \sigma_{12}^{\infty}(s) \\ \sigma_{32}^{\infty}(s) \end{vmatrix} ds$$
$$+ \frac{\mathbf{X}(z)}{2\pi} \int_{a}^{b} [\mathbf{X}_+(s)]^{-1} \frac{\phi(s)}{s-z} \widehat{N}^{-1} ds \begin{vmatrix} -\widetilde{w}_3 \\ \widetilde{w}_1 \end{vmatrix}$$
$$+ \frac{\mathbf{X}(z)}{2\pi} \int_{-L}^{L} \frac{[\mathbf{X}_+(x_1)]^{-1}}{\pi(x_1-z)} [\int_{a}^{b} \frac{\phi(s)}{(s-x_1)} ds] \widehat{N}^{-1} dx_1 \begin{vmatrix} \widetilde{d}_{12} \\ \widetilde{d}_{23} \end{vmatrix} \quad (209)$$

where,

$$\mathbf{X}(z) = \frac{V\Delta(z;\epsilon)}{\sqrt{z^2-L^2}}; \qquad \Delta(z;\epsilon) = \mathrm{diag}[(\frac{z-L}{z+L})^{i\epsilon}, (\frac{z-L}{z+L})^{-i\epsilon}] \quad (210)$$

In equation (210), $V = [\mathbf{v}_1, \mathbf{v}_2]$ is 2×2, the constants matrix which can be normalized as $\bar{V}^T \widehat{N} V = I$, and(Appendix G)

$$\epsilon = \frac{1}{2\pi} \log[\frac{1+\widetilde{\beta}}{1-\widetilde{\beta}}], \quad \widetilde{\beta} = \frac{\widetilde{w}_2}{\sqrt{\widetilde{d}_{11}\widetilde{d}_{33} - \widetilde{d}_{13}^2}} \quad (211)$$

where $\widetilde{\beta}$ is real since $\widetilde{D}$ is positive definite. Here in equation (211) the bimaterial parameter $\widetilde{\beta}$ depends only on $\widetilde{w}_2$, i.e. the oscillatory character on the shear stress and displacement fields will disappear if the $\widetilde{w}_2$ is zero. This interesting result is in agreement with the one in [51] by using an other method, but more compact in form than those in [51]. The current study is also much more complete and general than those in literature.

By using the contour integral technique, the equation (207) can be further calculated as (Appendix G):

$$\begin{vmatrix} \Phi_1'(z) \\ \Phi_3'(z) \end{vmatrix} = \frac{\mathbf{X}(z)}{2\pi} \int_{-L}^{L} \frac{[\mathbf{X}_+(s)]^{-1}}{s-z} \widehat{N}^{-1} \begin{vmatrix} \sigma_{12}^{\infty}(s) \\ \sigma_{32}^{\infty}(s) \end{vmatrix} ds$$
$$+ \frac{\mathbf{X}(z)}{2\pi} \int_{a}^{b} [\mathbf{X}_+(s)]^{-1} \frac{\phi(s)}{s-z} \widehat{N}^{-1} ds \begin{vmatrix} -\widetilde{w}_3 \\ \widetilde{w}_1 \end{vmatrix}$$
$$+ [\frac{\mathbf{X}(z)}{2\pi} \int_{a}^{b} \frac{\Xi(s)\phi(s)}{s-z} \widehat{N}^{-1} ds \; - \frac{\Lambda(z;\epsilon)}{\pi} \int_{a}^{b} \frac{\phi(s)}{s-z} ds] \begin{vmatrix} \widetilde{d}_{12} \\ \widetilde{d}_{23} \end{vmatrix} \quad (212)$$

where,

$$\Xi(s) = \frac{1}{\pi} \int_{-L}^{L} \frac{[\mathbf{X}_+(t)]^{-1}}{t-s} dt \quad (213)$$

and $\Lambda(z;\epsilon)$ is defined in (279) which can be rewritten here as

$$\Lambda(z;\epsilon) = iV[I - \frac{\Delta(z;\epsilon)}{\sqrt{z^2-L^2}} \mathrm{diag}[z+i2L\epsilon, z-i2L\epsilon]]V^{-1}[\widehat{N} + \overline{\widehat{N}}]^{-1} \quad (214)$$

It is worth mentioning that as $x_2 \to 0$

$$\frac{1}{s-(x_1 \pm p_\alpha x_2)} = \frac{1}{s-x_1} \pm i\pi\delta(s-x_1), \quad \text{and}$$
$$\int_{-L}^{L} \frac{F(s)}{s-(x_1 \pm p_\alpha x_2)} ds = \int_{-L}^{L} \frac{F(s)}{s-x_1} ds \pm \mathrm{i}\pi F(x_1), \quad (215)$$

for $\mathrm{Im}[p_\alpha] > 0$ and arbitrary function $F(s)$. Then, substitution of equations (212) and (205) into (203) yields

$$\mathcal{A}\,\phi(s) + \frac{\mathcal{B}}{\pi} \int_{a}^{b} \frac{\phi(s)}{s-x_1} ds + \frac{1}{2\pi} \int_{a}^{b} \frac{\varrho(s,x_1)\phi(s)}{s-x_1} ds = \sigma_{22}^{\infty}(x_1) + \tau(x_1),$$
$$\mathrm{a} < x_1 < \mathrm{b} \quad (216)$$

where

$$\mathcal{A} = \frac{1}{2}[\widetilde{d}_{12} - i\widetilde{w}_3, \widetilde{d}_{23} + i\widetilde{w}_1][\widehat{N}^{-1} \begin{vmatrix} -\widetilde{w}_3 \\ \widetilde{w}_1 \end{vmatrix} + (\mathbf{X}_+(x_1)\Xi(x_1)\widehat{N}^{-1}$$
$$- \Lambda_+(x_1;\epsilon)) \begin{vmatrix} \widetilde{d}_{12} \\ \widetilde{d}_{23} \end{vmatrix}]$$
$$+ \frac{1}{2}[\widetilde{d}_{12} + i\widetilde{w}_3, \widetilde{d}_{23} - i\widetilde{w}_1][\, g(\epsilon)\widehat{N}^{-1} \begin{vmatrix} -\widetilde{w}_3 \\ \widetilde{w}_1 \end{vmatrix}$$
$$- (\mathbf{X}_-(x_1)\Xi(x_1)\widehat{N}^{-1} - \Lambda_-(x_1;\epsilon)) \begin{vmatrix} \widetilde{d}_{12} \\ \widetilde{d}_{23} \end{vmatrix}] \tag{217}$$

$$\mathcal{B} = -\widetilde{d}_{22} + i[\widetilde{d}_{12} - i\widetilde{w}_3, \widetilde{d}_{23} + i\widetilde{w}_1]\Lambda_+(x_1;\epsilon) \begin{vmatrix} \widetilde{d}_{12} \\ \widetilde{d}_{23} \end{vmatrix}$$
$$+ i[\widetilde{d}_{12} + i\widetilde{w}_3, \widetilde{d}_{23} - i\widetilde{w}_1]\Lambda_-(x_1;\epsilon) \begin{vmatrix} \widetilde{d}_{12} \\ \widetilde{d}_{23} \end{vmatrix} \tag{218}$$

$$\varrho(s,x_1) = -i[\widetilde{d}_{12} - i\widetilde{w}_3, \widetilde{d}_{23} + i\widetilde{w}_1]\mathbf{X}_+(x_1)h(s)$$
$$- i[\widetilde{d}_{12} + i\widetilde{w}_3, \widetilde{d}_{23} - i\widetilde{w}_1]\mathbf{X}_-(x_1)h(s) \tag{219}$$

$$h(s) = \mathbf{X}_+^{-1}(s)\widehat{N}^{-1} \begin{vmatrix} -\widetilde{w}_3 \\ \widetilde{w}_1 \end{vmatrix} + \Xi(s)\widehat{N}^{-1} \begin{vmatrix} \widetilde{d}_{12} \\ \widetilde{d}_{23} \end{vmatrix} \tag{220}$$

and

$$\tau(x_1) =$$
$$[\widetilde{d}_{12} - i\widetilde{w}_3, \widetilde{d}_{23} + i\widetilde{w}_1][i\ \frac{\mathbf{X}_+(x_1)}{2\pi} \int_{-L}^{L} \frac{[\mathbf{X}_+(s)]^{-1}}{s - x_1} \widehat{N}^{-1} \begin{vmatrix} \sigma_{12}^{\infty}(s) \\ \sigma_{32}^{\infty}(s) \end{vmatrix} ds$$
$$- \frac{1}{2} \widehat{N}^{-1} \begin{vmatrix} \sigma_{12}^{\infty}(x_1) \\ \sigma_{32}^{\infty}(x_1) \end{vmatrix}]$$
$$+ [\widetilde{d}_{12} + i\widetilde{w}_3, \widetilde{d}_{23} - i\widetilde{w}_1][i\ \frac{\mathbf{X}_-(x_1)}{2\pi} \int_{-L}^{L} \frac{[\mathbf{X}+(s)]^{-1}}{s - x_1} \widehat{N}^{-1} \begin{vmatrix} \sigma_{12}^{\infty}(s) \\ \sigma_{32}^{\infty}(s) \end{vmatrix} ds$$
$$- \frac{g(\epsilon)}{2} \widehat{N}^{-1} \begin{vmatrix} \sigma_{12}^{\infty}(x_1) \\ \sigma_{32}^{\infty}(x_1) \end{vmatrix}] \tag{221}$$

$$g(\epsilon) = V \mathrm{diag}[e^{\epsilon 2\pi}, e^{-\epsilon 2\pi}] V^{-1} \tag{222}$$

for arbitrary applied loading, or

$$\tau(x_1) = \{[\widetilde{d}_{12} - i\widetilde{w}_3, \widetilde{d}_{23} + i\widetilde{w}_1][i\ \Lambda_+(x_1;\epsilon)] +$$
$$[\widetilde{d}_{12} + i\widetilde{w}_3, \widetilde{d}_{23} - i\widetilde{w}_1][i\ \Lambda_-(x_1;\epsilon)]\} \begin{vmatrix} \sigma_{12}^{\infty} \\ \sigma_{32}^{\infty} \end{vmatrix} \tag{223}$$

for uniformly applied loading.

From equation (217), it is easy to see that for general anisotropic bimedia the coefficient $\mathcal{A}$ usually is not zero since it is possible that none of the $\widetilde{d}_{ij}$ and $\widetilde{w}_j$ $(i, j = 1, 2, 3)$ might be zero. This may imply that the solution of $\phi(s)$ $(|s| < 1)$ to equations (216) has the oscillatory property [37, pp.398]. This observation is different from the case of isotropic dissimilar bimedia, in which no such oscillatory property exists under Comninou's assumption. Therefore,

one important conclusion may be drawn here is that the Comninou model may not be able to completely eliminate the oscillatory, hence interpenetration or overlapping phenomenon in the solution to the interface crack problem for arbitrary anisotropic bimaterial media.

Mathematically, in order to solve equations (216), one needs some additional conditions such as single valuedness of displacement

$$\int_a^b \phi(\mathrm{s}) d\mathrm{s} = 0 \tag{224}$$

and positive crack opening displacements and negative contact zone traction

$$\begin{aligned} &\Phi_{2+}(x_1) - \Phi_{2-}(x_1) \geq 0, \qquad \mathrm{a} < x_1 < \mathrm{b}; \\ &\sigma_{22}(x_1) < 0, \qquad -\mathrm{L} < x_1 < \mathrm{a} \quad \text{and} \quad \mathrm{b} < x_1 < \mathrm{L} \end{aligned} \tag{225}$$

7.2 Solution by Contact Model to Some Dissimilar Anisotropic Bimaterial Composites

In previous section, it was shown that even using the Comninou model, one may not be able to eliminate the physically inadmissible interpenetration property in the solution to the interface crack problem of general anisotropic bimedia. But fortunately, for most engineering materials such as laminated composites which often have one symmetric plane, the $\widetilde{w}_2$ usually equals to zero. Hence, from equations (211), $\widetilde{\beta} = 0$ implies $\epsilon = 0$. Therefore, the oscillation in the shear stress and displacement fields disappears. Furthermore, one may readily show that the $\widetilde{d}_{12} = 0$ and $\widetilde{d}_{23} = 0$ for such type of materials. Then, a simple calculation can show that the coefficient $\mathcal{A} = 0$, which means the oscillatory character in the solution of $\phi(s)$ ($|s| < 1$) also disappears. Consequently, the equation (216) becomes

$$\frac{\widetilde{d}_{22}}{\pi}\int_a^b \frac{\phi(s)}{s-x_1}ds - \frac{1}{2\pi}\int_a^b \frac{\widetilde{\varrho}(s,x_1)\phi(s)}{s-x_1}ds = -\sigma_{22}^{\infty}(x_1) - \widetilde{\tau}(x_1), \qquad \text{a} < x_1 < \text{b} \tag{226}$$

where

$$\widetilde{\varrho}(s,x_1) = 2(\widetilde{w}_3^2/\widetilde{d}_{11} + \widetilde{w}_1^2/\widetilde{d}_{33})\frac{\sqrt{L^2-s^2}}{\sqrt{L^2-x_1^2}} \tag{227}$$

and

$$\widetilde{\tau}(x_1) = 2[\widetilde{w}_3, -\widetilde{w}_1]\frac{1}{2\pi\sqrt{L^2-x_1^2}}\int_{-L}^{L}\frac{\sqrt{L^2-s^2}}{s-x_1}\widehat{N}^{-1}\begin{vmatrix} \sigma_{12}^{\infty}(s) \\ \sigma_{32}^{\infty}(s) \end{vmatrix} ds \tag{228}$$

for arbitrary loading or

$$\widetilde{\tau}(x_1) = \frac{x_1}{\sqrt{L^2 - x_1^2}}[\frac{\widetilde{w}_1\sigma_{32}^{\infty}}{\widetilde{d}_{33}} - \frac{\widetilde{w}_3\sigma_{12}^{\infty}}{\widetilde{d}_{11}}] \tag{229}$$

for uniformly applied loading.

Let us consider a particular case, the isotropic bimedia case in which (Appendix F).

$$\widetilde{d}_{11} = \widetilde{d}_{22} = 1/[\eta(1-\beta^2)], \quad \widetilde{w}_3 = \beta/[\eta(1-\beta^2)] \qquad \text{and,} \quad \widetilde{w}_2 = 0 \tag{230}$$

If let

$$\sigma_{12}^{\infty}(x_1, 0) = \sigma_{32}^{\infty}(x_1, 0) = 0, \quad \sigma_{22}^{\infty}(x_1, 0) = T \quad \text{and,}$$

$$\gamma_a = |a/L|, \qquad \gamma_b = |b/L|. \tag{231}$$

then equation (226) can be reduced to

$$\widetilde{d}_{22}\int_{\gamma_a}^{\gamma_b} \frac{\phi(s)}{s - x_1} ds - \frac{\widetilde{w}_3^2}{\widetilde{d}_{11}}\int_{\gamma_a}^{\gamma_b} \frac{\sqrt{1-s^2}}{\sqrt{1-x_1^2}} \frac{\phi(s)}{s - x_1} ds = \pi T, \qquad \gamma_a < \ x_1 \ < \gamma_b \tag{232}$$

which is exactly the same as the equation (21) of [21]. This striking agreement justifies the validity of the method and deduction procedure in this paper. Similarly to the isotropic case, the stress intensity factors may be defined for practical engineering bimedia as

$$K = [K_2, K_1, K_3]^T = \begin{vmatrix} \lim\limits_{x_1 \to \pm L^+} \sqrt{2|x_1 \mp L|}\sigma_{12}(x_1, 0) \\ \lim\limits_{x_1 \to \pm L^-} \sqrt{2|x_1 \mp L|}\sigma_{22}(x_1, 0) \\ \lim\limits_{x_1 \to \pm L^+} \sqrt{2|x_1 \mp L|}\sigma_{32}(x_1, 0) \end{vmatrix} \tag{233}$$

From equations (207), (212) and (226), the stress intensity factors can be obtained as

$$
\begin{aligned}
K/\sqrt{L} &= [K_2, K_1, K_3]^T/\sqrt{L} \\
&= \left| \begin{array}{c} [\int_{-1}^{1} \sqrt{(1+s)/(1-s)}\sigma_{12}^{\infty}(s)ds \\ +\widetilde{w}_3 \int_{\gamma_a}^{\gamma_b} \sqrt{(1+s)/(1-s)}\phi(s)ds]/\pi, \\ [\widetilde{w}_1\sigma_{32}^{\infty}/\widetilde{d}_{33} - \widetilde{w}_3\sigma_{12}^{\infty}/\widetilde{d}_{11}] \\ +[\widetilde{w}_3^2/\widetilde{d}_{11} + \widetilde{w}_1^2/\widetilde{d}_{33}] \int_{\gamma_a}^{\gamma_b} \sqrt{(1+s)/(1-s)}\phi(s)ds/\pi \\ [\int_{-1}^{1} \sqrt{(1+s)/(1-s)}\sigma_{32}^{\infty}(s)ds - \widetilde{w}_1 \int_{\gamma_a}^{\gamma_b} \sqrt{(1+s)/(1-s)}\phi(s)ds]/\pi \end{array} \right|
\end{aligned} \tag{234}
$$

for arbitrary applied loading,or

$$
\begin{aligned}
K/\sqrt{L} &= [K_2, K_1, K_3]^T/\sqrt{L} \\
&= \left| \begin{array}{c} \sigma_{12}^{\infty} + [\widetilde{w}_3 \int_{\gamma_a}^{\gamma_b} \sqrt{(1+s)/(1-s)}\phi(s)ds]/\pi, \\ [\widetilde{w}_1\sigma_{13}^{\infty}/\widetilde{d}_{33} - \widetilde{w}_3\sigma_{12}^{\infty}/\widetilde{d}_{11}] \\ +[\widetilde{w}_3^2/\widetilde{d}_{11} + \widetilde{w}_1^2/\widetilde{d}_{33}] \int_{\gamma_a}^{\gamma_b} \sqrt{(1+s)/(1-s)}\phi(s)ds/\pi, \\ \sigma_{32}^{\infty} - [\widetilde{w}_1 \int_{\gamma_a}^{\gamma_b} \sqrt{(1+s)/(1-s)}\phi(s)ds]/\pi \end{array} \right|
\end{aligned} \tag{235}
$$

for uniformly applied loading.

Therefore, the energy release rate for which the interface crack tip extends from 'a' to $'a + \delta a'$ and 'L' to $'L + \delta L'$ can be calculated as

$$
\begin{aligned}
\mathcal{G}_0 = &\lim_{\delta a \to 0} \frac{1}{2} \int_a^{a+\delta a} \sigma_{11}(x_1, 0; L)\Delta u_2(x_1, 0; L)dx_1 \\
&+ \lim_{\delta L \to 0} \frac{1}{2} \int_L^{L+\delta L} \sigma_{12}(x_1, 0; L)\Delta u_1(x_1, 0; L)dx_1 \\
&+ \lim_{\delta L \to 0} \frac{1}{2} \int_L^{L+\delta L} \sigma_{32}(x_1, 0; L)\Delta u_3(x_1, 0; L)dx_1
\end{aligned} \tag{236}
$$

The first term has no contribution since $\Delta u_1(x_1) = 0$ for $a < x_1 < L$. Asymp-

totically,

$$\sigma_{12}(x_1, 0; L) \sim K_2/\sqrt{2(x_1 - L)}, \quad \sigma_{32}(x_1, 0; L) \sim K_3/\sqrt{2(x_1 - L)} \tag{237}$$

and

$$\begin{vmatrix} \Delta u_1(x_1, 0; L) \\ \Delta u_3(x_1, 0; L) \end{vmatrix} \sim \widehat{N}^{-1} \begin{vmatrix} K_2 \\ K_3 \end{vmatrix} \sqrt{2(L + \delta L - x_1)} \tag{238}$$

Substitution of equations (237) and (238) into (236) leads to

$$\mathcal{G}_0 = \frac{\pi}{4}[K_2, K_3]\widehat{N}^{-1} \begin{vmatrix} K_2 \\ K_3 \end{vmatrix} \tag{239}$$

For isotropic bimedia, equation (239) can be reduced to

$$\mathcal{G}_0 = \frac{\pi}{4}[K_2^2/\widetilde{d}_{11} + K_3^2/\widetilde{d}_{33}] \tag{240}$$

which is exactly the same as the equation (34) by Comninou in [21] if K_3 is not considered.

7.3 Some Examples for the Contact Zone Model

In this section, some numerical examples are given to illustrate the application of the theory and formulas for contact zone model to some practical engineering materials.

Making the change of variables with non-dimensional $|\mathrm{t}| < 1$ and $|\mathrm{t}_0| < 1$ such that

$$\mathrm{s} = \frac{b+a}{2} + \frac{b-a}{2}\mathrm{t}, \qquad x_1 = \frac{b+a}{2} + \frac{b-a}{2}\mathrm{t}_0. \tag{241}$$

then the equation (226) can be rewritten as

$$\frac{1}{\pi}\int_{-1}^{1} \frac{\widetilde{\mathcal{B}}\,\phi(t)}{t-t_0}dt + \int_{-1}^{1} k(t,t_0)\phi(t)dt = p(t_0), \qquad \text{-1} < \mathrm{t}_0 < 1 \tag{242}$$

where

$$\widetilde{\mathcal{B}}(t_0) = -\widetilde{d}_{22} + \widetilde{\varrho}(t_0,t_0)/2, \quad k(t,t_0) = \frac{1}{2\pi}\frac{\widetilde{\varrho}(t,t_0) - \widetilde{\varrho}(t_0,t_0)}{t-t_0},$$
$$p(t_0) = \sigma_{22}^{\infty}(t_0) + \widetilde{\tau}(t_0) \tag{243}$$

where

$$\widetilde{\varrho}(t,t_0) = 2(\widetilde{w}_3^2/\widetilde{d}_{11} + \widetilde{w}_1^2/\widetilde{d}_{33})\frac{\sqrt{1-[(\gamma_a+\gamma_b)/2 + (\gamma_a-\gamma_b)\mathrm{t}/2]^2}}{\sqrt{1-[(\gamma_a+\gamma_b)/2 + (\gamma_a-\gamma_b)\mathrm{t}_0/2]^2}} \tag{244}$$

and

$$\widetilde{\tau}(\mathrm{t}_0) = \frac{(\gamma_a+\gamma_b)/2 + (\gamma_a-\gamma_b)\mathrm{r}_0/2}{\sqrt{1-[(\gamma_a+\gamma_b)/2 + (\gamma_a-\gamma_b)\mathrm{r}_0/2]^2}}[\widetilde{w}_1\sigma_{32}^{\infty}/\widetilde{d}_{33} - \widetilde{w}_3\sigma_{12}^{\infty}/\widetilde{d}_{11}] \tag{245}$$

Since the contact zone is assumed to be smooth, there should be no singularity at $t_0 = \pm 1$. One can therefore let

$$\phi(t) = w(t)\sqrt{1-t^2} \tag{246}$$

where $w(t)$ is continuous, bounded function on the interval $t \in [-1,\ 1]$. And also one can have

$$\sigma_{22} = 0, \quad \text{at} \quad t_0 = \pm 1 \tag{247}$$

The equation (242) then can be discretized with Chebyshev polynomials of the second kind [18] and it reads as

$$\sum_{j=1}^{\mathrm{n}} \frac{1-t_j^2}{\mathrm{n}+1}[\frac{\mathcal{B}(t_{0k})}{t_j - t_{0k}} + \pi k(t_{0k}, t_j)]w(t_j) = p(t_{0k}) \tag{248}$$

where

$$t_j = \cos[\frac{j\pi}{\mathrm{n}+1}], \quad j = 1, 2, ...\mathrm{n} \tag{249}$$

$$t_{k0} = \cos[\frac{(2k-1)\pi}{2(\mathrm{n}+1)}], \quad k = 1, 2, ...\mathrm{n}{+}1 \tag{250}$$

Equation (248) provides n+1 equations to determine the n-values $\phi(t_j)$ and $\gamma_a = |a/L|$ and $\gamma_b = |b/L|$. It may need to be mentioned that n should be chosen to be an even number, and the equation (n/2) + 1 then can to be singled out. It is easily seen that equation (248) is a system of nonlinear equations due to the presence of the unknown ratios $|a/L|$ and $|b/L|$. In practical computation, the ratios γ_a and γ_b are assumed first, then equations (248) are solved with n unknown $w(t_j)$. By repeating this process, a plot of

σ_{22} at $t_0 = -1$ and $t_0 = 1$ versus $|a/L|$ and $|b/L|$, respectively can be obtained. The corresponding values of 'a' and 'b' at which the $\sigma_{22} = 0$ are determined as the root of these curves.

Without loss of generality and simplifying the calculation, it can be further assumed that a = −b, then $\gamma_a = \gamma_b = \gamma$, and the equations (244) and (245) become as

$$\widetilde{\varrho}(t, t_0) = 2(\widetilde{w}_3^2/\widetilde{d}_{11} + \widetilde{w}_1^2/\widetilde{d}_{33})\frac{\sqrt{1-[\gamma \mathrm{t}]^2}}{\sqrt{1-[\gamma \mathrm{t}_0]^2}} \tag{251}$$

and

$$\widetilde{\tau}(\mathrm{t}_0) = \frac{\gamma \mathrm{t}_0}{\sqrt{1-[\gamma \mathrm{t}_0]^2}}[\widetilde{w}_1\sigma_{32}^{\infty}/\widetilde{d}_{33} - \widetilde{w}_3\sigma_{12}^{\infty}/\widetilde{d}_{11}] \tag{252}$$

The stress intensity factors of equation (235) can be expressed in a discretized form as

$$\begin{aligned} K/\sqrt{L} &= [K_2, K_1, K_3]^T/\sqrt{L} \\ &= \left| \begin{array}{c} \sigma_{12}^{\infty} - \widetilde{w}_3\gamma \sum_j^n w(t_j)(1-t_j^2)\sqrt{1-\gamma^2 t_j^2}/(n+1)/(\gamma t_j - 1) \\ [\widetilde{w}_1\sigma_{32}^{\infty}/\widetilde{d}_{33} - \widetilde{w}_3\sigma_{12}^{\infty}/\widetilde{d}_{11}] - \frac{[\widetilde{w}_3^2/\widetilde{d}_{11} + \widetilde{w}_1^2/\widetilde{d}_{33}]}{(n+1)(\gamma t_j - 1)}\gamma \sum_j^n w(t_j)(1-t_j^2)\sqrt{1-\gamma^2 t_j^2} \\ \sigma_{32}^{\infty} + \widetilde{w}_1\gamma \sum_j^n w(t_j)(1-t_j^2)\sqrt{1-\gamma^2 t_j^2}/(n+1)/(\gamma t_j - 1) \end{array} \right| \end{aligned} \tag{253}$$

Let's first consider the fiber-reinforced composites $[\pm\theta^o]$ with the following elastic constants

$$E_T = E_Z = 2.1E, \quad E_L = 20E; \quad G_{LT} = G_{LZ} = G_{TZ} = 0.85E$$

$$E = 0.6895GPa, \quad \nu_{LT} = \nu_{LZ} = \nu_{TZ} = 0.21. \tag{254}$$

where, subscripts L, T, and z refer to longitudinal,. transverse, and through-thickness directions, respectively.

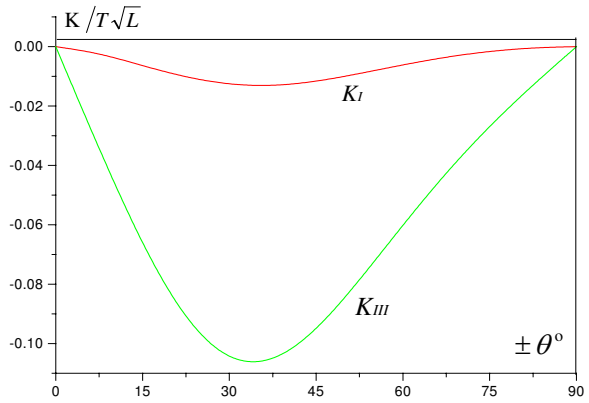

Fig.7.2 Stress Intensity Factors for an interface crack in $[\theta^o/-\theta^o]$ composites under pure tension $\sigma_{22}^{\infty} = T$

In this case, the upper half space is occupied by material $'I'$, which is located at orientation angle θ^o with respect to x_3, and the lower half space is occupied by material $'II'$ oriented at -θ^o with respect to x_3. Due to the symmetry, it is easy to see that $\widetilde{d}_{12} = \widetilde{d}_{23} = 0$, and $\widetilde{w}_2 = \widetilde{w}_3 = 0$. The equations (253) and (240) show that we need only to consider $K_I(L)$ and

$K_{III}(L)$ and G_{III}. Plotted in Fig. 7.2 are the mode I and mode III stress intensity factors under pure tension. Fig. 7.3 is the corresponding energy release rate.

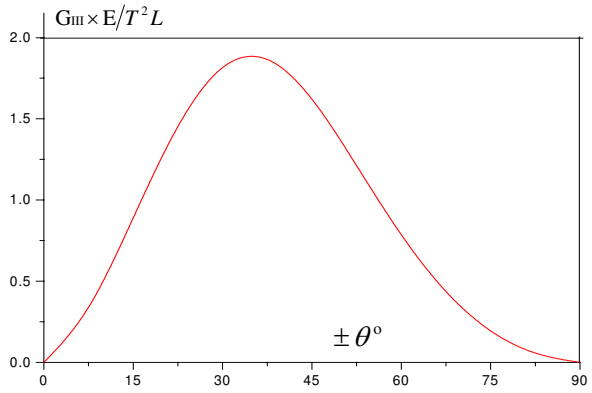

Fig. 7.3 Energy Release Rate($E = 10^6$)for an interface delamination in $[\theta^o/-\theta^o]$ composites under pure tension $\sigma_{22}^{\infty} = T$

The negative $K_I(L^-)$ in Fig. 7.2 means that the interaction between the two interfaces of the bimedia within the contact zone is pressure, not tension. This verifies the correctness of the Comninou assumption and theory or formulas developed in this chapter. The $K_{III}(L)$ and G_{III} in our calculation are in good agreement with the K_{III} in Fig. 4 and G_{III} in Fig. 5 of [48]. The $K_{III}(L)$ in Fig. 3 of [50] looks similar to ours except its opposite sign. But the energy release rate G_{III} in Fig. 4 of [50] is different from those in [48] and ours. The difference may come from the fact that the formulas in [50] were simply the extension of these corresponding formulas for isotropic bimedia. The study in

previous sections of this chapter shows that the phenomena of interface crack of anisotropic bimedia and isotropic bimaterials are quite different. Therefore, the results of isotropic cases may not be extend directly to anisotropic cases. For example, the discontinuity in K_{III} at $\theta = 0^0$ and $\theta = 90^0$ in Fig. 3 and Fig. 5 in [50], which corresponds to the homogeneous anisotropic media, may not be in agreement with the result of equation (29) and (31) by Sih and Paris [39].

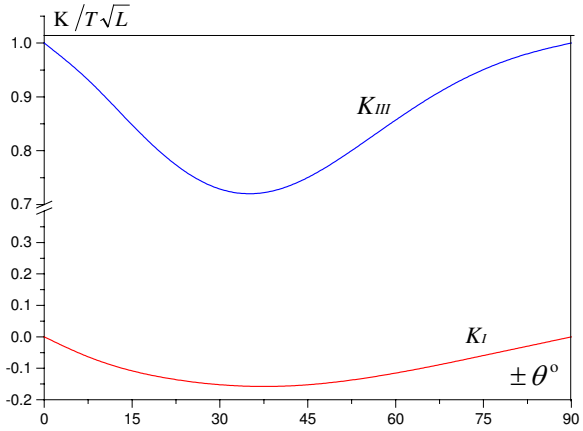

Fig .7.4 Stress Intensity Factors for an interface delamination in $[\theta^o/-\theta^o]$ composites under applied loading $\sigma_{22}^{\infty} = \sigma_{32}^{\infty} = T$

Fig. 7.4 and Fig. 7.5, respectively are the stress intensity factors and energy release rate for this material system under a combined tensile and anti-plane shear loading. An interesting result in these plots is that the minimum K_{III} and G occurs around $\theta = \pm 37.5^o$ and $\theta = \pm 30^o$, respectively. This observation could tell that this study would present the optimum angles for the fibers orientation which could be useful for manufacturing the fiber-reinforced composites.

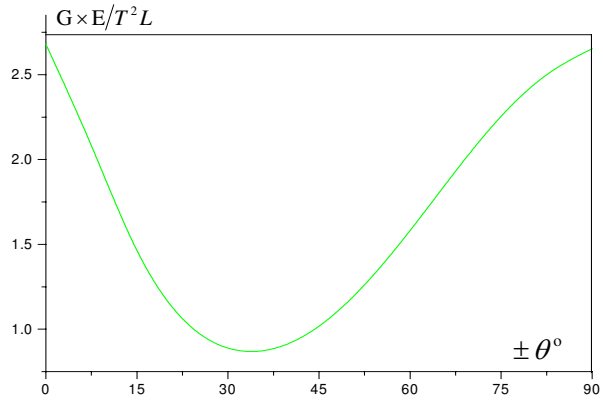

Fig .7.5 Energy Release Rate($E = 10^4$) for an interface delamination in $[\theta^o/-\theta^o]$ composites under applied loading $\sigma_{22}^{\infty} = \sigma_{32}^{\infty} = T$

Next, we consider a laminated composites system of $[30^o/\theta^o]$, in which $\widetilde{d}_{12} = \widetilde{d}_{23} = 0$ and $\widetilde{w}_2 = 0$ since the system is symmetric with respect to $x_2 = 0$. The stress intensity factors K_{II} and K_{III} for the composites under pure tension change their sign across $\theta = 30^0$ as shown on Fig. 7.6. K_{II} reaches its maximum value at $\theta = 0^o$ while K_{III} at $\theta = 60^o$. This tendency can also be seen on Fig. 7.8, which shows the results of K_{II} and K_{III} under combined tensive and anti-plane shear loading. The energy release rate G for pure tension and combined loading cases are presented on Fig. 7.7 and Fig. 7.9, respectively.

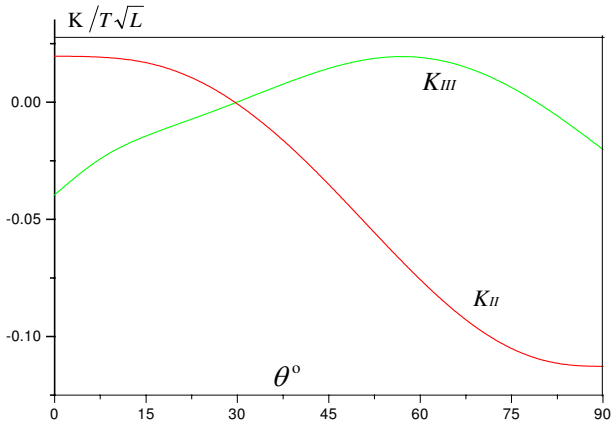

Fig .7.6 Stress Intensity Factors for an interface delamination in $[30^o/\theta^o]$ composites under pure tension $\sigma_{22}^{\infty} = T$

The minimum value $G_{\min}$ of G for combined loading happens when $\theta = 90^o$ (Fig. 7.9), at which the G attains its maximum value $G_{\max}$ under pure tension(Fig. 7.7). But the magnitude of $G_{\min}$ of the combined loading case is much larger than that of $G_{\max}$ under pure tension. This result together with the result for K_{II} and K_{III} on Fig. 7.6 and Fig. 7.8 may imply that the optimum orientation angle value between these two media is 60^0 in order to minimize the possibility of the interface crack growth.

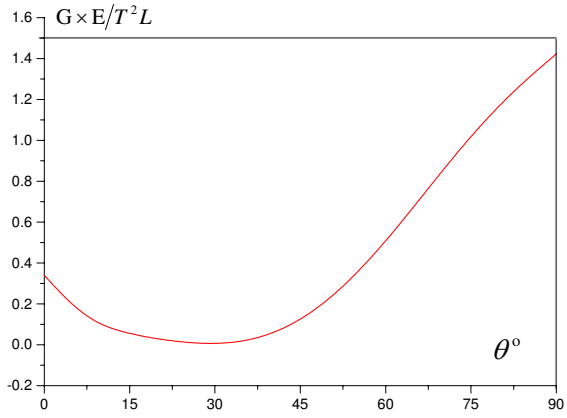

Fig. 7.7 Energy Release Rate($E = 10^6$) for an interface delamination in $[30^o/\theta^o]$ composites under pure tension $\sigma_{22}^{\infty} = T$

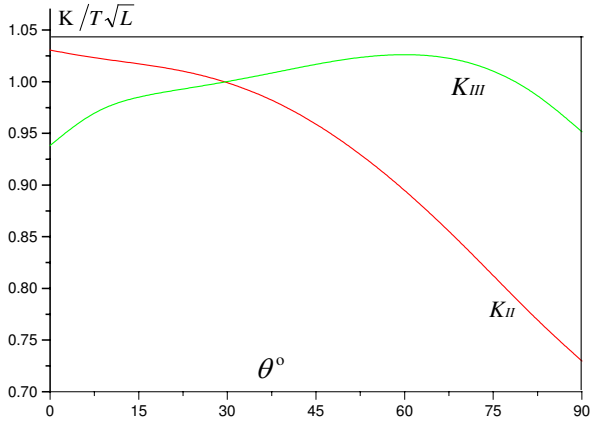

Fig. 7.8 Stress Intensity Factors for an interface delamination in $[30^o/\theta^o]$ composites under applied loading $\sigma_{12}^{\infty} = \sigma_{22}^{\infty} = \sigma_{32}^{\infty} = T$

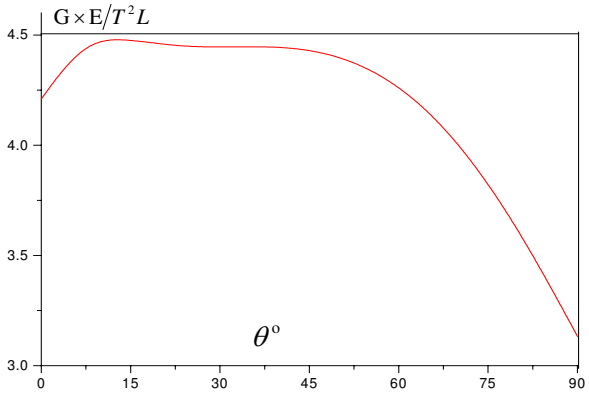

Fig. 7.9 Energy Release Rate($E = 10^4$) for an interface delamination in $[30^o/\theta^o]$ composites under applied loading $\sigma_{12}^{\infty} = \sigma_{22}^{\infty} = \sigma_{32}^{\infty} = T$

Chapter VIII

Conclusions and Recommendation

In this chapter, some conclusions will be drawn based on the results of the current research. Besides these results, the method developed in the present work may also have further applications in some more complicated problems such as three dimensional (3-D) thermal-elastic interface delamination branching behavior for dissimilar anisotropic bimaterials. Some insight on how to expand the two dimensional method to 3-D problem will also offered in this chapter.

8.1 Conclusions and Discussions

In the present research, the study of the thermo-elastic interface delamination branching behavior has been carried out for anisotropic bimaterial media. In this study, Stroh's dislocation formulas, extended to thermo-elasticity were used. The analytic continuation principle of complex analysis was incorporated into this research. A compact form of a general solution was presented in solving the problem of thermo-elastic interface delamination of dissimilar anisotropic bimaterial media. A closed form solution was also formulated

here for the interaction between the dislocations (heat vortex and conventional dislocation) and the interface delamination in terms of matrix notation. The thermo-elastic interface delamination branching phenomenon for dissimilar anisotropic bimaterial media was subsequently investigated in detail. The influence of thermal loading on the onset of interface delamination branching was addressed. The results in this study also justify that the method and formulas in the present work could be applied to isotropic bimaterial media and homogeneous anisotropic/isotropic delamination branching problems.

From the general solution in this paper, we can observe that the delamination tip (point 'a' in Fig. 5.1) stress fields and the displacement fields along the interface usually have the convectional oscillatory character depending on the bimaterial property ϵ. These results are in agreement with those in literature [1]. We also found that the fields around 'b' have no singular but oscillatory character which depends not only on the bimaterial property but also on the branching angle. This observation can be explained well from the physical point of view. Before the delamination branched, the point 'b' had singular fields. Once the crack branched, a large amount of strain energy was released, therefore the singularity of those fields around point 'b' relaxed, or disappeared.

Here, we may also need to mention that some results regarding crack branching without thermal effects in the literature, especially for those con-

cerned with energy release rate, obviously contradicts the secondary delamination phenomenon in laminated composites and matrix cracks phenomenon in reinforced composites. But all the results in the current research are consistent with the observed fracture phenomena in composites and sandwich coupons with delaminations. The simulation results from extensive cases analysis in this paper suggest the following important conclusions:

(1). K-based criteria and G-based criteria are consistent in isotropic cases. But for anisotropic monolithic and bimaterial media cases, the predications based on K criteria contradict the observed fracture phenomena while the G-criteria gives a very reasonable predications. For example, the maximum values of K_I occurs when the crack branches into the stiffer material of the bimedia, which is rarely observed; while the $\mathcal{G}$ attains its maximum values when the interface crack extends into the weaker (more compliant) medium and tries to follow the stronger principal material axis of this weaker medium, which remarkably agrees with the well-known observed facts in fracture phenomena.

(2). The degree of anisotropy has a great influence on the crack branching modes, e.g. for a crack located along the stiffer material axis of the monolithic anisotropic solid, when s_{22}/s_{11} below is 4.15, the crack branch may not happen in some material or a secondary delamination which is close and parrel to the original delamination may be created in laminated composites; but when s_{22}/s_{11} is above 4.15, the delamination between the reinforcing fibers and the

matrix branches into the matrix in a direction nearly perpendicular to the fibers which often happens in some materials like fiber strongly reinforced composites.

(3). For general dissimilar anisotropic bimaterial media, there usually exists a huge interaction energy between the thermal loading and the mechanical loading for a structure with defects. This may explain why a catastrophic failure could easily happen when an imperfect bimaterial structure being exposed to a sudden fire.

(4). For some anisotropic bimaterial media, negative K_I (overlapping of the delamination faces around the crack tip) is possible under certain loading conditions due to the thermal effects.

(5). There exists an optimal orientation angle difference between the two constituents of a bimaterial media. This optimal difference could minimize the value of maximum energy release rate.

Therefore, the maximum energy release rate criterion may be an adequate criterion for the prediction of monolithic anisotropic crack branching phenomenon and interface delamination branching phenomenon in dissimilar anisotropic bimaterial media. The results in the current research would provide some useful guidelines for practical engineering design.

Furthermore, one may see that the oscillatory property vanishes if the matrix $W = 0$ of (72). But even for no-null $W \neq 0$, the introduction of the contact zone model works well for most practical materials. Theoretical solution from rigorous mathematical deduction and numerical results of the contact model on eliminating the interface interpenetration presents the following suggestions:

(1). For arbitrary anisotropic bimaterial, the usage of the Comninou model may not be able to eliminate the oscillatory property in the solution for the interface crack. This observation is different from the isotropic bimaterial case for which Comninou assumption was originally proposed.

(2). Under Comninou Assumption, the oscillatory character in shear stress and displacement fields depends only on the parameter $\widetilde{w}_2$ of the bimaterial matrix $\widetilde{W}$. If the two other elements $\widetilde{d}_{12}$ and $\widetilde{d}_{23}$ of the bimaterial matrix $\widetilde{D}$ are also zero, then the overlapping or interpenetration phenomenon will disappear. Therefore, Comninou model may be generally valid for such dissimilar anisotropic bimaterial media that the three parameters $\widetilde{d}_{12} = 0$, $\widetilde{d}_{23} = 0$ and $\widetilde{w}_2 = 0$.

(3). Fortunately, for most practical engineering anisotropic materials such as laminated composites with one symmetric plane, these three elements ($\widetilde{d}_{12}$, $\widetilde{d}_{23}$ and $\widetilde{w}_2$) usually equal to zeros. This implies that the Comninou contact model would work well for engineering practice on eliminating the oscillatory

property in the solution of dissimilar anisotropic bimedia interface crack problem.

(4). Observations from the numerical results here may provide some good criteria on manufacturing fiber reinforced composites. For a symmetric material system, the optimum orientation between two lamina may be around $\theta = \pm 30^0$ with respect to the coordinate x_3. If one of the two lamina is already located at an angle of 30^0 with respect to x_3, then the optimum angle for the other lamina is 60^0 with respect to the first lamina. These observations may be helpful on the design of fiber reinforced composites.

8.2 Recommendation for Future Work

It is well known that three dimensional (3-D) interface branching problems often happen in reality. Due to the complexity introduced, the 3-D interface branching problems become very hard to deal with, and no single work on this subject is available so far. Fortunately, the approach of the current research on two dimension issues can be extended to 3-D problems. Some insight will be offered on how to extend the current method to the 3-D problems the sake of future work.

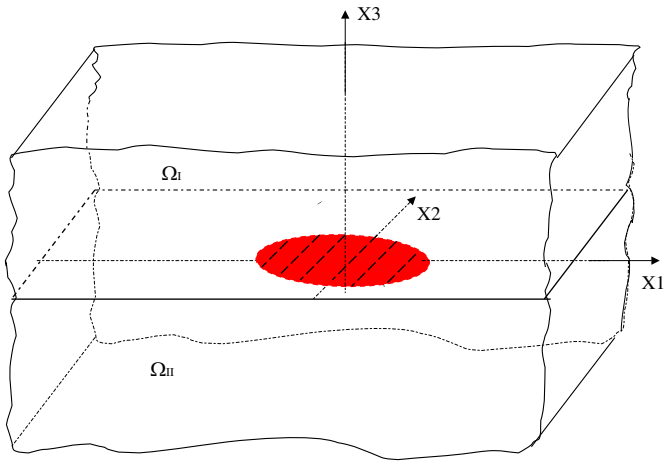

Fig.8.1 An interface delamination in a 3D dissimilar anisotropic bimedium

The procedure to solve the 3-D problem of thermo-elastic interface delamination branching can be as follows:

(1). by employing the Radon transform [41] combined with method of complex analysis and the analytic continuation principle to the extended Stroh's dislocation formulas in matrix notation, the 3-D problem can become a two dimensional (2-D) problem in the Radon transformation space;

(2). in the transformed space, the 2-D problem would be solved by a similar approach as in the current research;

(3). by using the inverse Radon transform to turn the solution back to the original 3-D physical space, the study of the 3-D thermo-elastic interface delamination branching could be completed.

Extension of 2D Stroh's Formulation to 3-D Anisotropic Elasticity

To use the above procedure to solve the 3-D thermo-elastic delamination branching problem, one may need first to extend the 2D Stroh's Formulation to 3D anisotropic elasticity. This section serves this purpose.

As described in Chapter II, the linear relationship, in a fixed Cartesian coordinate system (x_1, x_2, x_3), of the stresses $\sigma_{ij}(x_1, x_2, x_3)$, the displacements $u_k(x_1, x_2, x_3)$, and the heat flux $h_i(x_1, x_2, x_3)$ and temperature $\Theta(x_1, x_2, x_3)$ in an anisotropic elastic medium could be rewritten as follows,

$$h_i = -k_{ij}\Theta_{,j}, \tag{255}$$

$$\sigma_{ij} = C_{ijkl}\, u_{k,l} - \beta_{ij}\Theta. \tag{256}$$

where i, j, k, l range in $(1, 2, 3)$ and the repeated indices imply summation, the comma stands for differentiation with respect to the corresponding coordinate variables, C_{ijkl} is the elastic moduli tensor with properties of

$$C_{ijkl} = C_{jikl} = C_{ijlk} = C_{klij} \tag{257}$$

k_{ij} are coefficients of heat conduction and β_{ij} are the stress-temperature coefficients. The conservation of energy and equilibrium equations in terms of

displacements in the absence of body force can be rewritten as:

$$h_{i,i} = 0, \quad \text{i.e.} \qquad k_{ij}\frac{\partial^2 \Theta}{\partial x_l \partial x_j} = 0, \tag{258}$$

$$\sigma_{ij,j} = 0, \quad \text{i.e.} \qquad C_{ijkl}\,\frac{\partial^2 \mathbf{u}_k(x_1, x_2, x_3)}{\partial x_l \partial x_j} - \beta_{ij}\frac{\partial \Theta}{\partial x_j} = 0. \tag{259}$$

The traction and in-plane stress are denoted , respectively, as

$$\begin{aligned}\mathbf{t} &= (\sigma_{13}, \sigma_{23}, \sigma_{33}) \\ &= (C_{13kl}\mathbf{u}_{k,l} - \beta_{13}\Theta,\ C_{23kl}\mathbf{u}_{k,l} - \beta_{23}\Theta,\ C_{33kl}\mathbf{u}_{k,l} - \beta_{33}\Theta), \qquad (260)\\ \mathbf{s} &= (\sigma_{11}, \sigma_{12}, \sigma_{22}) \\ &= (C_{11kl}\mathbf{u}_{k,l} - \beta_{11}\Theta,\ C_{12kl}\mathbf{u}_{k,l} - \beta_{12}\Theta,\ C_{22kl}\mathbf{u}_{k,l} - \beta_{23}\Theta) \qquad (261)\end{aligned}$$

The Radon transforms for the space R^2 are defined as [52]

$$\begin{aligned}\mathcal{R}\{\mathbf{\Theta}\} = \hat{\mathbf{\Theta}}(\rho, \theta, x_3) \ &= \ \iint_{R^2} \mathbf{\Theta}(x_1, x_2, x_3)\delta(\rho - \mathbf{n}\cdot\mathbf{x})d\mathbf{x}, \\ \mathcal{R}\{\mathbf{\Theta}_{,lj}\} &= n_l n_j \frac{\partial^2 \hat{\mathbf{\Theta}}}{\partial \rho^2} \qquad (262)\\ \mathcal{R}\{\mathbf{u}_k\} = \hat{\mathbf{u}}_k(\rho, \theta, x_3) \ &= \ \iint_{R^2} \mathbf{u}_k(x_1, x_2, x_3)\delta(\rho - \mathbf{n}\cdot\mathbf{x})d\mathbf{x}, \\ \mathcal{R}\{\mathbf{u}_{k,lj}\} &= n_l n_j \frac{\partial^2 \hat{\mathbf{u}}_k}{\partial \rho^2} \qquad (263)\end{aligned}$$

and the inverse Radon transforms[52] are

$$\mathbf{\Theta}(x_1, x_2, x_3) = \oint\limits_{|\mathrm{n}|=1} d\mathrm{n} \int_{-\infty}^{\infty} \frac{\hat{\mathbf{\Theta}}_{,\rho}(\rho, \mathrm{n}, x_3)}{\rho - \mathrm{n} \cdot \mathrm{x}} d\rho,$$

$$\mathbf{u}_k(x_1, x_2, x_3) = \oint\limits_{|\mathrm{n}|=1} d\mathrm{n} \int_{-\infty}^{\infty} \frac{\hat{\mathbf{u}}_{k,\rho}(\rho, \mathrm{n}, x_3)}{\rho - \mathrm{n} \cdot \mathrm{x}} d\rho \tag{264}$$

where

$$\mathbf{x} = (x_1, x_2), \quad \mathbf{n} = [n_1, n_2, n_3]^T = [\cos\theta,\ \sin\theta,\ 0]^T \tag{265}$$

and a superscript 'T' stands for the transpose of a matrix.

Applying the Radon transforms to the equation (259) leads to

$$C_{ijks} n_j n_s \frac{\partial^2 \hat{\mathbf{u}}_k}{\partial \rho^2} + (C_{ijks} + C_{iskj}) n_j m_s \frac{\partial^2 \hat{\mathbf{u}}_k}{\partial \rho \partial x_3} + C_{ijks} m_j m_s \frac{\partial^2 \hat{\mathbf{u}}_k}{\partial x_3^2}$$
$$- (\beta_{ij} n_j \frac{\partial \hat{\Theta}}{\partial \rho} + \beta_{is} m_s \frac{\partial \hat{\Theta}}{\partial x_3}) = 0 \tag{266}$$

where, $\mathbf{m} = [m_1, m_2, m_3]^T = [0,\ 0,\ 1]^T$.

Without loss of generality, one non-trivial solution to (266) takes the following form

$$\hat{\mathbf{u}}_k = a_{kj} \phi(\zeta_j) + \bar{a}_{kj} \bar{\phi}(\bar{\zeta}_j) + c_k \chi(\zeta_\tau) + \bar{c}_k \bar{\chi}(\bar{\zeta}_\tau), \tag{267}$$

$$\hat{\Theta} = \chi^{'}(\zeta_\tau) + \bar{\chi}^{'}(\bar{\zeta}_\tau), \qquad \zeta_j = \rho + p_j x_3, \quad \zeta_\tau = \rho + \tau x_3 \tag{268}$$

if $a_k = [a_{k1}, a_{k2}, a_{k3}]^T$ and p satisfy the eigenequations

$$[C_{ijks} n_j n_s + (C_{ijks} + C_{iskj}) n_j m_s\ p + C_{ijks} m_j m_s\ p^2] a_k = 0, \tag{269}$$

and, $\mathbf{c} = [c_1, c_2, c_3]^T$ and τ are solutions of the following equations

$$k_{js}n_jn_s + (k_{js} + k_{sj})n_jm_s\tau + k_{js}m_jm_s\tau^2 = 0, \tag{270}$$

$$[C_{ijks}n_jn_s + (C_{ijks} + C_{iskj})n_jm_s\ \tau + C_{ijks}m_jm_s\ \tau^2]c_k = (\beta_{ij}n_j + \beta_{is}m_s\tau) \tag{271}$$

In equation (268), $\bar{\zeta}$ denotes the conjugate of an complex ζ, p_j is the j^{th} eigenvalue , a_k is the k^{th} eigenvector (269) and $\phi(\zeta_j)$ is an eigenfunction vector of equation(269), χ is the temperature potential.

The stress functions corresponding to equation (268) can be written as

$$\hat{\varphi}_k = b_{kj}\phi(\zeta_j) + \bar{b}_{kj}\bar{\phi}(\bar{\zeta}_j) + d_k\chi(\zeta_\tau) + \bar{d}_k\bar{\chi}(\bar{\zeta}_\tau), \tag{272}$$

If three material property matrices Q, R, T are defined as

$$Q_{ik} = C_{ijks}n_jn_s, \quad R_{ik} = C_{ijks}n_jm_s, \quad T_{ik} = C_{ijks}m_jm_s \tag{273}$$

then one can easily show the following relations by making use of $\sigma_{ij} = \sigma_{ji}$,

$$\mathbf{b}_k = (R^T + p\ T)\mathbf{a}_k = -\frac{1}{p}(Q + pR)\mathbf{a}_k,$$
$$d = (R^T + \tau\ T)\mathbf{c} - \beta_2 = -\frac{1}{\tau}(Q + \tau R)\beta_1$$

where

$$\beta_1 = [\beta_{1j}n_j,\ \beta_{2j}n_j,\ \beta_{3j}n_j]^T,$$

$$\beta_2 = [\beta_{1s}m_s,\ \beta_{2s}m_s,\ \beta_{3s}m_s]^T$$

By denoting $A = [\mathbf{a}_1, \mathbf{a}_2, \mathbf{a}_3]$, $B = [\mathbf{b}_1, \mathbf{b}_2, \mathbf{b}_3]$, equation $()_2$ could be recast in the following matrix form,

$$N \begin{vmatrix} \mathbf{a} \\ \mathbf{b} \end{vmatrix} = p \begin{vmatrix} \mathbf{a} \\ \mathbf{b} \end{vmatrix}, \qquad N \begin{vmatrix} \mathbf{c} \\ \mathbf{d} \end{vmatrix} = \tau \begin{vmatrix} \mathbf{c} \\ \mathbf{d} \end{vmatrix} - \begin{vmatrix} 0 & N_2 \\ I & N_1^T \end{vmatrix} \begin{vmatrix} \beta_1 \\ \beta_2 \end{vmatrix}$$

where,

$$N_1 = -T^{-1}\, R^{\mathrm{T}},\ N_2 = T^{-1},\ N_3 = R\, T^{-1}\, R^{\mathrm{T}} - Q,\ N_4 = N_1^T$$

The displacement functions, stresses functions and traction can be rewritten in the transformed space in the matrix form

$$\hat{\mathbf{u}}(\rho, \theta, x_3) = A\ \phi(\zeta_j) + \bar{A}\ \bar{\phi}(\bar{\zeta}_j) + c\ \chi(\zeta_\tau) + \bar{c}\ \bar{\chi}(\bar{\zeta}_\tau),$$

$$\hat{\varphi}(\rho, \theta, x_3) = B\ \phi(\zeta_j) + \bar{B}\ \bar{\phi}(\bar{\zeta}_j) + d\ \chi(\zeta_\tau) + \bar{d}\ \bar{\chi}(\bar{\zeta}_\tau),$$

$$\hat{\mathbf{t}}(\rho, \theta, x_3) = B\ \phi^{'}(\zeta_j) + \bar{B}\ \bar{\phi}^{'}(\bar{\zeta}_j) + d\ \chi^{'}(\zeta_\tau) + \bar{d}\ \bar{\chi}^{'}(\bar{\zeta}_\tau),$$

$$\hat{\mathbf{s}}(\rho, \theta, x_3) = \mathcal{B}\ \phi^{'}(\zeta_j) + \bar{\mathcal{B}}\ \bar{\phi}^{'}(\bar{\zeta}_j) + \mathcal{S}\ \chi^{'}(\zeta_\tau) + \mathcal{S}\ \bar{\chi}^{'}(\bar{\zeta}_\tau),$$

$$\zeta_j = \rho + p_j\ x_3, \quad \zeta_\tau = \rho + \tau\ x_3.$$

where

$$\mathcal{B} = (n_s + p\ m_s) \begin{vmatrix} C_{111s} & C_{112s} & C_{113s} \\ C_{211s} & C_{212s} & C_{213s} \\ C_{221s} & C_{222s} & C_{223s} \end{vmatrix} A,$$

$$\mathcal{S} = (n_s + \tau\ m_s) \begin{vmatrix} C_{111s} & C_{112s} & C_{113s} \\ C_{211s} & C_{212s} & C_{213s} \\ C_{221s} & C_{222s} & C_{223s} \end{vmatrix} c - \begin{vmatrix} \beta_{11} \\ \beta_{12} \\ \beta_{22} \end{vmatrix}$$

As pointed in Chapter II, with the positive definite property of the strain energy density for an elastic system in stable equilibrium, p_j are complex values. The roots p_j will be assumed all distinct, and equal roots are viewed as the limiting case of the distinct roots and if p_j is an eigenvalue of equation () then $\bar{p}_j$ is also an eigenvalue of equation () since C_{ijkl} are real numbers.

By the same token, the 3-D boundary conditions would also be turned into 2-D boundary conditions in the transformed space.

Having obtained the above formulas, one then may investigate the 3-D thermo-elastic interface delamination branching behavior in dissimilar anisotropic bimaterial media.

Appendix A

Contour Integral for the Interaction Function

From equations (68) and (83), the interaction stress functions read as

$$\Phi'(z) = \frac{1}{2\pi} X(z)[\int_a^b \frac{X_+^{-1}(x_1)}{x_1 - z} N^{-1}[p_0 + p_1^* x_1 + p_2^* \, \mathrm{i}\sqrt{(x_1 - a)(b - x_1)}] \, dx_1 + Q_1(z)]$$

where,

$$p_1^* = (\rho_1 + \rho_2)h_0^*, \quad p_2^* = (\rho_2 - \rho_1)h_0^*, \quad h_0^* = -\mathrm{i}\frac{k_{\mathrm{I}} + k_{\mathrm{II}}}{2k_{\mathrm{I}} \, k_{\mathrm{II}}} h_0$$

By using contour integral one can get

$$J_1 \equiv \frac{X(z)}{2\pi} \int_a^b \frac{X_+^{-1}(x_1)}{x_1 - z} N^{-1} p_0 \, dx_1 = \mathrm{v} \, \{\mathrm{I} - \mathrm{x}(z)\Delta(z;\epsilon)[\Xi(z) + \Pi_1]\} \, \mathrm{v}^{-1}(N + \overline{N})^{-1}(\mathrm{i}p_0)$$

$$J_2 \equiv \frac{X(z)}{2\pi} \int_a^b \frac{x_1 \, X_+^{-1}(x_1)}{x_1 - z} N^{-1} p_1^* \, dx_1$$
$$= \mathrm{v}\{\Xi(z) - \mathrm{x}(z)\Delta(z;\epsilon)[\Xi(z^2) + \Pi_1\Xi(z) - \Pi_2]\}\mathrm{v}^{-1}(N + \overline{N})^{-1}(\mathrm{i}p_1^*);$$

$$J_3 \equiv \frac{X(z)}{2\pi} \int_a^b \frac{\mathrm{i}\sqrt{(x_1 - a)(b - x_1)} \, X_+^{-1}(x_1)}{x_1 - z} N^{-1} p_2^* \, dx_1$$
$$= \mathrm{v}\{\mathrm{x}^{-1}(z) - \mathrm{x}(z)\Delta(z;\epsilon)[\Xi(z^2) - \Pi_3\Xi(z) + \Pi_4\}\mathrm{v}^{-1}(N + \overline{N})^{-1}(\mathrm{i}p_2^*)$$

$$
\begin{aligned}
J_4 &\equiv \frac{X(z)}{2\pi} Q_1(z) \\
&= \mathrm{vdiag}[0,\ 0\ , -\frac{(a-b)^2}{8}\frac{1}{\sqrt{(z-a)(z-b)}}]\mathrm{v}^{-1}(N+\overline{N})^{-1}\mathrm{i}(p_1^* + p_2^*) \\
&\quad + \mathrm{vdiag}[0, 0, \frac{1}{\sqrt{(z-a)(z-b)}}][\Pi_2 \mathrm{v}^{-1}(N+\overline{N})^{-1}(\mathrm{i}p_1^*) \\
&\quad + ({\Pi_1}^2 + \Pi_1\Pi_3 + \Pi_4)\mathrm{v}^{-1}(N+\overline{N})^{-1}(\mathrm{i}p_2^*)] \\
&\quad + \mathrm{v}[\frac{(a-b)^2}{8\sqrt{(z_1-a)(z_1-b)}}, \frac{(a-b)^2}{8\sqrt{(z_2-a)(z_2-b)}}, \\
&\quad \frac{(a-b)^2}{8\sqrt{(z_3-a)(z_3-b)}}]\mathrm{v}^{-1}(N+\overline{N})^{-1}(\mathrm{i}p_2^*) \\
&= \mathrm{vdiag}[0, 0, \frac{(b-a)^2}{8\sqrt{(z-a)(z-b)}}]\mathrm{v}^{-1}(N+\overline{N})^{-1}\mathrm{i}p_1^* \\
&\quad + \mathrm{vdiag}[\frac{(b-a)^2}{8\sqrt{(z_1-a)(z_1-b)}}, \frac{(b-a)^2}{8\sqrt{(z_2-a)(z_2-b)}}, \\
&\quad \frac{-(b-a)^2}{2\sqrt{(z_3-a)(z_3-b)}}]\mathrm{v}^{-1}(N+\overline{N})^{-1}\mathrm{i}p_2^* \\
&= \mathrm{v}\ \mathrm{x}(z)\Pi_5\mathrm{v}^{-1}(N+\overline{N})^{-1}(\mathrm{i}p_1^*) + \mathrm{v}\ \mathrm{x}(z)\Pi_6\mathrm{v}^{-1}(N+\overline{N})^{-1}(\mathrm{i}p_2^*)
\end{aligned}
$$

where,

$$\Xi(z) = \mathrm{diag}[z_1, z_2, z_3]$$

$$\Pi_1 = \mathrm{diag}[(b-a)\mathrm{i}\epsilon - \frac{a+b}{2}, (b-a)(\text{-}\mathrm{i}\epsilon) - \frac{a+b}{2}, -\frac{a+b}{2}$$

$$\Pi_2 = \mathrm{diag}[(\frac{b-a}{2})^2(1+4\epsilon^2), (\frac{b-a}{2})^2(1+4\epsilon^2), (\frac{b-a}{2})^2]$$

$$\Pi_3 = \mathrm{diag}[(a+b) + (b-a)\mathrm{i}\epsilon, (a+b) + (b-a)(\text{-}\mathrm{i}\epsilon), (a+b)],$$

$$\begin{aligned}
\Pi_4 = \mathrm{diag}[&ab + \frac{b^2-a^2}{2}\mathrm{i}\epsilon - (1+4\epsilon^2)(\frac{b-a}{2})^2, \\
&ab + \frac{b^2-a^2}{2}(\text{-}\mathrm{i}\epsilon) - (1+4\epsilon^2)(\frac{b-a}{2})^2, ab - (\frac{b-a}{2})^2]
\end{aligned}$$

$$\Pi_5 = \mathrm{diag}[0,\ 0,\ \frac{(b-a)^2}{8}]$$

$$\Pi_6 = \mathrm{diag}[1/8,\ 1/8,\ -1/2]$$

then

$$\Phi'(z) = J_1 + J_2 + J_3 + J_4$$

Integration of equation () yields

$$\begin{aligned}
\Phi(z) = {} & \mathrm{v}\ [\Xi(z) - \mathrm{x}^{-1}(z)\Delta(z;\epsilon)]\ \mathrm{v}^{-1}(N+\overline{N})^{-1}(\mathrm{i}p_0) \\
& + \mathrm{v}[\Xi(z^2) - x^{-1}\Delta(z;\epsilon)\Xi(z)]\ \mathrm{v}^{-1}(N+\overline{N})^{-1}(\mathrm{i}p_1^*) \\
& - \mathrm{v}[x^{-1}\Delta(z;\epsilon)(\Xi(z) - \Pi_1 - \Pi_3]\ \mathrm{v}^{-1}(N+\overline{N})^{-1}(\mathrm{i}p_2^*) \\
& - \mathrm{v}Y_1(z;\epsilon)\ \mathrm{v}^{-1}(N+\overline{N})^{-1}\mathrm{i}(p_1^* + p_2^*) \\
& - \mathrm{v}Y_2(z;\epsilon)[\Pi_2\ \mathrm{v}^{-1}(N+\overline{N})^{-1}(\mathrm{i}p_1^*) \\
& + (\Pi_1^2 + \Pi_1\Pi_3 + \Pi_4)\ \mathrm{v}^{-1}(N+\overline{N})^{-1}(\mathrm{i}p_2^*)] \\
& + \mathrm{v}Y_3(z)\mathrm{v}^{-1}(N+\overline{N})^{-1}(\mathrm{i}p_2^*)
\end{aligned}$$

where,

$$\begin{aligned}
Y_1(z;\epsilon) = \mathrm{diag}[& \frac{(a-b)^{0.5+i\epsilon}}{1.5-i\epsilon}(z-a)^{1.5-i\epsilon}\ {}_2F_1(1.5-i\epsilon, -0.5-i\epsilon, 2.5-i\epsilon, \frac{z-a}{b-a}), \\
& \frac{(a-b)^{0.5-i\epsilon}}{-1.5-i\epsilon}(z-a)^{1.5+i\epsilon}\ {}_2F_1(1.5+i\epsilon, -0.5+i\epsilon, 2.5+i\epsilon, \frac{z-a}{b-a}), \\
& \sqrt{(z-a)(z-b)}(z-a+z-b)/4]
\end{aligned}$$

$$Y_2(z;\epsilon) = \mathrm{diag}[\frac{(a-b)^{-0.5+i\epsilon}}{0.5-i\epsilon}(z-a)^{0.5-i\epsilon}\ {}_2F_1(0.5-i\epsilon, 0.5-i\epsilon, 1.5-i\epsilon, \frac{z-a}{b-a}),$$
$$\frac{(a-b)^{-0.5-i\epsilon}}{-0.5-i\epsilon}(z-a)^{0.5+i\epsilon}\ {}_2F_1(0.5+i\epsilon, 0.5+i\epsilon, 1.5+i\epsilon, \frac{z-a}{b-a}), 0]$$

$$Y_3(z_\alpha) = \mathrm{diag}[\sqrt{(z_1-a)(z_1-b)}\frac{(z_1-a+z_1-b)}{4},$$
$$\sqrt{(z_2-a)(z_2-b)}\frac{(z_2-a+z_2-b)}{4},$$
$$\sqrt{(z_3-a)(z_3-b)}\frac{(z_3-a+z_3-b)}{4}]$$

Appendix B

A Green's Function for Heat Vortex

The thermal dislocation is also referred as heat vortex in literature. A temperature distribution which vanishes at infinity may reasonably be assumed as:

$$T = q_{0\tau}\frac{1}{z_\tau} + \bar{q}_{0\tau}\frac{1}{\bar{z}_\tau}; \quad z_\tau = x_1 + \tau x_2, \quad \text{with } \mathrm{Im}[\tau] > 0$$

Let the temperature discontinuity along the cut $(x_1 < 0, x_2 = 0)$ be T_0 for an infinite anisotropic medium, then from the condition

$$T(x_1, x_2 = 0^+) - T(x_1, x_2 = 0^-) = T_0,$$

one can obtain a solution as

$$q_{0\tau} = \frac{T_0}{4\pi \mathrm{i}}$$

where, the relationship

$$\frac{1}{x_1 + \tau x_2} = \frac{1}{x_1} \mp \mathrm{i}\pi \text{ as } x_2 \to 0^{\pm}$$

is used. If the heat vortex is located at z_0 in this infinite anisotropic medium, one may write the temperature distribution as

$$T = q_{0\tau}\frac{1}{z_\tau - z_0} + \bar{q}_{0\tau}\frac{1}{\bar{z}_\tau - \bar{z}_0}.$$

Appendix C

Solution to the Thermal-dislocation of Bimedia

From the boundary condition $(117)_{1,2}$ along the interface, one can obtain

$$\begin{aligned}
&\mathrm{Re}[\frac{q_{0\tau}}{x_1 - z_{\tau 0}} + \frac{q_{1\tau}}{x_1 - \overline{z}_{\tau 0}}] = \mathrm{Re}[\frac{q_{2\tau}}{x_1 - z_{\tau 0}}] \\
&k_{\mathrm{I}}\ \mathrm{Im}[\frac{q_{0\tau}}{(x_1 - z_{\tau 0})^2} + \frac{q_{1\tau}}{(x_1 - \overline{z}_{\tau 0})^2}] = k_{\mathrm{II}}\ \mathrm{Im}[\frac{q_{2\tau}}{(x_1 - z_{\tau 0})^2}]
\end{aligned} \tag{243}$$

Differentiation of $(243)_1$ with respect to x_1 gives

$$\mathrm{Re}[\frac{q_{0\tau}}{(x_1 - z_{\tau 0})^2} + \frac{q_{1\tau}}{(x_1 - \overline{z}_{\tau 0})^2}] = \mathrm{Re}[\frac{q_{2\tau}}{(x_1 - z_{\tau 0})^2}] \tag{244}$$

Solving equations $(243)_2$ and (244) leads to:

$$q_{1\tau} = \frac{k_{\mathrm{I}} - k_{\mathrm{II}}}{k_{\mathrm{I}} + k_{\mathrm{II}}}\overline{q}_{0\tau}, \quad q_{2\tau} = \frac{2\ k_{\mathrm{I}}}{k_{\mathrm{I}} + k_{\mathrm{II}}}q_{0\tau} \tag{245}$$

The boundary condition $(117)_{3,4}$ along the interface yields

$$\begin{aligned}
&\sum_{1}^{3}\{[A_{\mathrm{I}}\log(x_1-z_{\mathrm{d0k}})\mathrm{I}_k q_{\mathrm{d0}}+\overline{A}_{\mathrm{I}}\log(x_1-\overline{z}_{\mathrm{d0k}})\mathrm{I}_k\overline{q}_{\mathrm{d0}}]\\
&\quad+[A_{\mathrm{I}}\log(x_1-\overline{z}_{\mathrm{d0k}})q_{1\mathrm{k}}+\overline{A}_{\mathrm{I}}\log(x_1-z_{\mathrm{d0k}})\overline{q}_{1\mathrm{k}}]\}\\
&\quad+[A_{\mathrm{I}}\log(x_1-z_{\tau 0})q_{1\mathrm{d}\tau}+\overline{A}_{\mathrm{I}}\log(x_1-\overline{z}_{\tau 0})\overline{q}_{1\mathrm{d}\tau}]\\
&\quad+[C_{\mathrm{I}}\log(x_1-z_{\tau 0})q_{0\tau}+\overline{C}_{\mathrm{I}}\log(x_1-\overline{z}_{\tau 0})\overline{q}_{0\tau}]\\
&\quad+[C_{\mathrm{I}}\log(x_1-\overline{z}_{\tau 0})q_{1\tau}+\overline{C}_{\mathrm{I}}\log(x_1-z_{\tau 0})\overline{q}_{1\tau}]\\
&=\sum_{1}^{3}[A_{\mathrm{II}}\log(x_1-z_{\mathrm{d0k}})q_{2\mathrm{k}}+\overline{A}_{\mathrm{II}}\log(x_1-\overline{z}_{\mathrm{d0k}})\overline{q}_{2\mathrm{k}}]\\
&\quad+[A_{\mathrm{II}}\log(x_1-\overline{z}_{\tau 0})q_{2\mathrm{d}\tau}+\overline{A}_{\mathrm{II}}\log(x_1-z_{\tau 0})\overline{q}_{2\mathrm{d}\tau}]\\
&\quad+[C_{\mathrm{II}}\log(x_1-z_{\tau 0})q_{2\tau}+\overline{C}_{\mathrm{II}}\log(x_1-\overline{z}_{\tau 0})\overline{q}_{2\tau}];
\end{aligned}\tag{246}$$

$$\begin{aligned}
&\sum_{1}^{3}\{[B_{\mathrm{I}}\log(x_1-z_{\mathrm{d0k}})\mathrm{I}_k q_{\mathrm{d0}}+\overline{B}_{\mathrm{I}}\log(x_1-\overline{z}_{\mathrm{d0k}})\mathrm{I}_k\overline{q}_{\mathrm{d0}}]\\
&\quad+[B_{\mathrm{I}}\log(x_1-\overline{z}_{\mathrm{d0k}})q_{1\mathrm{k}}+\overline{B}_{\mathrm{I}}\log(x_1-z_{\mathrm{d0k}})\overline{q}_{1\mathrm{k}}]\}\\
&\quad+[B_{\mathrm{I}}\log(x_1-z_{\tau 0})q_{1\mathrm{d}\tau}+\overline{B}_{\mathrm{I}}\log(x_1-\overline{z}_{\tau 0})\overline{q}_{1\mathrm{d}\tau}]\\
&\quad+[D_{\mathrm{I}}\log(x_1-z_{\tau 0})q_{0\tau}+\overline{D}_{\mathrm{I}}\log(x_1-\overline{z}_{\tau 0})\overline{q}_{0\tau}]\\
&\quad+[D_{\mathrm{I}}\log(x_1-\overline{z}_{\tau 0})q_{1\tau}+\overline{D}_{\mathrm{I}}\log(x_1-z_{\tau 0})\overline{q}_{1\tau}]\\
&=\sum_{1}^{3}[B_{\mathrm{II}}\log(x_1-z_{\mathrm{d0k}})q_{2\mathrm{k}}+\overline{B}_{\mathrm{II}}\log(x_1-\overline{z}_{\mathrm{d0k}})\overline{q}_{2\mathrm{k}}]\\
&\quad+[B_{\mathrm{II}}\log(x_1-\overline{z}_{\tau 0})q_{2\mathrm{d}\tau}+\overline{B}_{\mathrm{II}}\log(x_1-z_{\tau 0})\overline{q}_{2\mathrm{d}\tau}]\\
&\quad+[D_{\mathrm{II}}\log(x_1-z_{\tau 0})q_{2\tau}+\overline{D}_{\mathrm{II}}\log(x_1-\overline{z}_{\tau 0})\overline{q}_{2\tau}]
\end{aligned}\tag{247}$$

The following two sets of equations can be derived by grouping the coefficients

of terms $\log(x_1 - z_{\mathrm{d0k}})$, and $\log(x_1 - z_{\tau 0})$ in the above equation:

$$
\begin{aligned}
-\overline{A}_{\mathrm{I}}\overline{q}_{1\mathrm{k}} + A_{\mathrm{II}}q_{2\mathrm{k}} &= A_{\mathrm{I}}\mathrm{I}_k q_{\mathrm{d0}} \\
-\overline{B}_{\mathrm{I}}\overline{q}_{1\mathrm{k}} + B_{\mathrm{II}}q_{2\mathrm{k}} &= B_{\mathrm{I}}\mathrm{I}_k q_{\mathrm{d0}}
\end{aligned} \tag{248}
$$

and

$$
\begin{aligned}
A_{\mathrm{I}}q_{1\mathrm{d}\tau} - \overline{A}_{\mathrm{II}}\overline{q}_{2\mathrm{d}\tau} &= C_{\mathrm{II}}q_{2\tau} - \overline{C}_{\mathrm{I}}\overline{q}_{1\tau} - C_{\mathrm{I}}q_{0\tau} \\
B_{\mathrm{I}}q_{1\mathrm{d}\tau} - \overline{B}_{\mathrm{II}}\overline{q}_{2\mathrm{d}\tau} &= D_{\mathrm{II}}q_{2\tau} - \overline{D}_{\mathrm{I}}\overline{q}_{1\tau} - D_{\mathrm{I}}q_{0\tau}
\end{aligned} \tag{249}
$$

Equations (248) and (248), respectively, give

$$
\begin{aligned}
B_{\mathrm{I}}q_{1\mathrm{k}} &= N[-N^{-1} + 2L_1^{-1}]\overline{B}_{\mathrm{I}}\mathrm{I}_k\overline{q}_{\mathrm{d0}} \\
B_{\mathrm{II}}q_{2\mathrm{k}} &= 2\overline{N}L_1^{-1}B_{\mathrm{I}}\mathrm{I}_k q_{\mathrm{d0}}
\end{aligned} \tag{250}
$$

and

$$
B_{\mathrm{I}}q_{1\mathrm{d}\tau} = N[\overline{M}_{\mathrm{II}}^{-1}D + \mathrm{i}C]q_{0\tau} \tag{251}
$$

$$
B_{\mathrm{II}}q_{2\mathrm{d}\tau} = -\overline{N}[\overline{M}_{\mathrm{I}}^{-1}\overline{D} + \mathrm{i}\overline{C}]q_{0\tau} \tag{252}
$$

where,

$$
\begin{aligned}
C &= \frac{2k_{\mathrm{I}}}{k_{\mathrm{I}} + k_{\mathrm{II}}}C_{\mathrm{II}} - \frac{k_{\mathrm{I}} - k_{\mathrm{II}}}{k_{\mathrm{I}} + k_{\mathrm{II}}}\overline{C}_{\mathrm{I}} - C_{\mathrm{I}}, \\
D &= \frac{2k_{\mathrm{I}}}{k_{\mathrm{I}} + k_{\mathrm{II}}}D_{\mathrm{II}} - \frac{k_{\mathrm{I}} - k_{\mathrm{II}}}{k_{\mathrm{I}} + k_{\mathrm{II}}}\overline{D}_{\mathrm{I}} - D_{\mathrm{I}}
\end{aligned} \tag{253}
$$

Appendix D

Proof of the Equation (167)

From equation (26a) in [39], for the x_3-plane of symmetry and two modes present,

$$\mathcal{G}_1 = -\frac{K_I}{2} s_{22} \mathrm{Im}[\frac{K_I(p_1+p_2)+K_{II}}{p_1 p_2}],$$
$$\mathcal{G}_2 = \frac{K_{II}}{2} s_{11} \mathrm{Im}[K_{II}(p_1+p_2)+K_I p_1 p_2] \tag{254}$$

then

$$\begin{aligned} \mathcal{G} &= \mathcal{G}_1 + \mathcal{G}_2 \qquad (255)\\ &= \frac{s_{11}}{2}\mathrm{Im}[K_{II}^2(p_1+p_2) + K_{II}K_I\, p_1p_2 - K_I^2(p_1+p_2)\frac{s_{22}}{s_{11}}\frac{1}{p_1p_2} \\ &\qquad - K_I K_{II}\frac{s_{22}}{s_{11}}\frac{1}{p_1p_2}] \end{aligned}$$

where, the p_i and $\bar{p}_i (i = 1, 2)$ satisfy the characteristic equation (Lekhnitskii, 1963) [25],

$$s_{11}\, p^4 - 2\, s_{16} p^3 + (2\, s_{12} + s_{66})\, p^2 - 2 s_{26}\, p + s_{22} = 0 \tag{256}$$

and from the equation (256), the following relationship can be obtained,

$$s_{22}/s_{11} = p_1 p_2 \bar{p}_1 \bar{p}_2 \tag{257}$$

Substitution of (257) into (255) leads to:

$$\mathcal{G} = \frac{s_{11}}{2}\mathrm{Im}[K_{II}^2(p_1+p_2) + K_{II}K_I\, p_1p_2 - K_I^2(p_1+p_2)\bar{p}_1\bar{p}_2 - K_I K_{II}\bar{p}_1\bar{p}_2] \tag{258}$$

which is

$$\mathcal{G} = \frac{s_{11}}{2}\mathrm{Im}[K_{II}^2(p_1+p_2) - 2\ K_{II}K_I\ \bar{p}_1\bar{p}_2 - K_I^2(p_1+p_2)\bar{p}_1\bar{p}_2]$$

Appendix E

Proof of the Existence of Quasi-bimaterials

It is easy to show that SL^{-1} is antisymmetric. Actually, from the definition of matrices S, L and using equation (262)

$$SL^{-1} = i\ (2\ AB^T - \mathrm{I})(-2\ iBB^T)^{-1}$$
$$= \frac{B^{-T}B^{-1}}{2} - AB^{-1}\ = \frac{B^{-T}B^{-1}}{2} - L^{-1}(S^T - i\mathrm{I})\ = -L^{-1}S^T = -[SL^{-1}]^T \tag{259}$$

It follows that $\mathrm{W} = S_1L_1 - S_2L_2$ is antisymmetric.

If x_3 is an axis of material symmetry, then the third components of the first and second vector in the matrices A and B are zero, so are the first and second component of the third vector. Therefore, the matrix SL^{-1} can only has the following form

$$SL^{-1} = \begin{vmatrix} 0 & b & 0 \\ -b & 0 & 0 \\ 0 & 0 & d \end{vmatrix} \tag{260}$$

Hence,

$$S_2L_2^{-1} = \Omega^T S_1 \Omega[\Omega^T L_1^{-1}\Omega]^{-1}\ = \Omega^T S_1 L_1^{-1}\Omega$$

$$= \begin{vmatrix} 0 & b[\cos^2(\omega) + \sin^2(\omega)] & 0 \\ -b[\cos^2(\omega) + \sin^2(\omega)] & 0 & 0 \\ 0 & 0 & d \end{vmatrix} = S_1L_1^{-1} \tag{261}$$

This shows that W is a null matrix, then it follows that the bimaterial parameter $\epsilon = 0.0$ by equation (73).

Appendix F

Properties of Some Bimaterial Matrices

As defined in Chapter II, we have three matrices:

$$H = 2\,i\,AA^T, \qquad L = -2\,i\,BB^T, \qquad S = i\,(2AB^T - I), \tag{262}$$

where, A and B are the coefficient matrices in equation (21). It is easily[10] to show that H, L are real positive definite and S is real. The related bimaterial property matrices $D = L_1^{-1} + L_2^{-1}$ are symmetric, positive definite and $W = S_1 L_1^{-1} - S_2 L_2^{-1}$ antisymmetric [10]. From equation (262), the following relationship can be obtained

$$iAB^{-1} = 2AB^T \frac{B^{-T}B^{-1}}{-2i} = (\frac{S}{i} + I)(-2iBB^T)^{-1} = (I - iS)L^{-1} \tag{263}$$

Next we shall prove the matrix N defined in equation (189) is equivalent to $N = (D - iW)^{-1}$. From equations (189), $(262)_2$ and $(262)_3$

$$\begin{aligned} N^{-1} &= iA_1\,B_1^{-1} + \overline{iA_2\,B_2^{-1}} = iA_1B_1^T(B_1B_1^T)^{-1} + \overline{iA_2B_2^T(B_2B_2^T)^{-1}} \\ &= \frac{(S_1 + iI)}{2}\,(\frac{L_1}{-2i})^{-1} + \overline{\frac{(S_2 + iI)}{2}\,(\frac{L_2}{-2i})^{-1}} \\ &= L_1^{-1} - iS_1L_1^{-1} + L_2^{-1} + iS_2L_2^{-1} = D - iW \end{aligned} \tag{264}$$

The positive definite D in (264) imply that N is nonsingular. In fact, N is also Hermitian since

$$\overline{N^{-1}}^T = \overline{D - iW}^T = D^T + iW^T = D + i(-W) = D - iW = N^{-1} \tag{265}$$

i.e. N^{-1} is Hermitian and $N = \widetilde{D} + i\widetilde{W}$, where

$$\widetilde{D} = (D - WD^{-1}W)^{-1} = \begin{vmatrix} \widetilde{d}_{11} & \widetilde{d}_{12} & \widetilde{d}_{13} \\ \widetilde{d}_{12} & \widetilde{d}_{22} & \widetilde{d}_{23} \\ \widetilde{d}_{13} & \widetilde{d}_{23} & \widetilde{d}_{33} \end{vmatrix} \tag{266}$$

$$\widetilde{W} = D^{-1} W \widetilde{D} = \begin{vmatrix} 0 & \widetilde{w}_3 & -\widetilde{w}_2 \\ -\widetilde{w}_3 & 0 & \widetilde{w}_1 \\ \widetilde{w}_2 & -\widetilde{w}_1 & 0 \end{vmatrix} \tag{267}$$

For isotropic bimedia[3],

$$L_\alpha = \frac{4\mu_\alpha}{k_\alpha + 1} \text{diag}[1,\ 1,\ (k_\alpha + 1)/4], \qquad \alpha = 1,\ 2 \tag{268}$$

$$S_\alpha = \frac{1}{k_\alpha + 1} \begin{vmatrix} 0 & -(k_\alpha - 1) & 0 \\ k_\alpha - 1 & 0 & 0 \\ 0 & 0 & \end{vmatrix}, \qquad \alpha = 1,\ 2 \tag{269}$$

Where, $k_\alpha = 3 - 4\nu_\alpha$ for plane strain and $k_\alpha = (3 - \nu_\alpha)/(1 + \nu_\alpha)$ for plane stress; ν is Poisson's ratio and μ is shear modulus. Then by equation (81) of [3], the following can be found

$$\widetilde{D} = \text{diag}[\frac{1}{\eta(1-\beta^2)},\ \frac{1}{\eta(1-\beta^2)},\ \frac{1}{1/\mu_1 + 1/\mu_2}] \tag{270}$$

$$\widetilde{W} = \frac{\beta}{\eta(1-\beta^2)} \begin{vmatrix} 0 & 1 & 0 \\ -1 & 0 & 0 \\ 0 & 0 & 0 \end{vmatrix} \tag{271}$$

where, $\eta = (k_1 + 1)/4\mu_1 + (k_2 + 1)/4\mu_2$, $\beta = [\Gamma(k_1 - 1) - (k_2 - 1)/[\Gamma(k_1 + 1) + (k_2 + 1)]$ and $\Gamma = \mu_2/\mu_1$.

Appendix G

Solution to Hilbert Equation to (207)

The homogenous equation corresponding to the equation(207) is

$$\widetilde{N}\begin{vmatrix} \Phi'_{1+}(x_1) \\ \Phi'_{3+}(x_1) \end{vmatrix} + \overline{\widetilde{N}}\begin{vmatrix} \Phi'_{1-}(x_1) \\ \Phi'_{3-}(x_1) \end{vmatrix} = 0, \quad |x_1| < L \tag{272}$$

Let us try a solution of the form

$$\chi(z) = \mathbf{c}(z+L)^{-\mu}(z-L)^{1-\mu} \tag{273}$$

Substitution of (273) into (272) leads

$$[\widehat{N}e^{i2\pi\mu} + \overline{\widehat{N}}]\mathbf{c} = [(\widehat{D} + i\widehat{W})e^{i2\pi\mu} + (\widehat{D} - i\widehat{W})]\mathbf{c} = 0 \tag{274}$$

where,

$$\widehat{D} = \begin{vmatrix} \widetilde{d}_{11} & \widetilde{d}_{13} \\ \widetilde{d}_{13} & \widetilde{d}_{33} \end{vmatrix} \qquad \text{and} \qquad \widehat{W} = \begin{vmatrix} 0 & -\widetilde{w}_2 \\ \widetilde{w}_2 & 0 \end{vmatrix} \tag{275}$$

For non-trivial constant vector $\mathbf{c}$, one has

$$|(I - i\widehat{W}\widehat{D}^{-1})e^{i2\pi\mu} - (I + i\widehat{W}\widehat{D}^{-1})| = |(1+e^{i2\pi\mu})I + i(1-e^{i2\pi\mu})\widehat{W}\widehat{D}^{-1}| = 0 \tag{276}$$

where $|A|$ denotes the determinant of the matrix A. Let $\lambda = (1+e^{i2\pi\mu})/(1-e^{i2\pi\mu})$, then

$$|\widehat{W}\widehat{D}^{-1} + i\lambda| = \{\frac{\widetilde{w}_2}{\widetilde{d}_{11}\widetilde{d}_{33} - \widetilde{d}_{13}^2}\begin{vmatrix} \widetilde{d}_{13} & -\widetilde{d}_{11} \\ \widetilde{d}_{33} & -\widetilde{d}_{13} \end{vmatrix} + \mathrm{i}\lambda I\} = 0 \tag{277}$$

It can be easily seen, if $\widetilde{w}_2 = 0$, $\lambda = 0$. Otherwise

$$\lambda = \pm\widetilde{\beta}, \quad \widetilde{\beta} = \frac{\widetilde{w}_2}{\sqrt{\widetilde{d}_{11}\widetilde{d}_{33} - \widetilde{d}_{13}^2}} \tag{278}$$

Appendix H

A Contour Integral for Stress Functions

$$\Lambda(z;\epsilon) = \frac{X(z)}{2\pi}\int_{-L}^{L}\frac{[X_+(x_1)]^{-1}}{(x_1-z)}\,dx_1$$
$$= iV[I - \frac{\Delta(z;\epsilon)}{\sqrt{z^2-L^2}}\mathrm{diag}[z+i2L\epsilon, z-i2L\epsilon]]V^{-1}[\widehat{N}+\overline{\widehat{N}}]^{-1} \qquad (279)$$

where $\Delta(z;\epsilon)$ is defined by equation $(210)_2$.

The integral in equation (209) can be rewritten into two parties.

$$j_2 = \frac{X(z)}{2\pi}\int_{-L}^{L}\int_{a}^{b}\frac{[X_+(x_1)]^{-1}\phi(t)}{\pi\,(x_1-z)(t-x_1)}\,dtdx_1$$
$$= \int_a^b\{\frac{\phi(t)}{\pi(t-z)}\frac{X(z)}{2\pi}\int_{-L}^{L}(\frac{1}{x_1-z}-\frac{1}{x_1-t})[X_+(x_1)]^{-1}\,dx_1\}dt$$
$$= \int_a^b \mathbf{g}(t,z)\frac{\phi(t)}{\pi(t-z)}dt \qquad (280)$$

where

$$\mathbf{g}(t,z) = iV[\frac{\Delta(t;\epsilon)}{\sqrt{t^2-L^2}}\mathrm{diag}[t+i2L\epsilon,\ t-i2L\epsilon]$$
$$-\frac{\Delta(z;\epsilon)}{\sqrt{z^2-L^2}}\mathrm{diag}[z+i2L\epsilon,\ z-i2L\epsilon]]V^{-1}[I+\widehat{N}^{-1}\overline{\widehat{N}}]^{-1} \qquad (281)$$

Appendix I

Header File "vector_matrix_operator.h"

Since the C++ code is an important part of this research, by taking the advantage of C++ programming language features, such as operator overloading and data hiding, we have developed a system of operators to make the complex matrix, real matrix and complex number manipulation much more flexible. Using this code-system, the complex matrix operation works like ordinary '+'(plus or addition), '-'(substraction), '*'(multiplication), '/'(divided by) on real numbers. Thus it makes the complicated numerical simulations relatively easy. This code system may find other applications which involve complex number or complex matrix manipulation. Therefore, we list some of the important contents in Appendix-I to Appendix-K as a reference for the readers.

Following file is the declaration of the five classes, namely: **class number_complex, class vector, class vector_complex, class matrix, class matrix_complex.**

File "vector_matrix_operator.h"

```
#ifndef _VECTOR_MATRIX_H_
#define _VECTOR_MATRIX_H_
#include <iostream.h>
#include <math.h>
//—constant—//
#define EPSLON 1.0e-25
#define OPEN_FAILURE 1
#define PI 3.14159265358979
// forward declaration//
```

```
class vector;
class vector_complex;
class number_complex {
   private:
      double x, y;
      double r, theta;
      void mod_0(void);
      void argument_0(void);
   public:
      friend class vector_complex;
      friend class matrix;
      number_complex(void);
      number_complex(double ar, double ai);//constructor
      number_complex(number_complex &a);
      ~number_complex();
      double mod(number_complex &n_c);
      double argument(number_complex &n_c);
      //square_root of a complex number//
      number_complex sqrt_c(number_complex &n_c);
      number_complex number_complex::log_c(number_complex &nc);
      // power of a complex to a complex number//
      number_complex pow_c(const number_complex &a,
            const number_complex &n_c);
      number_complex conjugate(const number_complex &n_c);
      double re(const number_complex &n_c);//real part of a number
      double im(const number_complex &n_c);//imaginary part of a number
      number_complex & operator=(const number_complex &n_c);
```

```
    number_complex operator +(number_complex &n_c) const;
    number_complex operator +(double n) const;//substraction
    number_complex operator -(number_complex &n_c) const;
    number_complex operator -(double nx) const;
    number_complex operator -() const;//minus
    number_complex operator *(number_complex &n_c) const;
    number_complex operator *(double n_r); //scale multiplication
    number_complex operator /(number_complex &n_c) const;
    number_complex operator /(double n_r);// divided by a real number
  //friends//
    friend ostream & operator<<(ostream& os , const number_complex n_c);
};
//———real vector operator class——-//
class vector {
  private:
    int m; // dimension of a vector.
    double *v; // vector to be used as real part .
  public:
    friend class vector_complex;
    vector(void);
    vector(double *vr, int);//constructor
    vector(const vector & a);
    ~ vector(void);//destructor
    int dim_m(void);//report the m
    double mod(const vector & a);
    //operator overloading//
    vector operator +(const vector & b) const;//vector addition
```

```
    vector operator +(const double* b) const;
    vector operator -(const vector & b) const;//vector addition
    vector operator -(const double* b) const;
    double operator *(const vector &b) const;//scale product
    double operator*(const double *a) const;
    vector operator *(double x);//scale product
    vector operator -() const; //minus sign to a vector
    double operator [](int i) const ;
    vector & operator =(vector &b);//vector assignment
    vector & operator =(double *b);//vector assignment
    void vector::eq(int i, double x);//element assignment
  //friend class matrix//
    friend ostream& operator<<(ostream& os, vector v);
};
//———complex vector operator class——-//
class vector_complex//: public vector {
  private:
    int m;
    double *vr;
    double *vi;
  public:
    friend class matrix;
    vector_complex(void);
    vector_complex(const vector_complex &v);
    vector_complex(double *vr, double *vi, int n);//constructor
    ~vector_complex(void);//destructor
    int dim_m(void);//report the m
```

```
    double mod(const vector_complex &a);
    vector rev( vector_complex &v_c);//real part of a number
    vector imv( vector_complex &v_c);//imaginary part of a number
    vector_complex conjugate(const vector_complex &b)const;
    //operator overloading
    vector_complex operator +(const vector_complex &b) const;//vector addition
    vector_complex operator -(const vector_complex &b) const;//vector addition
    vector_complex operator *(double x)const ;
    vector_complex vector_complex::operator *(number_complex nc)const;
    vector_complex operator -()const; //minus sign to a vector
    vector_complex & operator =(const vector_complex &b);
    number_complex operator *(const vector_complex &b)const;//scale product
    number_complex operator *(const vector &b) const;
    number_complex operator [](int i)const;
    void vector_complex::eq(int i, number_complex & n_c);
    // friends//
    friend ostream& operator<<(ostream& os , const vector_complex v_c);
};
//———real matrix operator class——-//
class matrix{
  private:
    int m, n; // dimension of a matrix.
    double **ar; // matrix to be used as real part.
  public:
    friend class matrix_complex;
    matrix(void);
    matrix(const matrix &a);
```

```
matrix(double **ar, int m, int n);//constructor
~matrix(void);//destructor
int dim_m(void);//report the m
int dim_n(void);//report the n
matrix transpose(matrix &b);//inverse of a matrix
matrix inverse(matrix &b);//inverse of a matrix
matrix unitk(int p, int q, int k);
matrix unit(int p, int q);
void dec(double **a, int n, double *aux, int *p);
void inv(double **a, int n, int *p);
void dupcolvec(int l, int u, int j, double** a, double*b);
double mattam(int l, int u, int i, int j, double **a, double **b);
void ichrow(int l, int u, int i, int j, double **a);
void ichcol(int l, int u, int i, int j, double **a);
double matmat(int l, int u, int i, int j, double **a, double **b);
void matrix::eq(int i, int j, double x );
//operator overloading
double operator ()(int i, int j) const;
double & operator=(double x);
matrix & operator=(const matrix & b);//assignment operator
matrix & operator=( double **a);//assignment operator
matrix operator +(const matrix & b) const ;// matrix addition
matrix operator +(double ** b) const ;// matrix addition
matrix operator -(const matrix & b) const ;// matrix addition
matrix operator -(double ** b) const ;// matrix addition
matrix operator *(const matrix & b) const ;// matrix multipilcation
matrix operator *(double ** b) const ;// matrix multipilcation
```

```
    vector operator *(vector & v) ;
    vector_complex operator *(vector_complex &v);
    matrix operator *(double x);// scale multipilcation
    matrix operator -() ; //minus sign to a matrix
    friend ostream& operator<<(ostream& os , const matrix a);
};
// complex matrix operator class
class matrix_complex : public matrix {
  private:
    int m, n;
    double **ar,**ai; // imaginary part of a matrix
  public:
    matrix_complex(void);//default constructor
    matrix_complex(double **ar, double **ai, int m, int n);// set data to ar
+ i ai
    matrix_complex(matrix &br, matrix &bi);
    matrix_complex(const matrix_complex & b);// copy constructor
    ~matrix_complex(); //destructor
    matrix_complex transpose(matrix_complex &b);
    int dim_m(void);
    int dim_n(void);
    void eqilbr(double **a, int n, double *em, double *d, int *inter);
    void tfmreahes(double **a, int n, double em[], int *index);
    int comvalqri(double **a, int n, double *em, double *re, double *im);
    void comveches(double **a, int n, double lambda, double mu,
      double *em, double *u, double *v);
    void reaveches(double **a, int n, double lambda, double *em, double *v);
```

```
void bakreahes2(double **a, int n, int n1, int n2, int *index,double **vec);

void baklbr(int n, int n1, int n2, double *d, int *inter, double **vec);
void comscl(double **a, int n, int n1, int n2, double *im);
double vecvec(int l, int u, int shift, double *a, double *b);
double tamvec(int l, int u, int i, double **a, double *b);
double matvec(int l, int u, int i, double **a, double *b);
double tammat(int l, int u, int i, int j, double **a, double **b);
matrix_complex diag(number_complex &a, number_complex &b,
        number_complex &c);
matrix_complex conjugate(matrix_complex & b);//conjugate of a matrix
matrix_complex inverse(matrix_complex &b);//inverse of a matrix
matrix re(matrix_complex &b);//real part of the complex matrix
matrix im(matrix_complex &b);//imaginary party
// assignment
void eq(int, int, number_complex & n_c);
//operator overloading
matrix_complex operator +(const matrix_complex & b) const ;
matrix_complex operator -(const matrix_complex & b) const ;
matrix_complex operator *(const matrix_complex & b) const ;//
matrix_complex operator *( matrix & b) const ;
vector_complex operator *( vector &) const ;
vector_complex operator *( vector_complex &a) const;
matrix_complex operator *(double x);
matrix_complex matrix_complex::operator *(number_complex x);
matrix_complex operator *(double **a) const;
matrix_complex & operator=(const matrix_complex & b);//assignment
```

```
operator
    matrix_complex operator -() const; //minus sign to a matrix
    number_complex operator ()(int i, int j) const;//get element a[i][j];
    //eigen values and eigen vectors of a real matrix//
    int matrix_eigvalue_eigvector(matrix b, vector_complex &eval,
            matrix_complex &evec);
    matrix_complex  matrix_complex::matrix_norm_eigvector(matrix_complex
&ab,
            matrix_complex &a,matrix_complex &b);//normalized
    friend matrix_complex operator *(const matrix &a, const matrix_complex
&b) ;
    friend vector_complex operator*(const vector_complex &ta,
            const matrix_complex &b);
    friend vector_complex operator*(const vector &ta, const matrix_complex
& b);
    friend ostream& operator<<(ostream& os , const matrix_complex a);
};
#endif
```

Appendix J

Header File "sie_solving.h"

```
    #ifndef _SIE_SOLVING_
#define _SIE_SOLVING_
/*———-constants———*/
#define epslon pow(10,-12)
class sie{
   private:
      int m, n;
      char *str;
      //material property constant//
      double E1, E2, E3, G12, G21, G31, G13, G23, G32;
      double nu12, nu21, nu13, nu31, nu23,nu32;
      double alpha, delt, si,cs ;
      double **k,**c;
   public:
      sie(void);
      sie(double *theta, char* st);
      ~sie();
      void set_material_constants(char*str);
      void set_material_const_matrix_0(void);
```

```
void set_transformation_matrix(void);
void set_material_const_matrix(void);
double get_alpha(void);
char* get_str(void);
matrix material_characteristic_matrix();
void point_t_x_T(vector &t, vector &x, int *mt);//points of x and t;
void point_t_x_b(vector & t, vector &x, int *n);
matrix matrix_a_T(vector& t, vector& x, int *m, double *l, double *K,
    double *ratio_a, double *ratio_b, double *oega,
    number_complex lambda_omega, vector &fb);
matrix matrix_a_b(vector& tb, vector &xb, int *n, double *ratio_al,
    double *ratio_bl, double *l, double *k , vector_complex& ps,
    matrix_complex &b1, vector_complex &d1, matrix &L1,
    double *omega, number_complex &lambda_omega, vector &fn);
/*—- for thermal bi-media—-*/
matrix matrix_a_T_bimedia(vector& t, vector& x, int *m, double *l,
    double *K1, double *K2, double *ratio_a, double *ratio_b, double
*oega,
    number_complex tau, vector &fb , double * );
matrix matrix_a_b_bimedia(vector& tb, vector &xb, int *m, double beta,
    double *ratio_al, double *ratio_bl, double *l, double *k, number_complex
```

```
        &tau, vector_complex & ps, matrix_complex &b1, vector_complex
&d1,
        vector_complex &c1, vector_complex &d2, vector_complex &c2, ma-
trix &L1,
        matrix_complex &mn, vector_complex &p1, vector_complex &p2,
        vector_complex &dc, matrix_complex& nc, double *Omeg, vector&
t,
        matrix_complex &M, vector_complex &v1, vector_complex &v2,
        double k1, double k2,vector &fn, double *);
    double L_interpolation(vector& fnT, vector& pt, double* t);
    vector Kbt(double * x, vector &t, vector &g);
    /*——- No Thermal Loading ——-*/
    void point_t_x(vector & t, vector &x, int *n);
    matrix matrix_a(vector& t, vector &x, int *n, double y, double*coe,
        vector_complex &ps, matrix_complex &b1, matrix &l2, matrix_complex
&mn,
        matrix_complex&c, vector &v,matrix &tp, double *omega);
    number_complex hg_2F1(number_complex &z, double epson);
    double gamma(double epson);
    matrix matrix_a_comnin_model(vector& t, vector& x, int *m,
        matrix &d, matrix &w, double *gamma, vector &fb, vector &load,
```

```
        vector &ca, double *cp);
    vector known_function_f(vector &x, int *m, double beta, double*ce,
        vector_complex& ps, matrix_complex &mn, matrix_complex&c);
    void gauss_elim_partial_pivoting(matrix &a, vector &b);
    void forward_substitutation(double**L, vector &b);
    void backward_substitutation(double**U, vector &fb);
    // assign overloading//
    sie & operator =( sie & b);//object assignment
};
#endif
_SIE_SOLVING_
```

Appendix K

C++ Source Code List for Simulating the Singular Integral Equations

Here are some important source codes for the numerical simulation in this research. As we know, the C++ have some very good features such as operator overloading which could make computing more convenient illustrated in the following codes. Since some techniques incorporated into this codes is very original, it would be a good reference for those who intend to use C++ to develop their own codes in computational mechanics.

K.1 the main.cpp– this program is used to obtain **sif** and energy release rate

```
#include "vector_matrix_operator.h"
#include "sie_solving.h"
#include <fstream.h>
#include <stdlib.h>
int main(void)
{
    //-----------------------------------------------//
    int i,j, m = 6, n = 3, km , count = 1, countk = 1, stop = 0;
    int N = 60; // the points
    double h0 = 1.0, k1, k2, k12;
    double theta = 0.0, beta = 0.0; //theta is the material axis orientation
    double ratio_al = -1, ratio_bl = 0.0, l = 0.001;// = l/L
```

```
double omega0 =PI/(40*18.*2), omega, // omega is branching angle
    deltomega = PI/2/18.0, degree =180.0/PI;
//————————————————————-//
h0 = 1.0;
//—-for upper medium—-//
double kI11 = 42.1, kI12 = 0.0, kI22 = 0.466;
double alphaI11 = 0.025*pow(10,-6), alphaI22 = 32.4*pow(10,-6),
    alphaI12 = 0.0, alphaI33 = alphaI22, coea11 =1.0, coea12 = 1.0;
//—-for lower medium—-//
double kII11= 53.7, kII12 = 0.0, kII22 = 0.73, coek1 = 1.0, coek2 = 1.0;
double alphaII11 = 0.034*pow(10,-6), alphaII22 = 34.2*pow(10,-6),
    alphaII12 = 0.0, alphaII33 = alphaII22, coea21 =1.0, coea22 = 1.0;
//————————————————————-//
double K1 = 0.0, K2 = 0.0, G = 1.0, G0 =1.0;
double coefk = 0.01, coefkmax = 0.0, omegamax = 0.0, Gmax = 0.0,
    cof = 2, y = 1.0, coef = 1.0;
double **Ari, *fnbeta, *cdr,*cdi, **U, **L, *g, *K, **Omega, *t0;
    double **tpNtau, **tpNbeta, *Beta;
double *T0 ;
char *ch1 = "medium_I", *ch2 = "medium_II";
char *ch = "laminates";
```

```
int openmode;
/*————————— thermal property ————————————*/
number_complex nc, z1, z2(2,3), i1 = number_complex(0,1),//(i1)^2 = -1;
      u1 = number_complex(1,0), hstar, G0t;
vector t, x, tb, xb, fn, ft, fb, vtp ;
vector_complex ps, ps1, ps2, c1, c2, d1, d2;
vector_complex rho1, rho2, e1, e2, e3, estr, dc, p1, p2, dtilde, ctilde;
/*————————— linear eq: a X = fn;————————————-*/
matrix a, atb, c, H1, L1, S1, H2, L2, S2, d, w, M, // c is the material matrix;
      tm, I = I.unit(n,n), Itau = Itau.unit(m,m), Itp = I-I,
I1 = I1.unitk(3,3,1),I2 = I2.unitk(3,3,2),I3 = I3.unitk(3,3,3);
matrix_complex ab, tp, b, a1, b1, a2, b2, M_1, M_2,
      mn, cc, Ic = matrix_complex(I, Itp);
omega0 = -omega0;
//theta = PI/6; // (1)
//theta = PI/4; //(2)
//theta = PI/3; //(3)
sie slu, upper(&theta, ch2);
// theta = 0.0;
theta = -PI/(6.*4.);
//theta = -PI/6; // (1)
```

```
//theta = -PI/4.001; //(2)
theta = -PI/3; //(3)
sie lower(&theta,ch2);
kII11 = kI11; kII12 = kI12; kII22 = kI22;
alphaII11 = alphaI11; alphaII22 = alphaI22;
alphaII12 = alphaI12; alphaII33 = alphaI33;
//-----------------------------------------------------------------------//
Dyanmic Memory Allocation and Initialization of arrays
//-----------------------------------------------------------------------//
cout << "begin: running....."<<"\ n";
//========== upper medium ==========//
c = upper.material_characteristic_matrix();
// cout << "c_upper:" << c << "\ n";
//-------------------------//
omega = upper.get_alpha();
coea11 = alphaI11*cos(omega)*cos(omega) + alphaI12*sin(2.*omega) +
    alphaI22*sin(omega)*sin(omega);
coea12 = (alphaI22-alphaI11)*sin(2.*omega)/2.0 + alphaI12*
    (cos(omega)*cos(omega) - sin(omega)*sin(omega));
coea22 = alphaI11*sin(omega)*sin(omega) - alphaI12*sin(2.*omega) +
    alphaI22*cos(omega)*cos(omega);
```

```
alphaI11 = coea11; alphaI12 = coea12; alphaI22 = coea22;
//————————————————————//
coea11 = kI11*cos(omega)*cos(omega) + kI12*sin(2.*omega) +
     kI22*sin(omega)*sin(omega);
coea12 = (kI22-kI11)*sin(2.*omega)/2.0 + kI12*
     (cos(omega)*cos(omega) - sin(omega)*sin(omega));
coea22 = kI11*sin(omega)*sin(omega) - kI12*sin(2.*omega) +
     kI22*cos(omega)*cos(omega);
kI11 = coea11; kI12 = coea12; kI22 = coea22;
coea11 = 1.0; coea12 = 1.0; coea22 = 1.0;
//————————————————————-//
Beta[1] = c(1,1)*alphaI11 + c(1,2)*alphaI22 + c(1,3)*alphaI33;//beta11;
Beta[2] = 0.0; //beta21;
Beta[3] = 0.0;//beta31;
Beta[4] = Beta[2]; //beta12;
Beta[5] = c(1,2)*alphaI11 + c(2,2)*alphaI22 + c(2,3)*alphaI33;
Beta[6] = 0.0;//beta32;        km = tp.matrix_eigvalue_eigvector(c, ps1, ab);
ab = tp.matrix_norm_eigvector(ab, a1, b1);//eigen vector A & B of eq(11-1)
tp = a1*a1.transpose(a1)*cof; H1 = -tp.im(tp);//H = 2i A A^t;
tp = -b1*b1.transpose(b1)*cof; L1 = -tp.im(tp);//L = - 2i B B^t
tp = a1*b1.transpose(b1)*cof-Ic; S1 = -tp.im(tp);//S = i(2AB^t -I)
```

```
//————————————————//

k1 = sqrt(kI11*kI22 - kI12*kI12);

number_complex tau1(-kI12/kI22, k1/kI22);

for( i = 1; i ¡= 6; i++){

for( j = 1; j ¡= 6; j++)

tpNtau[i][j] = c(i,j);

tpNtau[i][i] = tpNtau[i][i] - tau1.re(tau1);

tpNbeta[i][i] = -tau1.im(tau1);

}

matrix_complex Ntau(tpNtau, tpNbeta, 6, 6);

tpNbeta[4][1] = -1.0; tpNbeta[5][2] = -1.0; tpNbeta[6][3] = -1.0;

for(i = 1; i <= 6; i++)

   for(j = 4; j <= 6; j++)

      tpNbeta[i][j] = -c(i,j);

matrix Nbeta(tpNbeta, 6, 6);

vector Vbeta(Beta,6),

fNbeta = Nbeta*Vbeta ; // RHS_2 of eq (11-2)

for(i = 1; i<= 6; i++) {

   for( j = 1; j <= 6; j++){

      Ari[i][j] = Ntau.re(Ntau)(i,j); Ari[i+6][j+6] = Ari[i][j];

      Ari[i+6][j] = Ntau.im(Ntau)(i,j); Ari[i][j+6] = - Ari[i+6][j];
```

```
   }
   fnbeta[i] = fNbeta[i];
}
a = matrix(Ari,12,12);
vector fbeta(fnbeta,12);
slu.gauss_elim_partial_pivoting(a,fbeta);
//————————————————————————————————-//
Dynamic Memory Allocation and Initialization for U and L
//————————————————————————————————-//
fbeta = fbeta;
slu.forward_substitutation(L, fbeta);
slu.backward_substitutation(U, fbeta);
/*normalization of C and D vector*/
for(i = 1; i <= 3; i++){
   cdr[i] = fbeta[i];
   cdi[i] = fbeta[6+i];
}
c1 = vector_complex(cdr, cdi,3);
c1 = c1*(1/c1.mod(c1));
for(i = 1; i ¡= 3; i++){
cdr[i] = fbeta[3+i];
```

```
cdi[i] = fbeta[6+3+i];
}
d1 = vector_complex(cdr,cdi,3);
d1 = d1*(1/d1.mod(d1));
//——— Lower Medium———//
c = lower.material_characteristic_matrix();
//————————————//
omega = lower.get_alpha();
coea11 = alphaII11*cos(omega)*cos(omega) + alphaII12*sin(2.*omega) +
   alphaII22*sin(omega)*sin(omega);
coea12 = (alphaII22-alphaII11)*sin(2.*omega)/2.0 + alphaII12*
   (cos(omega)*cos(omega) - sin(omega)*sin(omega));
coea22 = alphaII11*sin(omega)*sin(omega) - alphaII12*sin(2.*omega) +
   alphaII22*cos(omega)*cos(omega);
alphaII11 = coea11; alphaII12 = coea12; alphaII22 = coea22;
//————————————————————————————//
coea11 = kII11*cos(omega)*cos(omega) + kII12*sin(2.*omega) +
   kII22*sin(omega)*sin(omega);
coea12 = (kII22-kII11)*sin(2.*omega)/2.0 + kII12*
   (cos(omega)*cos(omega) - sin(omega)*sin(omega));
coea22 = kII11*sin(omega)*sin(omega) - kII12*sin(2.*omega) +
```

```
   kII22*cos(omega)*cos(omega);
kII11 = coea11; kII12 = coea12; kII22 = coea22;
coea11 = 1.0; coea12 = 1.0; coea22 = 1.0;
//————————————————————//
Beta[1] = c(1,1)*alphaII11 + c(1,2)*alphaII22 + c(1,3)*alphaII33;//beta11;
Beta[2] = 0.0; //beta21;
Beta[3] = 0.0;//beta31;
Beta[4] = Beta[2]; //beta12;
Beta[5] = c(1,2)*alphaII11 + c(2,2)*alphaII22 + c(2,3)*alphaII33;
Beta[6] = 0.0;//beta32;
km = tp.matrix_eigvalue_eigvector(c, ps2, ab);
ab = tp.matrix_norm_eigvector(ab, a2, b2);//eigen vector A & B of eq(11-1)
tp = a2*a2.transpose(a2)*cof; H2 = -tp.im(tp);//H = 2i A A^t;
tp = -b2*b2.transpose(b2)*cof; L2 = -tp.im(tp);//L = - 2i B B^t
tp = a2*b2.transpose(b2)*cof-Ic; S2 = -tp.im(tp);//S = i(2AB^t -I)
//————————————————//
k2 = sqrt(kII11*kII22 - kII12*kII12);
number_complex tau2(-kII12/kII22, k2/kII22);
for( i = 1; i <= 6; i++){
   for( j = 1; j<=6; j++)
      tpNtau[i][j] = c(i,j);
```

```
   tpNtau[i][i] = tpNtau[i][i] - tau2.re(tau2);
   tpNbeta[i][i] = -tau2.im(tau2);
}
Ntau = matrix_complex(tpNtau, tpNbeta, 6, 6);
tpNbeta[4][1] = -1.0; tpNbeta[5][2] = -1.0; tpNbeta[6][3] = -1.0;
for(i = 1; i <= 6; i++)
   for(j = 4; j <= 6; j++)
      tpNbeta[i][j] = -c(i,j);
Nbeta = matrix(tpNbeta, 6, 6);
Vbeta = vector(Beta,6);
fNbeta = Nbeta*Vbeta ; // RHS_2 of eq (11-2)
for(i = 1; i <= 6; i++) {
   for( j = 1; j <= 6; j++){
      Ari[i][j] = Ntau.re(Ntau)(i,j); Ari[i+6][j+6] = Ari[i][j];
      Ari[i+6][j] = Ntau.im(Ntau)(i,j); Ari[i][j+6] = - Ari[i+6][j];
   }
   fnbeta[i] = fNbeta[i];
}
a = matrix(Ari,12,12);
fbeta = vector(fnbeta,12);
slu.gauss_elim_partial_pivoting(a,fbeta);
```

```
for(i =1; i <= 12; i++){
for(j = 1 ; j <=12; j++){
U[i][j] =0.0; L[i][j] = 0.0;
}
}
for(i = 1; i <= 12; i++) {
for(j=i; j <= 12; j++) U[i][j] = a(i,j);
for(j =i; j >= 1; j–) L[i][j] = a(i,j);
L[i][i] = 1.0;
}
fbeta = fbeta ;
slu.forward_substitutation(L, fbeta);
slu.backward_substitutation(U, fbeta);
/*normalization of C and D vector*/
for(i = 1; i <= 3; i++) {
   cdr[i] = fbeta[i]; cdi[i] = fbeta[6+i];
}
c2 = vector_complex(cdr, cdi,3); c2 = c2*(1/c2.mod(c2));
for(i = 1; i <= 3; i++){
cdr[i] = fbeta[3+i]; cdi[i] = fbeta[6+3+i];
}
```

d2 = vector_complex(cdr,cdi,3); d2 = d2*(1/d2.mod(d2));

//————————————————————————————————-//

Free Memory used by U and L

//————————————————————————————————-//

//=======——bimaterial property matrix—-=====//

d = L1.inverse(L1) + L2.inverse(L2);

w = S1*L1.inverse(L1) - S2*L2.inverse(L2);

matrix wtp = - w;

tp = matrix_complex(d, wtp);

mn = tp.inverse(tp);//mn = (d - i w)$^{-1}$//

c = d.inverse(d)*w*d.inverse(d)*w;//cc - is the constant matrix

y = -.5*(c(1,1) + c(2,2) + c(3,3));

if(fabs(y) ¡ EPSLON) y = 0.0;

beta = sqrt(y);

if(ch1 ! = “medium_isotropic”){

c = w*d.inverse(d);

km = tp.matrix_eigvalue_eigvector(c, ps, ab);

cc = ab; //cc - the constant matrix v

ch1 = upper.get_str();

ch1 = lower.get_str();

}

```
else cc = Ic;
/*—— Defined Bi-material Constants ——*/
M = S1*L1.inverse(L1) ;
M_1 = matrix_complex(L1.inverse(L1), -M);//M inverse
M = S2*L2.inverse(L2) ;
M_2 = matrix_complex(L2.inverse(L2), -M);
// matrix_complex Nstr = (mn + mn.conjugate(mn))*i1;
//———++++++++++———//
/*—— Defined Thermail Constants ——*/
e1 = (c1*k2 + c2.conjugate(c2)*k1)*(u1/(k1+k2));
e2 = (d1*k2 + d2.conjugate(d2)*k1)*(u1/(k1+k2));
e3 = (d1*k2 + d2*k1)*(u1/(k1+k2));
estr = (mn*e1 + mn.conjugate(mn)*e1.conjugate(e1))*i1;
estr = estr - (mn*M_1*e2 - mn.conjugate(mn)*M_1.conjugate(M_1)
   *e2.conjugate(e2)) + e2 + e3;
dc = mn*e1*i1 + mn*M_2.conjugate(M_2)*e2 - d1*(k2/(k1+k2));
//————————————————————//
rho1 = d1*k2*(u1/(k1+k2)) - mn*(e1*i1 + M_2.conjugate(M_2)*e2) ;
rho2 = d2*k1*(u1/(k1+k2))
- mn.conjugate(mn)*(e1.conjugate(e1)*i1
   + M_1.conjugate(M_1)*e2.conjugate(e2));
```

```
ctilde = c2*k1*(2/(k1+k2)) - c1.conjugate(c1)*((k1-k2)/(k1+k2)) - c1;
dtilde = d2*(2*k1/(k1+k2)) - d1.conjugate(d1)*((k1-k2)/(k1+k2)) - d1;
//————————//
omega = omega0;
if(omega < 0.0){
   e1 = (c2*k1 + c1.conjugate(c1)*k2)*(u1/(k1+k2));
   e2 = (d2*k1 + d1.conjugate(d1)*k2)*(u1/(k1+k2));
   e3 = (d2*k1 + d1*k2)*(u1/(k1+k2));
   estr = (mn*e1 + mn.conjugate(mn)*e1.conjugate(e1))*i1;
   estr = estr - (mn*M_2*e2 - mn.conjugate(mn)*M_2.conjugate(M_2)
      *e2.conjugate(e2)) + e2 + e3;
dc = mn*e1*i1 + mn*M_1.conjugate(M_1)*e2 - d2*(k1/(k1+k2));
//————————————————————//
rho1 = d2*k1*(u1/(k1+k2)) - mn*(e1*i1 + M_1.conjugate(M_1)*e2) ;
rho2 = d1*k2*(u1/(k1+k2))
   - mn.conjugate(mn)*(e1.conjugate(e1)*i1
   + M_2.conjugate(M_2)*e2.conjugate(e2));
ctilde = c1*k2*(2/(k1+k2)) - c2.conjugate(c2)*((k1-k2)/(k1+k2)) - c2;
dtilde = d1*(2*k2/(k1+k2)) - d2.conjugate(d2)*((k1-k2)/(k1+k2)) - d2;
}
/*———- equivalent loading ———-*/
```

number_complex h_0s(0, -(k1+k2)/(k1*k2)/2) ; h_0s = h_0s*h0;

p1 = (rho1 + rho2)*h_0s; p2 = (rho2 - rho1)*h_0s;

vector_complex p_0(t0, g,3);

t0[1] = p1.rev(p1)[1]; t0[2] = p1.rev(p1)[2]; t0[3] = p1.rev(p1)[3];

g[1] = p1.imv(p1)[1]; g[2] = p1.imv(p1)[2]; g[1] = p1.imv(p1)[3];

vector_complex p_1t(t0, g,3);

t0[1] = p1.rev(p1)[1]; t0[2] = p1.rev(p1)[2]; t0[3] = p1.rev(p1)[3];

t0[3] = t0[3]*1.5;

g[1] = p1.imv(p1)[1]; g[2] = p1.imv(p1)[2]; g[3] = p1.imv(p1)[3];

g[3] = 1.5*g[3];

vector_complex p_tild(t0,g,3);

t0[1] = p1.rev(p1)[1]; t0[1] = t0[1]*(ratio_bl+ratio_al);

t0[2] = p1.rev(p1)[2]; t0[2] = t0[2]*(ratio_bl+ratio_al);

t0[3] = p1.rev(p1)[3]; t0[3] = t0[3]*(ratio_bl+3*ratio_al)/2.0;

g[1] = p1.imv(p1)[1]; g[1] = g[1]*(ratio_bl+ratio_al);

g[2] = p1.imv(p1)[2]; g[2] = g[2]*(ratio_bl+ratio_al);

g[3] = p1.imv(p1)[3]; g[3] = g[3]*(ratio_bl+3*ratio_al)/2.0;

vector_complex p_1h(t0,g,3);

//————-for K0————-//

matrix_complex kk1, kk2, kk3;

kk1 = kk1.diag(i1*beta + 0.5, -i1*beta +0.5, i1*0+0.5);

```
kk1 = - kk1;        kk2 = kk2.diag(-i1*(beta*ratio_bl)
    + beta*beta-(ratio_bl+ratio_al)/(ratio_bl-ratio_al)/4,
  i1*(beta*ratio_bl) + beta*beta - (ratio_bl+ratio_al)/(ratio_bl-ratio_al)/4,
  i1*0-(ratio_bl+ratio_al)/(ratio_bl-ratio_al)/4 + 1/8);
kk2 = kk2 *(ratio_bl-ratio_al);
kk3 = kk3.diag(i1*2.*beta + beta*beta + 0.375, -i1*2.*beta
  + beta*beta + 0.375, i1*0 - 0.25);
kk3 = kk3 *(ratio_bl-ratio_al);
vector_complex KK0;
KK0 = kk1*p_0 + kk2*p1 + kk3*p2;
KK0 = -KK0*sqrt(2*PI*(ratio_bl-ratio_al));
vector K0 = KK0.rev(KK0);
//———-for G0————————//
G0t = ((L1.inverse(L1) + L2.inverse(L2))*p_0)*p_0/2.;
G0t = G0t + (((L1.inverse(L1) + L2.inverse(L2))*p_tild)*p_0)
  *(ratio_bl+ratio_al)/2.;
G0t = G0t + (((L1.inverse(L1)+ L2.inverse(L2))*estr)*p_0)*h_0s/2.;
G0t = G0t + (((L1.inverse(L1)+ L2.inverse(L2))*p_0)*p_1t)*ratio_bl/2.;
G0t = G0t + ((((L1.inverse(L1)+ L2.inverse(L2))*p_1h)*p_1t)*ratio_bl)/4./2.;
G0 = G0t.re(G0t);
G0 = G0*PI*(ratio_bl-ratio_al)/2.0;
```

```
omega = omega0;

if(omega < 0.0) {

k12 = k1; k1 = k2; k2 = k12;

ps = ps1; ps1 = ps2; ps2 = ps;

number_complex tau12 = tau1; tau1 = tau2; tau2 = tau12;

matrix_complex b12 = b1; b1 = b2; b2 = b12;

vector_complex c12 = c1, d12 = d1; c1 = c2; c2 = c12; d1 = d2; d2 = d12;

mmatrix_complex M_12 = M_1; M_1 = M_2; M_2 = M_12;

matrix L12 = L1; L1 = L2; L2 = L12;

}

//—for convergence—//

count = 1;

N = 120;

/*————————————*/        do {

n = N; // n = 120 points of discretization!!!

T0 = new double [N+1]; T0 = T0-1;

for( i = 1; i ¡= N+1; i++) T0[i] = 0.0;

ps = ps1;

/*–calculation of thermal dislocation density–*/

slu.point_t_x_T(t, x, &n);//create points t[n], x[n+1]

a = slu.matrix_a_T_bimedia(t,x, &n, &ratio_al, &ratio_bl, &l, &k1, &k2,
```

```
   &omega, tau1, ft, &h0);
slu.gauss_elim_partial_pivoting(a,ft);
//-----------------------------------------------------------------------//
Dynamic Memory Allocation and Initialization for U and L
//-----------------------------------------------------------------------//
for(i = 1; i <= n; i++){
   for(j=i; j <= n; j++) U[i][j] = a(i,j);
   for(j =i; j >= 1; j–) L[i][j] = a(i,j); L[i][i] = 1.0;
}
slu.forward_substitutation(L, ft);
slu.backward_substitutation(U, ft);
for(i = 1+1; i <= n+1; i++)
T0[i] = ft[i-1]*sqrt((1+t[i-1])*(1-t[i-1]));
ft = vector(T0, n+1);
//-----------------------------------------------------------------------//
Free Memory used by U and L
//-----------------------------------------------------------------------//
/*– end of the calcultion for thermal-dislocation density –*/
/*—solving singular integration equation for displ.-dislocation—*/
n = N;
fb = ft;
```

```
slu.point_t_x_b(tb, xb, &n);//create points t[n], x[n]
atb = slu.matrix_a_b_bimedia(tb, xb, &n, beta, &ratio_al, &ratio_bl, &l,
   tau1, ps, b1, d1, c1, d2, c2, L1, mn, p1, p2, dc, cc, &omega, t,
   M_2, ctilde, dtilde, k1, k2, fb, &h0);
//LU-decomposite a with partial poviting//
slu.gauss_elim_partial_pivoting(atb,fb);
//————————————————————————————————//
Dynamic Memory Allocation and Initialization for U and L
//————————————————————————————————//
for(i = 1; i <= 3*n; i++){
   for(j=i; j <= 3*n; j++) U[i][j] = atb(i,j);
   for(j =i; j >= 1; j–) L[i][j] = atb(i,j); L[i][i] = 1.0;
}
slu.forward_substitutation(L, fb);
slu.backward_substitutation(U, fb);
//————————————————————————————————//
Free Memory used by U and L
//————————————————————————————————//
Omega[1][1] = cos(omega); Omega[1][2] = sin(omega);
Omega[2][1] = -sin(omega); Omega[2][2] = cos(omega); Omega[3][3] = 1.0;
matrix Omega0 = matrix(Omega, 3,3);
```

```
number_complex zt1 = ps[1]*sin(omega) + cos(omega),

zt2 = ps[2]*sin(omega) + cos(omega),

zt3 = ps[3]*sin(omega) + cos(omega);

Omega[1][1] = sin(2*omega)/2; Omega[1][2] = sin(omega)*sin(omega);

Omega[2][1] = -Omega[1][2]; Omega[2][2] = Omega[1][1];

Omega[3][3] = sin(omega);

matrix Omegatp(Omega, 3,3);

matrix_complex Omega1(Omegatp, Omegatp-Omegatp);

Omega[1][1] = cos(omega)*cos(omega); Omega[1][2] = sin(2*omega)/2;

Omega[2][1] = -Omega[1][2]; Omega[2][2] = Omega[1][1];

Omega[3][3] = cos(omega);        Omegatp = matrix(Omega,3,3);

matrix_complex Omega2(Omegatp, Omegatp-Omegatp);

matrix_complex zta = zta.diag(u1/zt1, u1/zt2, u1/zt3),

palpha = palpha.diag(ps[1], ps[2], ps[3]);

matrix_complex kkb = Omega2*b1*zta*b1.transpose(b1)

  + Omega1*b1*zta*palpha*b1.transpose(b1);

matrix tpkb = kkb.im(kkb);

for(i= 1; i ¡= 3; i++){

g[i] = 0.0;

for(j = 1; j ¡= 3; j++)

g[i] = g[i] + tpkb(i,j)*fb[3*(n-1)+j]*(sqrt(l/2.0)/PI);
```

```
}
K[1] = -g[1]; K[2] = -g[2]; K[3] = -g[3];
//transformation matrix//
ofstream fout;
const char *file = "stress_intensitfy_factor.dat";
if((fabs(omega) == PI/(40*18.*2))——(fabs(omega) == PI))
   openmode = ios::out;
else openmode = ios::app;
   fout.open(file, openmode);
if(!fout.good()){
   cerr << "can't open " << file << "file for output. \ n"; exit(1);
}
if(openmode == ios::out){
fout <<"==branching/main crack v.s. stress intensity factor===" << "\n";
fout << "descritization point number " << "\ n";
fout << "n = " << n << ": " << "\ n";
fout << "\ n";
}
fout << "omega = " << omega*degree << ": ";
fout << K[2] ; fout << "" << K[1];
fout << "" << K[3] << "\ n";
```

```
fout.close();
ofstream fout1;
file = "stress_intensitfy_factor_plotting_KI.dat";
fout1.open(file, openmode);
if(!fout1.good()){
   cerr << "can't open " << file << "file for output.    n"; exit(1);
}
fout1 << omega*degree << "";
fout1 << K[2] << "\n";
fout1.close();
ofstream fout2;
file = "stress_intensitfy_factor_plotting_KII.dat";
fout2.open(file, openmode);
if(!fout2.good()){
   cerr << "can't open " << file << "file for output.\n"; exit(1);
}
fout2 << omega*degree << "";
fout2 << K[1] << "\n";
fout2.close();
ofstream fout3;
file = "stress_intensitfy_factor_plotting_KIII.dat";
```

```
fout3.open(file, openmode);
if(!fout2.good()){
   cerr << "can't open " << file << "file for output.\n"; exit(1);
}
fout3 << omega*degree << "";
fout3<< K[3] << "\n";
fout3.close();
vector t0t = vector(t0,3), t0tp;
matrix dtp = L1.inverse(L1)*2;
t0tp = dtp*t0t;
matrix L_1;
L_1 = Omega0.transpose(Omega0)*L1*Omega0;
L_1 = L_1.inverse(L_1);
if(K[2] ¡= 0) K[2] = 0.0; // contact of crack surfaces
y = K[1]; K[1] = K[2]; K[2] = y;
vector Kt = vector(K,3); //vector(K,3);
G = Kt*(L_1*Kt)*0.5; //energy release rate
ofstream fout4;
file = "energy_release_rate.dat";
fout4.open(file, openmode);
if(!fout4.good()){
```

```
    cerr << "can't open " << file << "file for output. n"; exit(1);
  }
  fout4 << omega*degree << "";
  fout4 << G << "\ n";
  fout4.close();
  if(omega0 >0){
    omega = omega + deltomega; //for upper half plane
  }
  else if (omega0 < 0) {
    omega = omega - deltomega;//for lower half plane
  }
  if(fabs(omega)>= PI/2) stop = 1;
  } while(stop !=1);
  stop = 0;
  cout << " n" << "——-end" << "\ n";
  //————————————————————————————————//
  Free Memory used by all arrays
  //————————————————————————————————//
  return 0;
}
```

K.2 the sie_solving_thermoelastic_bimedia_thmatrix_du.cpp

– these codes are used to calculate the terms in the

sigular integral equations

```
#include "vector_matrix_operator.h"
 #include "sie_solving.h"
/*———for thermal dislocation———-*/
 void sie::point_t_x_T(vector &t, vector &x, int *mt)//points of x and t;
 {
      int i, n;
      double *tp;
      n = *mt;
      tp = new double [n+1]; tp = tp -1;
      for(i = 1; i <= n; i++) tp[i] = cos(PI*i/(n + 1));
      t = vector(tp,n);
      for(i = 1; i <= n+1; i++) tp[i] = cos(0.5*PI*(2*i-1)/(n + 1));
      x = vector(tp, n+1);
      delete [] (char*) (tp+1);
 }
```

//coefficients matrix of SIE for voertix==========//

```
matrix sie::matrix_a_T_bimedia(vector& t, vector& x, int *mt, double *ratio_a,
    double *ratio_b, double *L, double *K1, double*K2, double *omega,
    number_complex tau, vector &fb, double* h)
{
    int i, j, m;
    double **kkt, *load, k1 = *K1, k2 = *K2, omegatp = *omega;
    double r, r0, l = *L, a = *ratio_a, b = *ratio_b, h0 = *h;
    matrix tp;
    number_complex u1 = number_complex(1,0);
    number_complex ktp, ktd, ktp1, ktp2, ktp3;
    number_complex mu = u1*cos(omegatp) + tau*sin(omegatp);
    m = *mt;
    kkt = new double *[m]; kkt = kkt - 1;
    for(i = 1; i ¡= m; i++){
      kkt[i] = new double [m]; kkt[i] = kkt[i] - 1;
    }
    for(i =1 ; i ¡= m; i++){
      for(j =1; j <= m; j++){
        kkt[i][j] = 0.0;
      }
    }
```

```
load = new double [m]; load = load -1;

for(i =1; i <=m; i++) load[i] = 0.0;

for(i = 1+1; i <= m+1; i ++){

   r = (1.0 + x[i])*l/2.0;

for( j = 1; j ¡= m; j++){

      r0 = (1.0 + t[j])*l/2.0;

      ktp1 = mu*(u1/(mu*r - mu.conjugate(mu)*r0));

      ktp1 = - ktp1*(k1-k2)/(k1+k2);

      ktp2 = (mu*r0 -a)*(mu*r0-b)/(mu*r -a)*(mu*r-b);

      ktp2 = ktp2.sqrt_c(ktp2);

      ktp2 = - ktp2 + 1.0;

      ktp2 = ktp2*(k2/(k1+k2)/(r-r0));

      ktp3 = (mu.conjugate(mu)*r0 -a)*(mu.conjugate(mu)*r0-b)

            /(mu*r -a)*(mu*r-b);

      ktp3 = ktp3.sqrt_c(ktp3);

      ktp3 = - ktp3 + 1.0;

      ktp3 = ktp3*mu/(mu*r-mu.conjugate(mu)*r0);

      ktp3 = ktp3 - mu*2/ktp3.sqrt_c((mu*r-a)*(mu*r-b));

      ktp3 = ktp3*(k2/(k1+k2));

      ktp = ktp1 + ktp2 + ktp3;

      ktp = ktp*l/2.0;
```

```
            ktp = -ktp + 1.0/(t[j] - x[i]);
            ktp = ktp*(1-t[j]*t[j])/(m + 1);
            kkt[i-1][j] = ktp.re(ktp);
          }
          ktd = mu*r - (a+b)/2;
          ktd = ktd/ktd.sqrt_c((mu*r-a)*(mu*r-b));
          ktd = (-ktd + 1.0)*(tau*sin(omegatp) + cos(omegatp));
          load[i-1] = 2*(cos(omegatp) + ktd.re(ktd))*h0/k1;
        }
        fb = vector(load, m);
        tp = matrix(kkt,m,m);
        delete [] (char*) (load+1);
        for(i = 1; i ¡= m; i ++)
        delete [] (char*) (kkt[i] +1);
        delete [] (char*) (kkt+1);
    return tp;
}
```

References

[1] Williams, M.L., 1959, "The Stress around a Fault or Crack in Dissimilar Media ", Bulletin of the Seismological Society of America , **49**, No.2, pp.199-204.

[2] Erdogan, F., 1963, "The Stress Distribution in a Non homogeneous Elastic Plane with Cracks", J. Applied Mechanics , **85**, pp.232-236.

[3] England, A.H., 1965, "A Crack Between Dissimilar Media", *Journal of Applied Mechanics* , Transaction ASME, **32**, pp.400-402.

[4] Rice, J.R. and Sih, G.C., 1965, "Plane problems of Cracks in Dissimilar Media", J. Applied Mechanics, **32**, pp.418-423.

[5] Suo, Z. and Hutchinson, J.W., 1990, "Interface Crack between two Elastic Layers ", Int. J. Fracture, **43**, pp.1-18.

[6] Muskhelishvili, N.I., 1953, *Some Basic Problems of the Mathematical Theory of Elasticity* , P. Noordoff and Company, New York, N.Y.

[7] Clements, D.L., 1971, "A Crack between Dissimilar Anisotropic Media ", Int. J. Engng . Sci., **9**, pp.257-265

[8] Stroh, A.N., 1958, "Dislocations and Cracks in Anisotropic Elasticity ", Phil. Mag. , Ser. 8, No.3 , pp.625-646.

[9] Willis, R.J., 1971, "Fracture mechanics of interfacial cracks ", J. Mech. Phys. Solids, **19**, pp.353-368.

[10] Ting, T.C.T, 1986, "Explicit Solution and Invariance of the Singularities at an Interface crack in anisotropic Composites", Int. J. Solids Structures, **22**, pp.965-983.

[11] Qu, J. and Li, Q.Q., 1991, "Interfacial Dislocation and its Applications to Interface Cracks in Anisotropic Bimaterials ", J. Elasticity, **26**, pp.169-195.

[12] Shi.G.C. , 1962 "On the Singular Character of Thermal Stresses Near

a Crack Tip ", ASME J. Applied Mechanics **29**, pp. 587-589.

[13] Barber, J.R. and Comninou, M., 1982 "The External Axisymmetric Interface Crack with Heat Flow ", Q.J.Mech.Appl. Math. **35**, pp. 403-417.

[14] Barber, J.R. and Comninou, M., 1983 "The Penny-shaped Interface Crack with Heat Flow, Part 2: Imperfect Contact ", J. Applied Mechanics **50**, pp. 770-776.

[15] Martin-Moran,C.J., Barber, J.R. and Comninou, M., 1983 "The Penny-shaped Interface Crack with Heat Flow, Part 1: Perfect Contact ", J. Applied Mechanics **50**, pp. 29-36.

[16] Atkinsion,C., and Clements, D.L., 1983 "A Thermoelastic Problem For a Crack Between Dissimilar Anisotropic Media ", Int. J. Solids Structures, **19**, pp. 121-130.

[17] Hwu, Chyanbin, 1992 "Thermoelastic Interface Crack Problems in Dissimilar Anisotropic Media ", Int. J. Solids Structures, **29**, No.16, pp.2077-2090

[18] Ting, T.C.T., 1988 "Some Identities and the Structures of N_i the Stroh Formalism of Anisotropic Elasticity ", Q. Appl. Math. **46**, pp.109-120

[19] Choi, H. J. and Thangjitham, S., 1993 "Thermally-Induced Interlaminar Crack-tip Singularities in Laminated Anisotropic Composites ", Int. J. Fracture, **60**, pp.327-347

[20] Herrmann, K. P., and Loboda, V.V., 2001 "Contact Zone Models for an Interface Crack in a Thermomechanically Loaded Anisotropic Bimaterials ", J. Thermal Stress, **24**, pp.479-506

[21] Comninou, M., 1977, "The Interface Crack ", J. Applied Mechanics, **44**, pp.631-636.

[22] Lo, K.K., 1978, "Analysis of Branched Crack ", ASME J. Applied Mechanics, **45**, pp.797-802.

[23] Hayashi, K and Nemat-Nasser, S., 1981a, "Energy-Release Rate and

Crack Kinking under Combined Loading ", ASME J. Applied Mechanics, **48**, pp.520-524.

[24] Hayashi, K. and Nemat-Nasser, S., 1981b, "On Branched Interface Cracks ", ASME J. Applied Mechanics, **48**, pp.529-533.

[25] He, M-Y and Hutchinson, J.W., 1989, "Kinking of a Crack Out of an Interface ", Transaction of the ASME, **56**, pp.271-278.

[26] Obata, M., Nemat-Nasser, S. and Goto, Y., 1989, "Branched Cracks in Anisotropic Elastic Solids ", Transaction of the ASME, **56**, pp.858-864

[27] Gao, H.J., and Chiu, C.H., 1992, "Slightly Curved or Kinked Cracks in Anisotropic Elastic Solids ", Int. J. Solid Structures, **29**, No.8, pp.947-972.

[28] Miller, G.R. and Stock, W.L., 1989, "Analysis of Branched Interface Cracks Between Dissimilar Anisotropic Media ", Transaction of the ASME , **56**, pp.844-849.

[29] Hasebe, N., Tamai, K., and Nakamura, T., 1986 "Analysis of Kinked Crack under Uniform Heat Flow ", J. Engineering Mechanics, **112**, No.1, pp.31-42

[30] Chao, C.K., and Shen, M.H., 1993 "Thermoelastic Problem of Curvilinear Cracks in the Bonded Dissimilar Materials ", Int. J. Solids Structures, **30**, No.22, pp.3041-3057

[31] Muskhelishvili, N.I., 1953, *Some Basic Problems of the Mathematical Theory of Elasticity* , English Translation, P.Noordoff and Company, New York, N.Y.

[32] Li, R. and Kardomateas, G.A., "Thermoelastic Crack Branching In General Anisotropic Media ", Proceeding of Fifth International Congress on Thermal Stresses and Related Topics Blacksburg, VA, 2003, pp WM-2-2-1 to WM-2-28

[33] Stroh, A.N., 1958, "Dislocations and Cracks in Anisotropic Elasticity ", Phil. Mag. , Ser. **8**, No.3 , pp.625-646.

[34] Conway, J.B., 1978 *Functions of One Complex Variable*, Springer-Verlag, New York, N.Y.

[35] Eshelby, J.D., Read, W.T. and Shockley, W., 1953, "Anisotropic Elasticity with Application to Dislocation Theory ", Acta Metallurgical, **2**, pp.251-259.

[36] Muskhelishvili, N.I., 1992, *Singular Integral Equations*, Dover Publications, Inc. N.Y.

[37] Erdogan, F., Gupta, G.D. and Cook, T.S., 1973, "Numerical solution of singular integral equation", *Mechanics of Fracture,* (Ed. G.C.Sih), **1** , pp.368-425.

[38] Barnett, D.M. and Asaro, R.J., 1972, "The fracture mechanics of slit-like cracks in anisotropic elastic media ", J. Mech. Phys. Solids, **20**, pp.356-366

[39] Sih, G.C., Paris, P.C. and Irwin, G.R., 1965, "On cracks in rectilinearly anisotropic bodies ", Int. J. Fracture of Mechanics, **1**, pp.189-203

[40] Li, R and Kardomateas, G.A., 2001 "On Delamination Branching of Anisotropic Bi-materials", Proceeding of the ASME Aerospace Division, ASME, New York, NY, A03-10766, Nov. 2001, pp.111-120. **1**, pp.189-203

[41] Hutchinson, J.W., Mear, M.E. and Rice, J.R., 1987, "Crack Paralleling an Interface Between Dissimilar Materials ", *Transaction of the ASME*, **54**, pp 828-832.

[42]Rice, J.R. 1988, "Elastic Fracture Mechanics Concepts for Interfacical Cracks ", J. Applied Mechanics, Transaction of the ASME, **55**, pp.98-103.

[43] Suo, Z. and Hutchinson, J.W., 1988, "On Sandwich Test Specimens for Measuring Interface Crack Toughness ", *Mater. Sci. Engng.*, **A 107**, pp 135-143.

[44] Qu, J. and Bassani, J.L., 1989, "Cracks on Bimaterial and Bicrystal Interfaces", *J. Mech. Phys. Solids*, **37**, pp 417-433.

[45] Qu, J. and Bassani, J.L., 1993, "Interfacial Fracture Mechanics for

Anisotropic Bimaterials ", *J. Applied Mechanics*, Transaction of the ASME, **37**, pp 417-433.

[46] Ting, T.C.T, 1996, *Anisotropic Elasticity: Theory and Application*, Oxford University Press, N.Y.

[47] Malyshev,B.M. and Salganik, R.L., 1965, "The Strength of Adhesive Joints Using the Theory of Fractures ", *Int. J. Fracture Mechanics*, **1**, pp.114-128.

[48] Wang, S.S. and Choi, I., 1983a, "The interface Crack Between Dissimilar Anisotropic Composite Materials ", *J. Applied Mechanics*, **50**, pp.169-178.

[49] Wang, S.S. and Choi, I. 1983b, "The interface Crack Behavior in Dissimilar Anisotropic Composites Under Mixed-Mode Loading ", *J. Applied Mechanics*, **50**, pp.179-183.

[50] Wu, K-C. and Hwang, S-J., 1990, "Corresponding Relations for the Interface Crack in Monoclinic Composites Under Mixed Loading ", *J. Applied Mechanics*, Transaction of the ASME, **57**, pp.894-899.

[51] Ni, L. and Nemat-Nasser, S., 1992, "Interface Craks in Anisotropic Dissimilar Materials:General Case ", *Q. Appl. Math.*, **50**, pp.305-322.

[52] Helgason, Sigurdur, 1999, *The Radon Transform* Birkhäuser Boston,N.Y.

Vita

Mr. Renfu Li was born in FengCheng, China, on February 6, 1966. In July 1988, he graduated with B.Sc. in Flight Vehicle Design & Applied Mechanics from Beijing University of Aeronautics and Astronautics. He also obtained his M.Sc degree in Computer Science from Beijing University. of Aeronautics and Astronautics in May 1995. Before he joined the School of Aerospace Engineering of Georgia Institute of Technology in August 1998, Mr. Li worked as a senior engineer in aerospace research institute in China. In August 2003, Mr. Li got his M.Sc in Aerospace Engineering and Mathematics Science from Georgia Institute of Technology.